AD-A141 691 A STUDY OF THERMAL PROPERTIES AND THE HEATING PROCESS 1/2
IN ASPHALTIC CONCRETE(U) TENNESSEE UNIV KNOXVILLE DEPT
OF CIVIL ENGINEERING W H HIGHTER ET AL. FEB 84
UNCLASSIFIED AFOSR-TR-84-0432 AFOSR-82-0250 F/G 11/2 NL

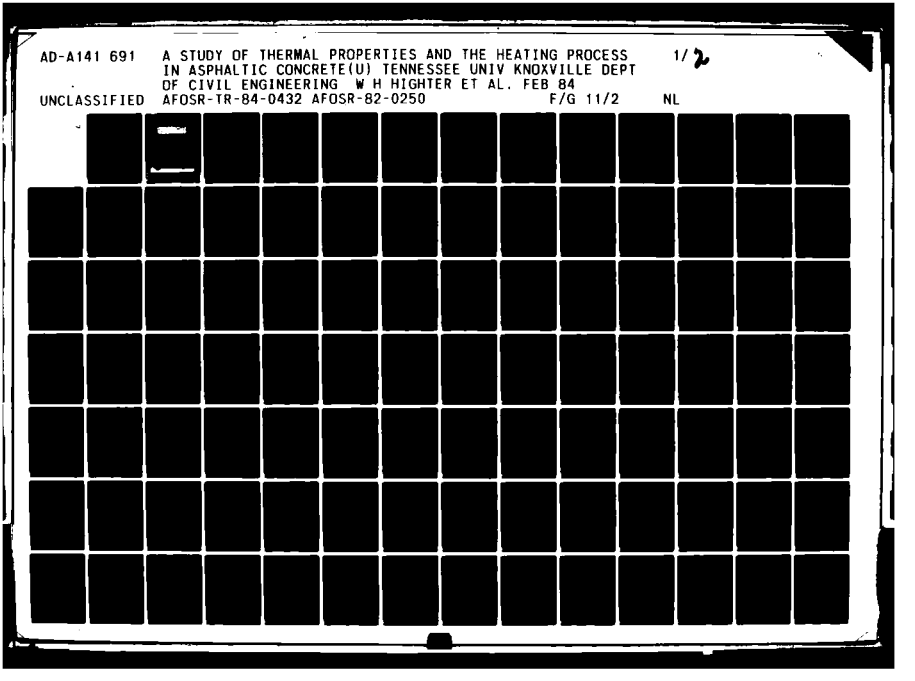

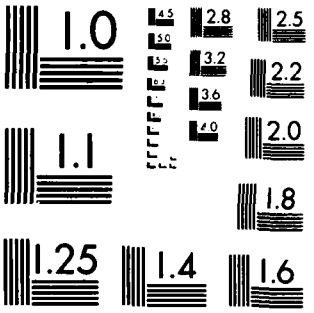

AFOSR-TR- 84-0432

(11)

THE UNIVERSITY OF TENNESSEE

A STUDY OF THERMAL PROPERTIES AND THE HEATING PROCESS IN ASPHALTIC CONCRETE

BY

WILLIAM H. HIGHTER
ROBERT J. KRANE
DOUGLAS J. WALL

A STUDY OF THERMAL PROPERTIES

AND THE

HEATING PROCESS IN ASPHALTIC CONCRETE

by

William H. Highter
Robert J. Krane
Douglas J. Wall

of

The University of Tennessee

February 1984

UNCLASSIFIED

SECURITY CLASSIFICATION OF THIS PAGE (When Data Entered)

REPORT DOCUMENTATION PAGE		READ INSTRUCTIONS BEFORE COMPLETING FORM
1. REPORT NUMBER AFOSR-TR- 84-0432	2. GOVT ACCESSION NO.	3. RECIPIENT'S CATALOG NUMBER
4. TITLE (and Subtitle) A STUDY OF THERMAL PROPERTIES AND THE HEATING PROCESS IN ASPHALTIC CONCRETE		5. TYPE OF REPORT & PERIOD COVERED FINAL 1 Jul 1982 - 31 Dec. 1983 6. PERFORMING ORG. REPORT NUMBER
7. AUTHOR(s) WILLIAM H. HIGHTER ROBERT J. KRANE DOUGLAS J. WALL		8. CONTRACT OR GRANT NUMBER(s) AFOSR-82-0250
9. PERFORMING ORGANIZATION NAME AND ADDRESS THE UNIVERSITY OF TENNESSEE DEPARTMENT OF CIVIL ENGINEERING KNOXVILLE, TN 37996		10. PROGRAM ELEMENT, PROJECT, TASK AREA & WORK UNIT NUMBERS 61102F 2307/C2
11. CONTROLLING OFFICE NAME AND ADDRESS AIR FORCE OFFICE OF SCIENTIFIC RESEARCH/NA BOLLING AFB, DC 20332		12. REPORT DATE February 1984 13. NUMBER OF PAGES 157
14. MONITORING AGENCY NAME & ADDRESS(if different from Controlling Office)		15. SECURITY CLASS. (of this report) Unclassified 15a. DECLASSIFICATION/DOWNGRADING SCHEDULE

16. DISTRIBUTION STATEMENT (of this Report)

Approved for Public Release; Distribution Unlimited.

17. DISTRIBUTION STATEMENT (of the abstract entered in Block 20, if different from Report)

18. SUPPLEMENTARY NOTES

19. KEY WORDS (Continue on reverse side if necessary and identify by block number)

ASPHALTIC CONCRETE
THERMAL PROPERTIES
NUMERICAL MODEL
PARAMETRIC STUDY
FIELD TESTS

20. ABSTRACT (Continue on reverse side if necessary and identify by block number)

The objectives of this study were to model the surface heating of asphaltic concrete pavements and to investigate the thermal properties (conductivity, specific heat, and diffusivity) of asphaltic concrete. The thermal properties of six laboratory prepared asphaltic concrete mixes at three asphalt contents were determined. As a result of testing four or five replicate samples of each

DD FORM 1 JAN 73 1473 EDITION OF 1 NOV 65 IS OBSOLETE

UNCLASSIFIED

SECURITY CLASSIFICATION OF THIS PAGE (When Data Entered)

20. ABSTRACT

of the eighteen mix combinations, it was concluded that average values of specific heat and diffusivity, independent of asphalt content but dependent aggregate gradation and mineralogy, could be used. Conductivity varied with asphalt content as well as aggregate type and gradation.

A parameter study using the transient heat transfer model which employed radiant and convection heating of the pavement surface and conduction through the asphaltic concrete indicated that: without exceeding the flash point of asphaltic concrete, it typically takes a field heater 25-35 minutes to heat the pavement at a depth of 25 mm to a temperature sufficient for easy removal (this was verified by field tests); combined convection-thermal radiation heating is more efficient than radiant heating, and; the best surface heating strategy is to operate the heater at a temperature such that the pavement surface reaches its maximum allowable temperature just as the desired temperature is reached at the prescribed removal depth without using insulation periods (soaking) between heat applications.

TABLE OF CONTENTS

TABLE OF CONTENTS (continued)

TABLE OF CONTENTS (continued)

TABLE OF CONTENTS (continued)

LIST OF TABLES

LIST OF FIGURES

LIST OF FIGURES (continued)

LIST OF FIGURES (continued)

APPENDIXES

ABBREVIATIONS AND SYMBOLS

Symbol	Description (SI Units)
A	radiation-conduction parameter
Bi	Biot number
°C	degrees Celsius
C_i^*	a set of constants
ERFC	error function
F_o	$= \alpha t/L^2$, Fourier Number, dimensionless time
J	Joule
°K	degrees Kelvin
L	thickness of sample, thickness of pavement (m)
L_c	thickness of copper disk (m)
M	number of nodes
Mg	megagram
Q	heat flux (J)
Ref.	reference
T	$= T^*/T_{REM}$, dimensionless pavement temperature
T*	pavement temperature (°K)
T_b	temperature at bottom of sample (°C)
T_f	final temperature of calorimeter and sample (°C)
T_H	$= T_H^*/T_{REM}^*$, dimensionless heater temperature
T_H^*	heater surface temperature (°K)
T_i	initial temperature of sample (°C), initial temperature (°K)
T_{ic}	initial temperature of calorimeter (°C)
T_R	$= T_R^*/T_{REM}^*$, dimensionless reference temperature for convection

ABBREVIATIONS AND SYMBOLS (continued)

Symbol	Description (SI Units)
T_R^*	reference temperature for convective heat transfer (°K)
T_{REM}^*	temperature to which pavement must be heated (=363°K) at depth x_{REM}^* at which it is to be removed
T_{soil}^*	temperature at bottom surface of pavement (°K)
$T_{SURFACE}$	dimensionless temperature at pavement surface
T_t	temperature at top of sample (°C)
$(T_1^*)_{MAX}$	maximum allowable pavement temperature, flash point of asphalt, (°K)
$(T_1)_{MAX}$	dimensionless maximum allowable pavement temperature
T_s	surface temperature (°K)
c	specific heat capacity (J/kg°C)
cm	centimeter
c_v	coefficient of consolidation (m^2/s)
dt	time increment (s)
h	unit-surface conductance (w/m°C)
h_c	convection heat transfer coefficient
k	thermal conductivity (w/m°C)
kg	kilogram
m	meter
s	seconds
t	$= \alpha t^*/L^2$, dimensionless time
t^*	time (s)
t_f	final time when $T_b = T_t$ (s)
t_{INSUL}	$= t_{INSUL}^* \alpha/L^2$, dimensionless insulation time
t_{INSUL}^*	time at which pavement surface is insulated after heating (s)

ABBREVIATIONS AND SYMBOLS (continued)

Symbol	Description (SI Units)
x	$= x^*/L$, dimensionless depth
x^*	spatial coordinate in the pavement
x_{REM}	$= x^*_{REM}/L$, dimensionless removal depth
x^*_{REM}	removal depth (m)
w	watt
α	thermal diffusivity (w/m^oC)
γ	radiation heat transfer modulus
Δx^*	distance between adjacent interior nodes (m)
ε_H	emissivity of heater surface
ε_s	emissivity of upper surface of pavement
υ	count parameter
ρ	density (Mg/m^3)
σ	Stefan Boltzman constant (5.6697×10^{-8} w/m^2 $^oK^4$), also used to denote property group ratio in Appendix II-A

INTRODUCTION

With the increasing cost of asphalt over the past decade, it has become more economically attractive for agencies such as the U. S. Air Force to recycle existing airfield pavements instead of overlaying them with new asphaltic concrete pavement. Several recycling methods are available, including some that apply heat to the surface of the pavement thereby increasing the temperature of the top portion of the pavement which decreases its shear strength and thus facilitates easier removal. The material is then either taken to a batch plant or recycled in-place. Additional asphalt, rejuvenators, or virgin materials are added before the reworked asphaltic concrete is laid down and compacted.

During the past several decades asphaltic concrete pavements have been recycled or improved using heater planer and heater scarifier techniques with little knowledge of the temporal and spatial temperature profile created during the process. This information is essential if such methods are to be optimized with respect to constraints on the maximum allowable temperature induced in the asphaltic concrete and the energy (usually fossil fuel) consumed during the process.

Few published studies have been conducted on the temporal-spatial temperature profiles resulting from the pavement heating process, and the literature contains little documented information on the thermal properties of asphaltic concrete pavement. The heating process must produce pavement temperatures that fall within certain constraints. Pavement temperature limits of interest are: (1) the temperature at the surface must be less than the flash point of asphalt and; (2) the temperature at the depth of removal must be sufficiently high for easy removal. A mathematical thermal model of asphaltic concrete pavement is necessary to predict the temporal-spatial temperature profiles that result from the heating process. The impetus for studying asphaltic pavement thermal pro-

perties stems from the lack of studies concerning how the thermal properties of asphaltic pavement vary with different mix designs and aggregate types. The objectives of this project were to model the heating process and study the thermal properties of asphaltic pavements. Four steps were taken to achieve these objectives:

1) Obtain in the laboratory an expected range of asphaltic pavement thermal properties and determine how the thermal properties vary with asphalt content, gradation, and aggregate type (Part I of this report).

2) Develop a heat transfer model and computer code specifically for the type of heating process encountered in in-place surface recycling methods (Part II of this report).

3) Validate the model by comparing the temporal-spatial temperature data observed in field tests to those predicted data determined from the computer program (Part III of this report).

4) Conduct a parametric study of the heating process to determined how sensitive the process is to the variation of thermal and physical parameters (Part IV of this report).

Part V of this report is a summary of important results and findings of the study.

PART I

THERMAL PROPERTIES OF SOME ASPHALTIC PAVEMENTS AND MIXES

CHAPTER I-A INTRODUCTION

Although thermal properties of asphalt and asphaltic concrete have been reported in the literature for at least 55 years (14), much of the data is undocumented in that variables that can be expected to influence the thermal properties such as asphalt content, density, and aggregate type and gradation were not published. Prediction of in situ temporal-spatial temperature profiles created by surface heating requires that thermal properties of the asphaltic concrete be known. Furthermore, the expected range of these properties for a wide variety of asphaltic concrete mixes would also be valuable.

This part of the report reviews the literature relevant to pavement thermal properties, describes an apparatus and procedure by which thermal properties were measured, and reports the results of experiments carried out on six aggregate mixes prepared in the laboratory and on field samples taken from Myrtle Beach Air Force Base and Loring Air Force Base.

CHAPTER I-B REVIEW OF THE LITERATURE

A review of the literature concerning asphaltic pavement thermal properties revealed few studies conducted solely on the thermal properties of asphaltic pavements. However, three allied areas were found that use the asphaltic pavements thermal properties as parameters in temperature-predicting thermal models. The allied areas, which are reviewed below, are (1) effects of climate on pavement temperatures, (2) asphaltic pavement cooling rates, and (3) thermal models of in-place surface recycling.

Effects of Climate on Pavement Temperatures

The effects of climate on pavement temperatures can be subdivided into frost

penetration studies and pavement temperature studies.

Frost Penetration Research. In cold climates, the deteriorating effects of frost action under pavements become increasingly important as maintenance costs, traffic frequency, and wheel loadings increase. Research has been conducted to offer a better understanding of the processes involved in frost penetration.

Carlson and Kersten (7) applied heat transfer theory to the pavement and soil subgrade to develop a model used to predict frost penetration below asphaltic pavement. Input parameters include the thermal conductivity of the pavement, the latent heat of fusion of water, and the surface freezing index of the pavement. The surface freezing index is defined as the time-average difference in temperature between the ground surface and the freezing point during the freezing period. The value of the thermal conductivity (a measure of the ease which heat energy will flow through a medium) used by Carlson and Kersten was 1.44 w/m°C (obtained from thermal property tests made at the University of Minnesota in 1948).

Aldrich (2) followed up on Carlson and Kersten's work and developed an improved method of calculating frost penetration. His method includes the effects of specific heat (the amount of energy necessary to change the temperature of a unit volume of a substance by one degree). Aldrich used a thermal conductivity value of 1.45 w/m°C in his analysis.

Dempsey and Thompson (15) used a one-dimensional transient heat flow model to predict temperature with depth in conjunction with highway frost studies. They reported that the accuracy of the temperatures predicted by their model depended more on the quality of the input data than the numerical method of calculation. They also pointed out the importance of accurately defining the boundary condition at the pavement surface, because it is this input which is the major factor contributing to the heat transfer process.

Minimum and Maximum Pavement Temperatures Due to Weather. Because the strength and stability of an asphaltic pavement are related to its temperature, research has been conducted to determine the minimum and maximum temperatures of pavement in natural field conditions. Studies indicate that given the thermal properties of the asphaltic concrete pavement and the history of the weather in the area, pavement temperatures can be predicted by heat transfer models.

Barber (3) used the diffusion equation to predict in-situ pavement temperatures. Weather parameters involved in the diffusion equation include wind speed, precipitation, air temperature, and solar radiation. Barber averaged several published values of asphaltic pavement thermal conductivity to obtain 1.21 w/m°C.

Southgate and Deen (25) analyzed the pavement temperatures recorded at various depths in a 0.3 m thick asphaltic pavement. They found that a fourth order polynomial fit the temperature as a function of depth data. No attempts were made to analyze the data using heat transfer theory. Rumney and Jimenez (23) recorded pavement temperatures with depth for one year in Arizona. Using the temperature data, they empirically derived curves which could be used to estimate the pavement temperature at any depth knowing the maximum air temperature and average daily radiation rates.

Straub, Schenk, and Przybycien (28) used weather data and pavement temperature data gathered from a test site for a period of one year to develop a heat transfer model which could predict pavement temperatures. Their forward difference, one-dimensional transient heat flow model used air temperature and solar radiation data and the thermal and physical properties of a specific locale to predict maximum and minimum pavement temperatures. They found that the pavements had a substantial temperature gradient and no one temperature was representative of that of the pavement. They used Barber's averaged value for thermal conductivity of 1.21 w/m°C.

Christison and Henderson (11) also used a finite difference approximation to predict temperatures in asphaltic concrete pavement. They assumed a value of 1.45 w/m°C for the thermal conductivity of asphaltic concrete and stated that "the thermal conductivity (k) and specific heat (c) of asphaltic concrete paving mixtures vary within narrow limits and for practical purposes can be considered independent." However, they did not indicate the basis for this statement nor their source for the assumed thermal properties.

Cooling Rates of Hot-Laid Asphaltic Pavements

During paving operations, a hot-laid asphaltic pavement must be compacted while the pavement is cool enough to have the stability needed to support a roller or other compacting device and warm enough to achieve a specified density with a minimum amount of compactive effort. Compaction attempts made when the pavement is too cool result in either more compactive effort needed to reach a specified density or the inability to reach the specified density at all. Strength and durability problems have been associated with improper compaction of asphaltic pavements.

The amount of time available for compaction depends upon the cooling rate of the hot asphalt mat. The cooling rate depends upon many thermal and physical properties of the asphaltic pavement, the temperature of the hot pavement mix, the temperature of the surrounding air, the temperature of the existing pavement, the wind speed, and the amount of solar radiation striking the pavement surface.

Corlew and Dickson (12) considered all of these factors in their one-dimensional transient heat flow equation to predict the temporal-spatial temperature field within a cooling layer of freshly placed hot-mix asphaltic concrete. The pertinent weather data and the temperature of the hot-laid asphaltic pavement were measured at the site, while the thermal and physical properties were assumed using values reported in the literature as a guide. Using a finite dif-

ference technique, they were able to predict temperatures in a six centimeter layer of asphaltic concrete within seven degrees centigrade of measured temperatures in the range at which asphaltic concrete is compacted (greater than 90°C).

With the impetus of extending the paving season into the cooler weather seasons, Frenzel et al. (16) developed a computer analysis to study the effect of preheating an existing asphaltic layer on the cooling of an overlay put down over the preheated base. They found, analytically, that preheating the base increased the cooling down period in thin overlays sufficiently to allow a compaction window long enough to make paving in early spring and late fall feasible. Later Corlew and Dickson (13) combined the base preheat model developed by Frenzel et al. and the previously described cooling model developed by Corlew and Dickson (12) to predict the temporal-spatial temperature field of an asphaltic concrete layer over a preheated base in a bench scale laboratory test. A sample with a 10 cm diameter base was heated by a direct-fired propane heater. Agreement between predicted and measured temperatures was considered to be good. Assumed thermal properties of asphaltic concrete were used in the analysis.

Another study of asphaltic pavement cooling rates was conducted by Wolfe and Colony (30) at the University of Toledo. They developed a computer simulation method to predict cooling rates using the same weather data and material property variables as Corlew and Dickson. The thermal properties of asphaltic pavement were taken from published values. Later Wolfe, Heath, and Colony (31) continued the research and further verified the computer model. In this study, the thermal conductivity of seven different mix designs of ashphaltic concrete was measured using a guarded hot-plate thermal conductivity instrument as specified in ASTM C-177. Thermal conductivity values ranged from 0.58 to 1.01 w/m°C. The specific heat of the seven mixes was also measured and found to range from 878 to 962 J/kg°C.

Thermal Models of In-Place Surface Recycling

In-place surface recycling of asphaltic pavements involves reworking the surface to a depth of approximately 2.5 centimeters using a heater scarifier. This operation may involve the addition of new materials (or recycled materials) including aggregates, modifiers, and/or asphalt cement. The reworked material is then compacted, and sometimes a seal coat is applied. Typically, heater planers and heater scarifiers developed by contractors use propane as a fuel to fire a grid of torches. The grid is on the order of 3 m wide and 5 m or more long and is attached to a self-propelled machine. The torch grid is covered on the top and sides to diminish heat loss. Typically, the machine advances at the rate of about 4.5 m/min giving a heat exposure time on the order of one minute. To prevent combustion of the pavement, the temperature at the pavement surface should be limited to about 230°C. Contractors claim that under these conditions, temperatures at a depth of about 2.5 cm in the asphaltic concrete are sufficiently high to allow easy scarification and/or removal of pavement to this depth. To increase the depth of influence of the heat source, a technique termed "soaking" is sometimes used. This method involves heating the surface as described above and then insulating the pavement surface. This, in principle, allows the heat to "soak" in thus producing greater heat penetration without exceeding the 230°C surface temperature requirement.

One of the few published studies undertaken in the area of heat transfer in asphaltic concrete recycling seems to refute many of the contractor claims mentioned above. Carmichael, Boyer, and Hokanson (8) modeled an asphaltic concrete pavement as a semi-infinite solid and used a forward difference numerical method to solve the governing differential equation. They assumed that the thermal conductivity, density, and specific heat of asphaltic concrete were independent of temperature and did not vary from point to point. The authors, using realistic source and initial pavement temperatures along with realistic pavement

parameters, found that even with an induced surface temperature of 540°C and a 30 second exposure time, there was no increase in temperature of the pavement at a depth of 1.6cm (See Figure I-1).

It was also shown that for surface temperatures between 200 and 300°C, the temperature of the pavement hardly changed from its initial condition. This is illustrated in Figure I-2. Although it can be argued that this study used restrictive assumptions, particularly with respect to the parameters used, and that the model has not been verified, it does indicate that the current development of pavement heating techniques and the present use of heater planer and heater scarifier equipment ignores some of the basic constraints of asphaltic concrete recycling--namely that to obtain sufficient temperature increases at depth it appears that the surface must be heated to a temperature greatly in excess of that at which damage to the pavement can occur. Carmichael et al. pointed out that it is important that the full depth of pavement be properly heated before scarifying because "cold asphalts do not bond well and any attempt to force cold, asphalt coated aggregates together after scarifying them by tensile failure can only lead to future problems."

Thermal Properties of Asphaltic Concrete and Its Components

Much of the literature cited above used assumed values of the thermal properties of asphaltic concrete. However, as shown in Tables I-1 and I-2 measured values of conductivity and specific heat of asphalt and asphaltic concrete as well as minerals and rocks commonly used as asphaltic concrete aggregate are available. Reported values of thermal conductivity range from 0.74 to 2.88 w/m°C for asphaltic concrete and from 0.14 to 0.17 w/m°C for "pure asphalt." Diffusivity values ranging from $5.8*10^{-7}$ to $14.4*10^{-7}$ m^2/s have been reported. The range of reported values of specific heat, c, is 879 to 963 J/kg°C for asphaltic concrete.

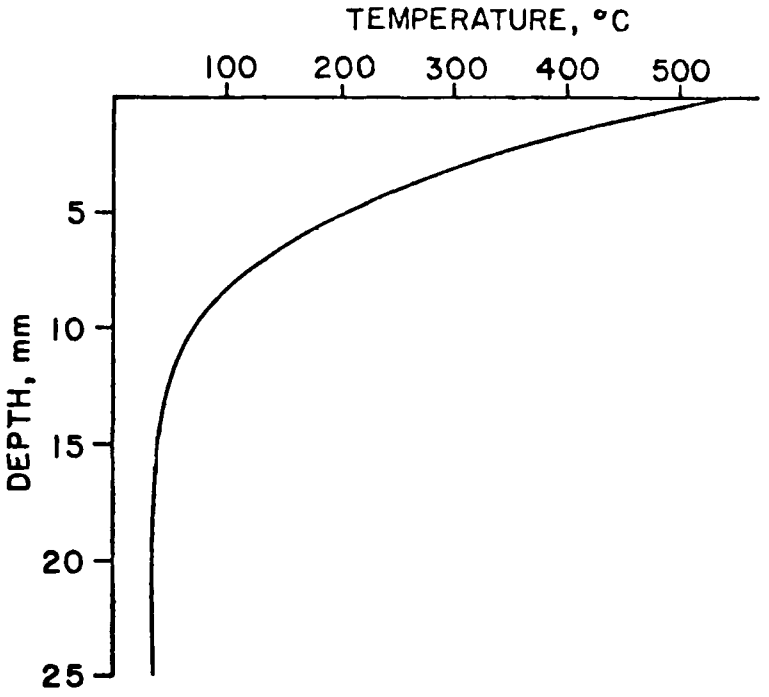

Figure I-1. Pavement Temperature vs. Depth for 1000°C Source and 30 s Exposure Time (8).

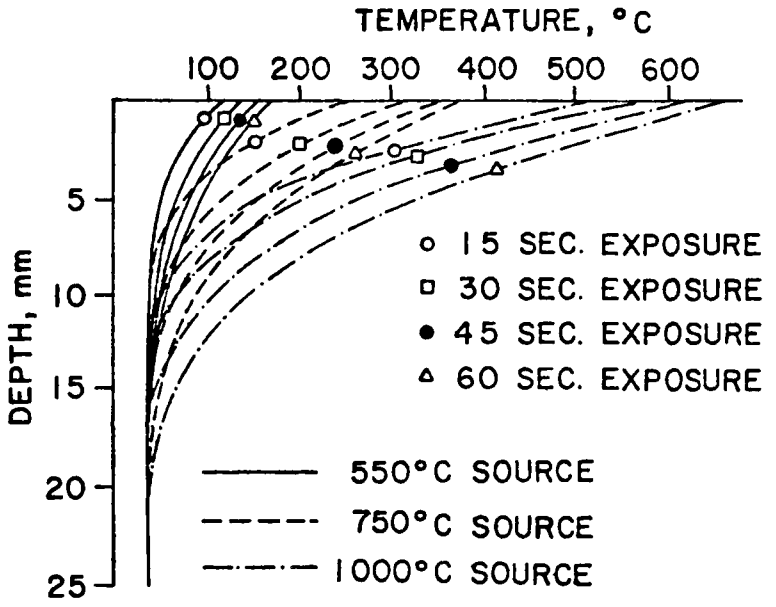

Figure I-2. Pavement Temperature vs. Depth as a Function of Source Temperature and Exposure Time (8).

Table I-1. Some Published Thermal Properties of Asphaltic Concrete.

Property				
k(w/m°C)	$\alpha(m^2/s)$	$\rho c(J/m^3°C)$	Ref.	Comment
1.454		$1.41*10^6$	32	
2.88	$14.4*10^{-7}$	$2.00*10^6$	19	18°C, Dry
2.28	$11.5*10^{-7}$	$1.97*10^6$	19	38°C, Dry
1.21	$5.75*10^{-7}$		8	Obtained from the Asphalt Institute
0.74-0.76			6	20°C-56°C
0.167-0.172			14	"Pure Asphalt" 20°C-80°C
0.65-0.75			14	Asphalt used in street paving
1.37-1.75	$7-8*10^{-7}$	c=879-963	31	
		c=879	14	100°C
0.80	$10*10^{-7}$		26	
1.21		c=920	3	
1.2	$5.9*10^{-7}$	$2.07*10^6$ c=921	12, 13	80°C-149°C
1.5			2	
0.82-2.32			22	
0.14-0.17		c=1528-2561	24	Asphaltic Bitumen free of paraffin 0°C-300°C

Table I-2. Some Published Thermal Properties of Asphaltic Concrete Aggregate.

Property				
k(w/m°C)	α(m^2/s)	c(J/kg°C)	Ref.	Comment
		790; 1000	18	Calcite 0°C; 200°C
		930	18	Dolomite 60°C
		698; 969	18	Quartz 0°C; 200°C
		1000	18	Limestone 58°C
		680	18	Limestone, mean of 3 at 50°C
		830	18	Limestone, mean of 10 at 65°C
		700; 970	18	Quartzite 0°C; 200°C
		650; 950	18	Granite 0°C; 200°C
		850; 1040	18	Basalt 0°C; 200°C
		930	18	Sandstone 59°C
		700; 870	18	Diabase 0°C; 200°C
		710; 1000	18	Slate 0°C; 200°C
1.82			17	Average value for sand and gravel
2.86			5	Calcite 100°C
6.45			5	Quartz 100°C
2.37			5	Granite 100°C
1.8-2.2			5	Basalt
2.0-3.4			5	"Compact" Limestone
1.1-2.2			5	"Porous" Limestone
1.8			5	Slate 100°C
3.99			5	Dolomite 100°C
5.2			5	Quartzite 100°C
1.8-2.8			5	Granite-Gneiss
2.7			5	Granite-Schist
2.6-4.5			5	Hard Sandstone
2.1			5	Diabase 100°C
1.1	$2*10^{-7}$		5	Quartz Sand
	$9*10^{-7}$		5	Sandy Soil

The predominant component of asphaltic concrete is aggregate. The thermal properties of the particular aggregate used in a given asphaltic concrete can be expected to have an important effect on the properties of the mix. The literature indicates that common minerals and rocks used as aggregate can have conductivities which range from about 1 to 8 w/m°C (Table I-2); the range of c can be expected to be on the order of 650 to 1040 J/kg°C. Wolfe et al. (31) suggest 920 J/kg°C as an average value based on their tests. Limited data on the diffusivity of the fine aggregate component indicate α is on the order of 2 to $9*10^{-7}$ m^2/s.

Thermal properties of asphaltic concrete reported in the literature do not indicate the mineralogy, grain size distribution, or density of the aggregate used in the mix; nor have the fraction of asphalt of density of mix been reported. Certainly these factors can be expected to influence the resulting thermal porperties of asphaltic concrete and thus the transfer of heat through and asphaltic concrete pavement.

CHAPTER I-C MEASUREMENT OF THERMAL PROPERTIES

Properties Required

The transient heat conduction process in a solid body is described by the energy balance equation,

Rate of Heat In-Flow	+	Rate of Heat Generation by Internal Sources	=	Rate of Heat Out-Flow	+	Rate of Change In Internal Energy	(1)

Without any internal heat generation in the solid, this equation can be written algebraically in rectangular coordinates as

$$\frac{\partial}{\partial x}\left(k_x \frac{\partial T}{\partial x}\right) + \frac{\partial}{\partial y}\left(k_y \frac{\partial T}{\partial y}\right) + \frac{\partial}{\partial z}\left(k_z \frac{\partial T}{\partial z}\right) = \rho\, c\, \frac{\partial T}{\partial t} \qquad (2)$$

where x, y, z are spatial coordinates (m)

T = temperature (°C)

k = thermal conductivity (w/m°C)

ρ = density (kg/m^3)

c = specific heat (J/kg°C)

t = time (s)

Field heaters are typically about 5 m long by 3 m wide. Since these dimensions are much greater than the thickness of the pavement, the conduction heat transfer can be assumed to be one-dimensional. Therefore, with the z-direction being vertical,

$$\frac{\partial T}{\partial x} = \frac{\partial T}{\partial y} \cong 0 \tag{3}$$

and Equation (2) becomes,

$$k_z \frac{\partial^2 T}{\partial z^2} = \rho\ c\ \frac{\partial T}{\partial t} \tag{4}$$

by defining the thermal diffusivity, α, as a measure of the rate at which a temperature change spreads through a solid or

$$\alpha = k\ /\ \rho\ c \tag{5}$$

and $k_z = k$, Equation (4) reduces to

$$\alpha \frac{\partial^2 T}{\partial z^2} = \rho\ c\ \frac{\partial T}{\partial t} \tag{6}$$

This equation is the one-dimensional transient heat conduction equation, and in similar forms can be used in other transient energy flow situations. One example of transient energy flow familiar to geotechnical engineers is

Terzaghi's one-dimensional consolidation theory. In Equation (6) the thermal diffusivity, α, is analogous to the coefficient of consolidation, c_v, and is an indicator of the rate of temperature (pore water pressure) dissipation within a solid (soil stratum).

Equation (6) can be written in finite difference form so that the temporal-spatial temperature field can be calculated for a pavement system having several layers, provided the initial and boundary conditions and the thermal properties, ρ, c, and k (or α) are known for each layer. The mathematics and computer coding for predicting the temperature profile with time for a layered asphaltic concrete pavement system for a known heat input are routine provided the asphaltic concrete thermal properties are known. This chapter describes the laboratory apparatus and procedure used to measure three thermal properties: thermal diffusivity, thermal conductivity, and specific heat.

Apparatus and Procedure

Many methods of measuring thermal properties have been used over the years. Most methods are for measuring a single property at a time, and they usually utilize closed form solutions for steady-state and transient cases. The method chosen for this research has some special advantages.

Beck and Al-Araji (4) developed a method of thermal property measurement capable of measuring the thermal conductivity, thermal diffusivity, and specific heat in a single test cycle. The thermal conductivity is considered constant in this method. The method requires the integration of some temperature data which can be easily accomplished with a microcomputer. The test procedure is quick, simple, and requires minimal equipment.

In concept, this method involves applying a given amount of heat, Q, to the top surface of a flat specimen of known thickness, and then measuring temperatures at the top (T_t) and bottom (T_b) surfaces of the insulated specimen over

time (see Figure I-3). The heat is applied with a calorimeter--an insulated copper disk of well known physical and thermal properties and at a uniform temperature different than that of the specimen (Figure I-3a). When the calorimeter and specimen are brought into contact, the top of the specimen will immediately assume the temperature of the calorimeter, and then will begin to cool as the heat is transferred to the specimen (Figure I-3C.). At the same time, the temperature at the bottom of the specimen will begin to rise. Provided there are no heat losses, the thermal energy will continue to travel into the specimen until the specimen and the calorimeter reach the same temperature, called T_f which occurs at time = t_f. Figure I-4 is an illustration of how the temperatures T_t and T_b are a function of time and how at time = t_f, $T_t = T_b = T_f$.

Beck and Al-Araji (4) showed that for flat-plate geometry, the thermal properties could be calculated from the following equations:

$$\alpha = \frac{L^2(T_f - T_i)}{\int_{t=0}^{t=t_f} (T_t - T_b)\, dt} \tag{7}$$

$$k = \frac{LQ}{\int_{t=0}^{t=t_f} (T_t - T_b)\, dt} \tag{8}$$

$$c = \frac{Q}{\rho L (T_f - T_i)} \tag{9}$$

where α = thermal diffusivity

L = thickness of asphaltic pavement disk

T_f = final pavement temperature

T_i = initial pavement temperature

Figure 3a. Calorimeter.

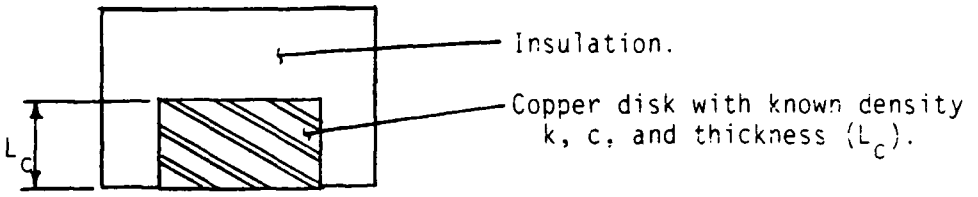

Figure 3b. Sample holder.

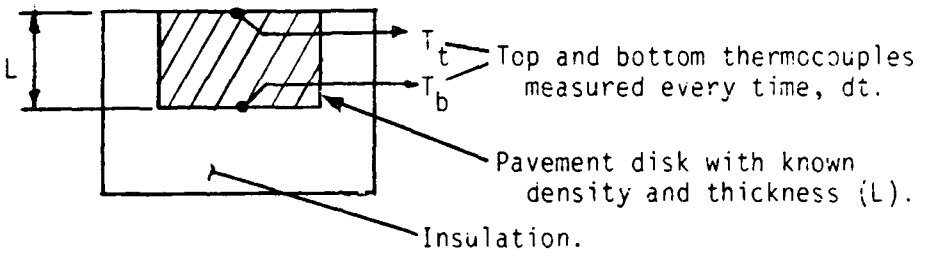

Figure 3c. Calorimeter in place atop the sample holder.

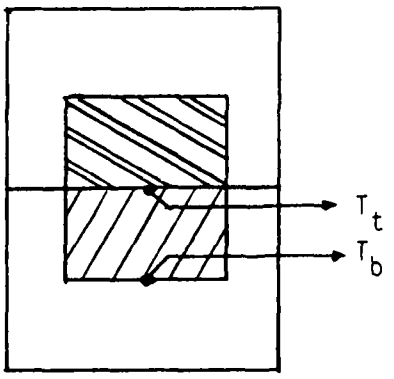

Figure I-3 (a, b, and c). Schematic of Calorimeter, Sample Holder and How the Two Fit Together.

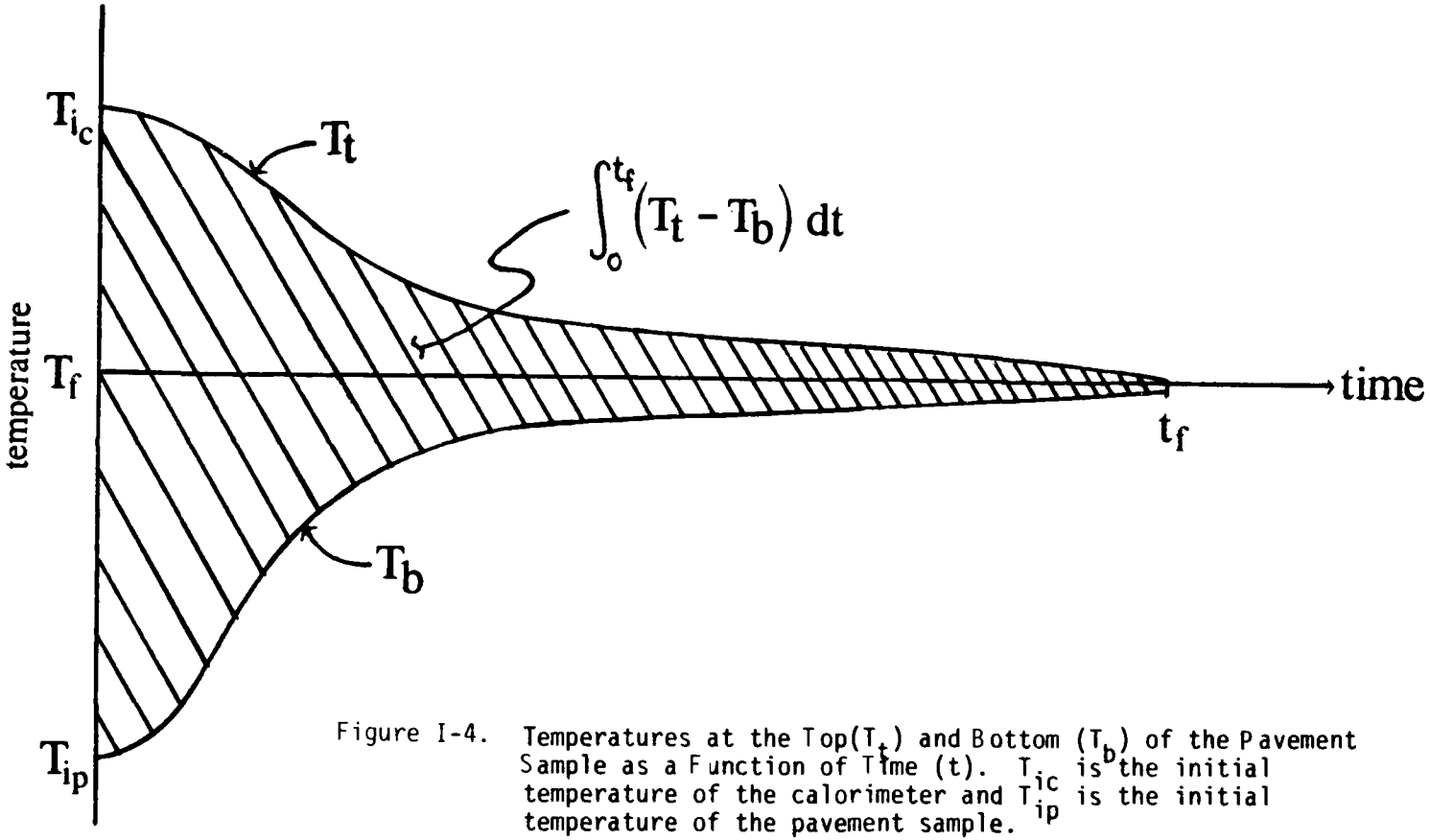

Figure I-4. Temperatures at the Top(T_t) and Bottom (T_b) of the Pavement Sample as a Function of Time (t). T_{ic} is the initial temperature of the calorimeter and T_{ip} is the initial temperature of the pavement sample.

T_t, T_b = temperature at the top and bottom of the pavement sample, respectively, at time t

dt = specified time increment (15 seconds)

Q = amount of heat transferred from the calorimeter to the asphaltic pavement sample

c = specific heat

ρ = previously (independently) measured density of the asphaltic pavement sample (ASTM D1188)

k = thermal conductivity of the asphaltic pavement sample

To find Q, the amount of heat transferred from the calorimeter to the sample, note that all surfaces are insulated when the calorimeter and sample are brought into contact (see Figure I-3c.). Therefore, all the thermal energy available in the calorimeter will be transferred to the pavement sample until the calorimeter and the sample reach the same temperature (see Figure I-4). The amount of heat transferred, Q, can be calculated using the following equation:

$$Q = \rho_c c_c L_c (T_i - T_f)_c \qquad (10)$$

where the subscript $_c$ refers to the calorimeter and c_c refers to the specific heat of the calorimeter at the average temperature. The procedure can be carried out in five steps:

1. Bring into contact an insulated calorimeter of known thickness, temperature, and thermal properties with an insulated specimen of known thickness, temperature, and density.
2. Measure the temperature at the top and the bottom of the specimen from the time of contact (time = 0) until all the thermal energy available in the calorimeter is transferred into the specimen (time = t_f when $T_t = T_b = T_f$, see Figure I-4).

3. Evaluate the integral in Equations 6 and 7 by summing the temperature difference, $T_t - T_b$, from time = 0 time = t_f and multiplying this sum by the sampling interval, dt, to get:

$$\int_{t=0}^{t=t_f} (T_t - T_b)\, dt \qquad (11)$$

4. Calculate Q, the amount of heat energy transferred from the calorimeter to the specimen (see Equation 10).
5. Calculate the thermal diffusivity (α), thermal conductivity (k), and specific heat (c) using Equations 7, 8, and 9, respectively.

The test apparatus used in this study consists of an insulated copper calorimeter, a calorimeter heater with heater controller, an insulated pavement sample holder, and a temperature measuring system with five copper-constantan thermocouples. The calorimeter (shown in Figure I-5) is composed of a pure copper disk (having accurately known thermal properties) 10.16 cm in diameter by 3.18 cm thick surrounded by 1.2 cm of firebrick insulation on the perimeter and on one face. An oak wood holder surrounds the insulation. A single thermocouple placed in the center of the copper disk is used to monitor and control the temperature of the calorimeter with the heater. During the calorimeter heating process, the heater controller regulates the power to the calorimeter heater (Figure I-6) in such a way as to bring the calorimeter to a constant prescribed temperature.

The 10.16 cm diameter asphaltic concrete pavement sample is held in a holder which insulates the perimeter and the bottom surface of the sample (Figure I-7). Two copper-constantan thermocouples are placed on both the top and bottom surfaces of the pavement sample with the top thermocouples recessed in shallow grooves sawn in the top of the pavement sample. These thermocouples

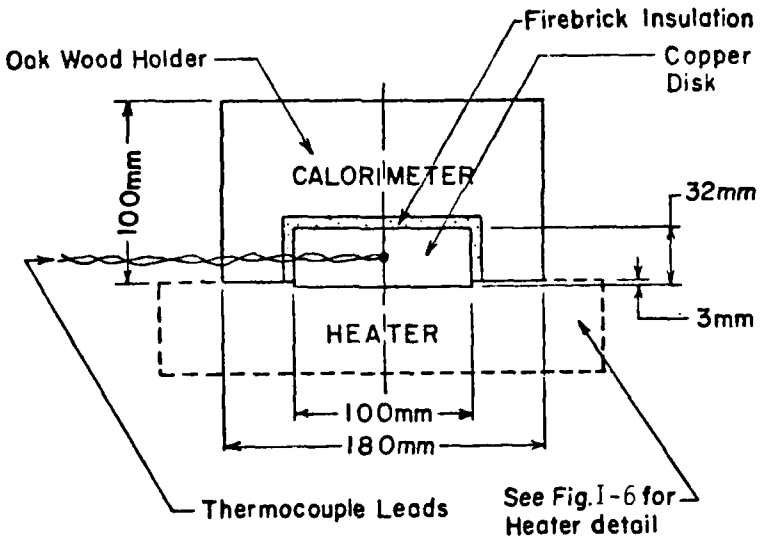

Figure I-5. Calorimeter.

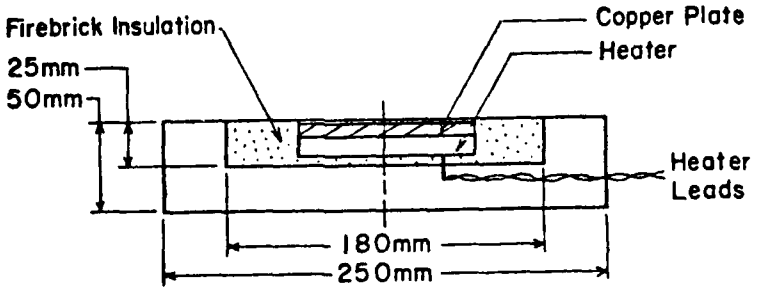

Figure I-6. Calorimeter Heater.

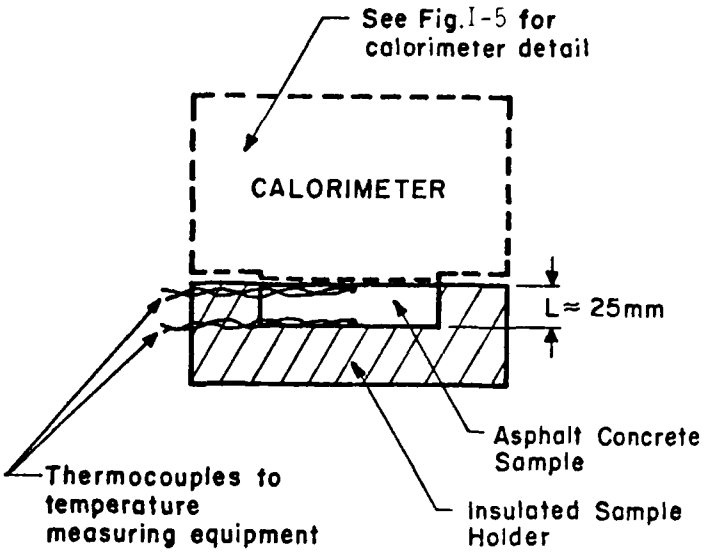

Figure I-7. Calorimeter in Contact with Sample After Being Heated.

lead to a temperature measurement system made by Interactive Microware (see Appendix I-A and Ref. 29) where the two top thermocouples are averaged giving T_t, and the two bottom thermocouples are averaged giving T_b at each specified time interval, dt.

The TEMPSENSE Temperature Monitoring System (29) in conjunction with an Apple II+ computer has user-controlled software which facilitates the calibration of the thermocouples and allows the operator to select the sampling frequency and the total duration of the temperature measurements. The time of each measurement is displayed on the screen along with the temperature of each thermocouple measured. The data are automatically stored on a floppy disk for later analysis.

To run a test, the calorimeter is placed on the heater, and the desired temperature of the calorimeter is set on the heater controller. The thickness, L, of the previously prepared pavement sample disk is measured, and the bottom thermocouples are fastened onto the center of the bottom surface of the sample with a viscid, high-conductivity silicon paste (Omegatherm 201 from Omega Engineering, Inc.) and masking tape. The sample is then placed in the insulated holder and a thin film of the silicon paste is applied to the top surface. The top thermocouples are then laid into the recessing grooves, and an insulating collar is placed over the sample and thermocouples. When the calorimeter reaches the prescribed temperature, the pavement sample is ready for contact with the heated calorimeter. The prescribed calorimeter temperature (145°C) was chosen to be approximately halfway between the minimum desirable pavement temperature for compaction (90°C) and the typical flash point temperature of asphalt cement (about 230°C).

The TEMPSENSE program prompts for the desired sampling interval, the duration of the temperature measurements, and the file name of the data to be gathered. A fifteen second sampling interval was chosen to provide reasonable

precision, and it was found that test durations of around 30 minutes (t_f = 30 min.) were sufficient for $T_t = T_b$. The temperature measurements are started, and two or three measurements are recorded to obtain the initial temperature of the sample (T_i). Then the calorimeter is removed from the heater and placed on the top of the sample. Measurements are made every 15 seconds until the temperature at the bottom of the pavement sample becomes equal or very close to the temperature at the top of the pavement sample, i.e. until t_f has elapsed. The temperature data is then stored on a floppy disk, and the calorimeter is removed and placed back on the heater in preparation for the next test.

The integral expression in the denominator of Equations 7 and 8 is approximated by summing the temperature difference between the top and bottom of the sample for each dt increment of time (dt = 15 seconds) over the duration of the test (see Equation 11). The duration of the test is defined as the time that elapses from the time the calorimeter and sample first contact (time = 0) to the time an equilibrium temperature is reached throughout the calorimeter and sample (time = t_f and $T_t = T_b$).

By using the collected data and the previously measured density of the pavement sample, Equations 7, 8, and 9 are solved for the thermal diffusivity, thermal conductivity, and the specific heat, respectively.

CHAPTER I-D PREPARATION OF LABORATORY ASPHALTIC CONCRETE SAMPLES

This chapter provides a brief description of asphaltic concrete and the variables considered in asphaltic concrete mix design. The reasons for choosing the specific mix designs used in this study are explained, and the designs are then summarized in Table I-3 and Figure I-8.

Typically, hot-laid asphaltic concrete pavements contain approximately 5% by weight asphalt cement and 95% by weight graded aggregate. Each aggregate

Table I-3. Summary of Mix Designs (each prepared with 3.5%, 5.0%, and 6.5% asphalt content).

	Gradations		
Aggregate Type	Dense	Open	Base
Limestone	√	√	√
Granite-Gneiss	√	√	
Expanded Shale	√		

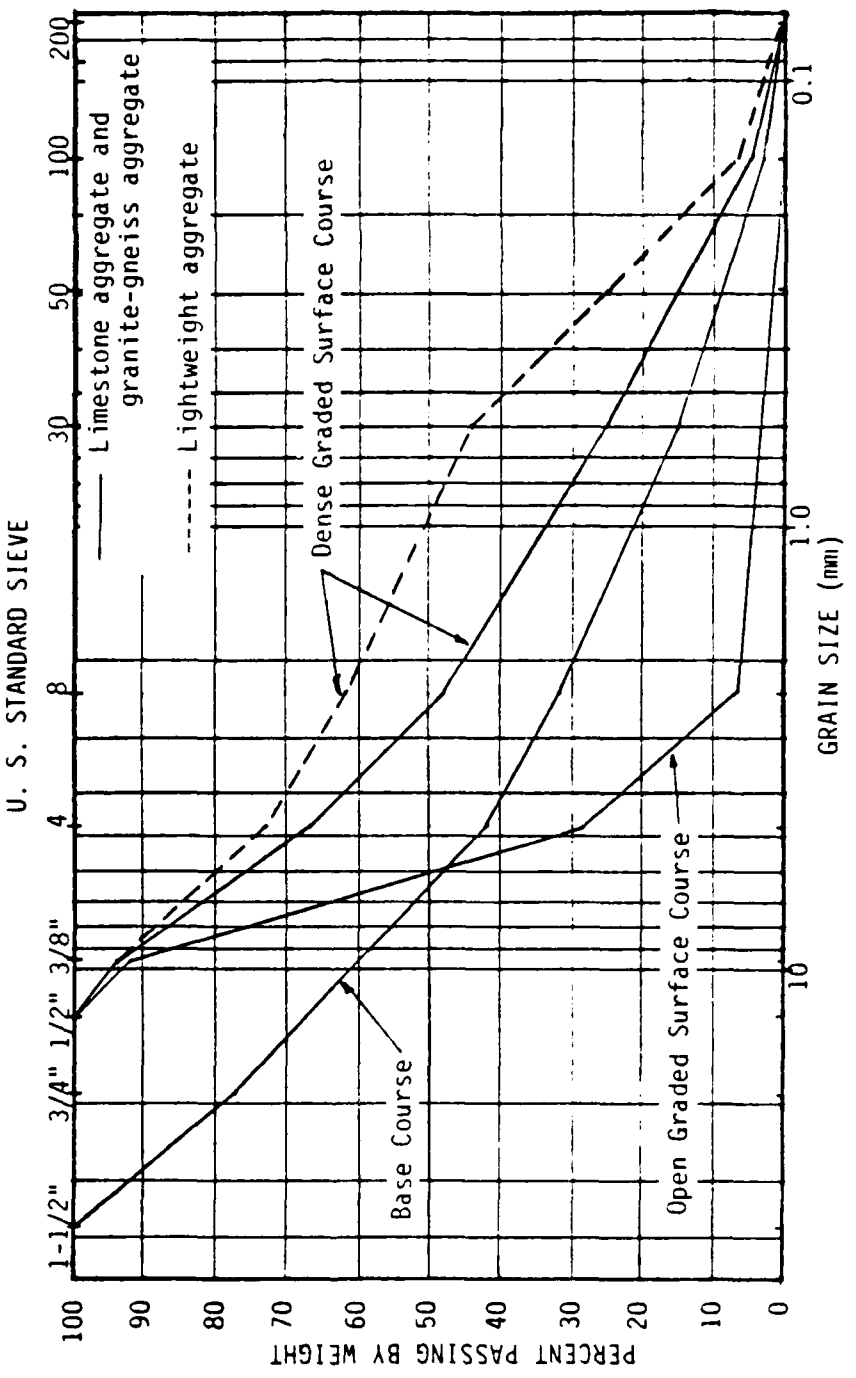

Figure I-8. Grain Size Distributions for the Six Aggregate Mixes.

type and gradation has associated with it a percentage of asphalt cement that provides an optimum mixture of durability, stability, and workablity.

The range of the variables, aggregate type, aggregate gradation, and percent asphalt cement used for this study were chosen for two purposes, (1) to cover a wide range of "typical" pavement mixes, and (2) to study the effects of asphalt content, particle size/shape distribution, aggregate mineralogy, and density on the thermal properties of asphaltic concrete pavement.

The type of aggregate used in an asphaltic concrete pavement, in a given geographical area, depends largely upon what is available in that region. These different types of aggregates, when classified by their specific gravity, are commonly catergorized as lightweight, medium weight, and heavy weight aggregates. Three types of aggregate were used in this research, (1) a lightweight, expanded shale aggregate, (2) a medium weight limestone aggregate, and (3) a medium weight granite-gneiss aggregate.

The aggregate gradation of an asphaltic pavement mix depends mainly upon the function of the mix. Usually, a very dense gradation is desirable for surface and base courses when a waterproof pavement is needed. Sometimes an open graded, porous gradation is used as the surface course to prevent the ponding of water on the surface. Gradations for three types of asphaltic pavements were used in this study: dense graded surface course, dense graded base course, and open graded surface course.

The particle size distributions (by weight) of the asphaltic concrete mixes are shown in Figure I-8. The base course and dense graded surface course mixes were similar except that the base course mix has particle sizes up to 38 mm whereas the largest particles present in the dense graded surface course mix were 12 mm. The open graded surface course mix has the same range of particle sizes as the dense graded surface course mix, but as Figure I-8 illustrates, aggregate size is much more uniform. The dense graded surface course made with

the lightweight aggregate shows a particle size distribution different from the other dense graded surface courses. This is because the curve is based on the percent passing by weight, and the lightweight mix contains a combination of lightweight, expanded shale aggregate and other medium weight aggregates.

The percent of asphalt cement used in a particular aggregate mix varies with the aggregate type and gradation. No attempts were made to optimize the percentage of asphalt cement for the aggregate types and gradations used in this research. Rather, three percentages by weight of asphalt cement were used with each aggregate mix so that the effects of asphalt content on the thermal properties could be studied independently of aggregate type and gradation. Type AC-20 asphalt cement was used in all the mixes.

Asphaltic concrete samples were compacted as specified by the Marshall Method of Mix Design (ASTM D1559). Samples of each mix were prepared at asphalt contents of 3.5%, 5.0%, and 6.5%. The bulk specific gravity (density) of each sample was determined according to ASTM D1188. Pavement disks, about 2.5 cm thick were cut with a diamond saw from the 10.2 cm diameter by nominal 6 cm thick Marshall samples, and thermocouple recessing grooves were sawn into one surface of each disk. The thermal properties of each disk were then obtained by the procedure described previously.

CHAPTER I-E PRESENTATION AND DISCUSSION OF RESULTS

The thermal properties (α, k, and c) were obtained for each asphaltic concrete mix (mixes summarized in Table I-3) using the method described in Chapter I-C. This chapter presents the results of these tests and indicates the variation of thermal properties with aggregate type, aggregate gradation, and asphalt content.

The density-asphalt content relationship for each of the mixes is shown in

Figure I-9. Each point on the curves represents the average of the results of either four or five samples. Thermal properties of each mix were obtained from the disk samples and the results for the thermal conductivity (k), specific heat (c), and thermal diffusivity (α) are shown in Figures I-10, I-11, and I-12, respectively, and in Table I-4. A comparison of Figures I-8 and I-9 indicates that thermal conductivity for the six mixes does not vary systematically with density or asphalt content.

For the dense graded surface course mix with limestone aggregate, the thermal conductivity increased as the asphalt content increased from 3.5% to 5.0%. That the density of the mix increased as well (Figure I-9) indicates that asphalt was replacing air in the mix voids. Since the thermal conductivity of asphalt is greater than that of air, the conductivity increased slightly (by about 4%). As the asphalt content of the mix was increased from 5.0% to 6.5%, the density remained constant. These data suggest that in this range of asphalt content for this mix, asphalt had filled the voids and some of the mineral aggregate itself was being replaced by asphalt. Since the conductivity of asphalt is less than that of limestone (Tables I-1 and I-2), the thermal conductivity of the mix decreased as shown in Figure I-10.

The dense graded surface course mix with granite-gneiss aggregate behaved very similarly to the dense graded surface course mix with limestone aggregate as the asphalt content was increased from 3.5% to 6.5%. The density (Figure I-9) and the thermal conductivity (Figure I-10) both increased as asphalt content changed from 3.5% to 5.0% indicating that the air voids in the mix were being filled with asphalt. From an asphalt content of 5.0% to 6.5%, the density decreased slightly (0.4%) indicating that the asphalt was displacing the mineral aggregate thus decreasing the thermal conductivity of the mix (Figure I-10). The values of the thermal conductivity for the granite-gneiss dense graded surface course mixes were all about 33% lower than that of the limestone dense

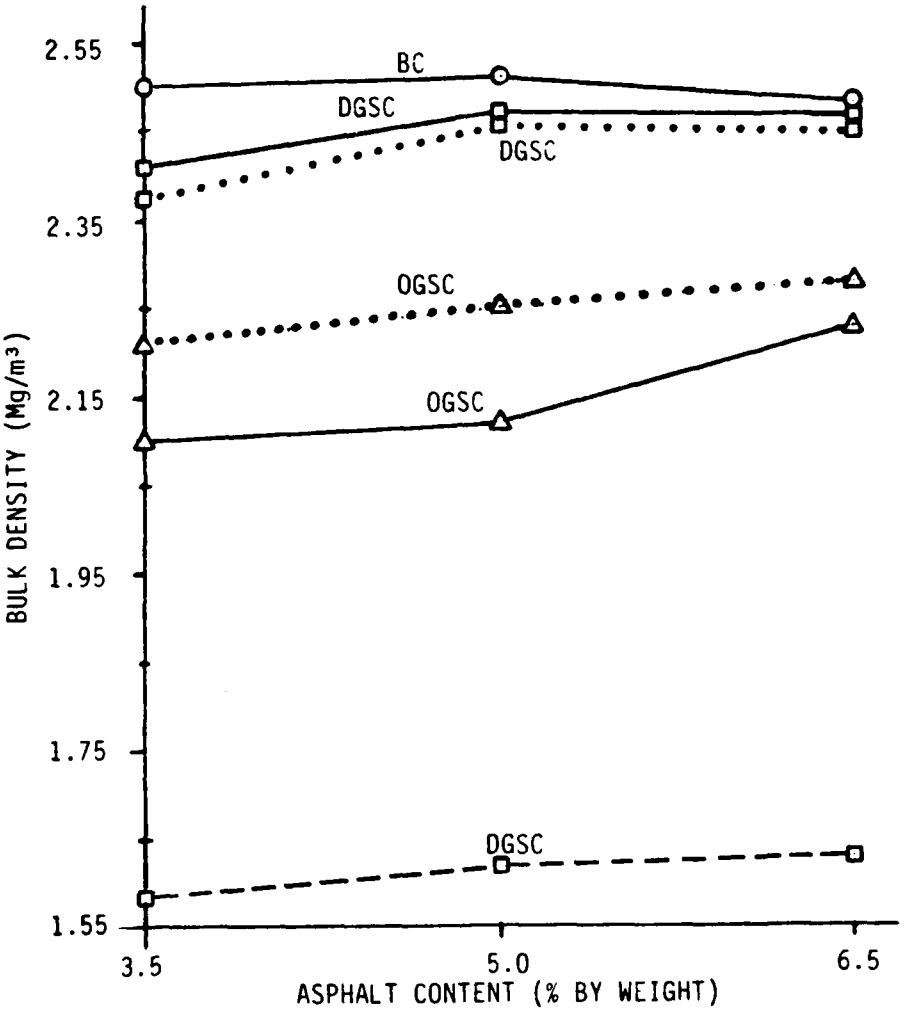

Legend

○ BC - Base Course
△ OGSC - Open Graded Surface Course
□ DGSC - Dense Graded Surface Course

——— Limestone Aggregate
– – – Lightweight Aggregate
. . . . . Granite-gneiss Aggregate

Figure I-9. Bulk Density as a Function of Asphalt Content for the Six Aggregate Mixes.

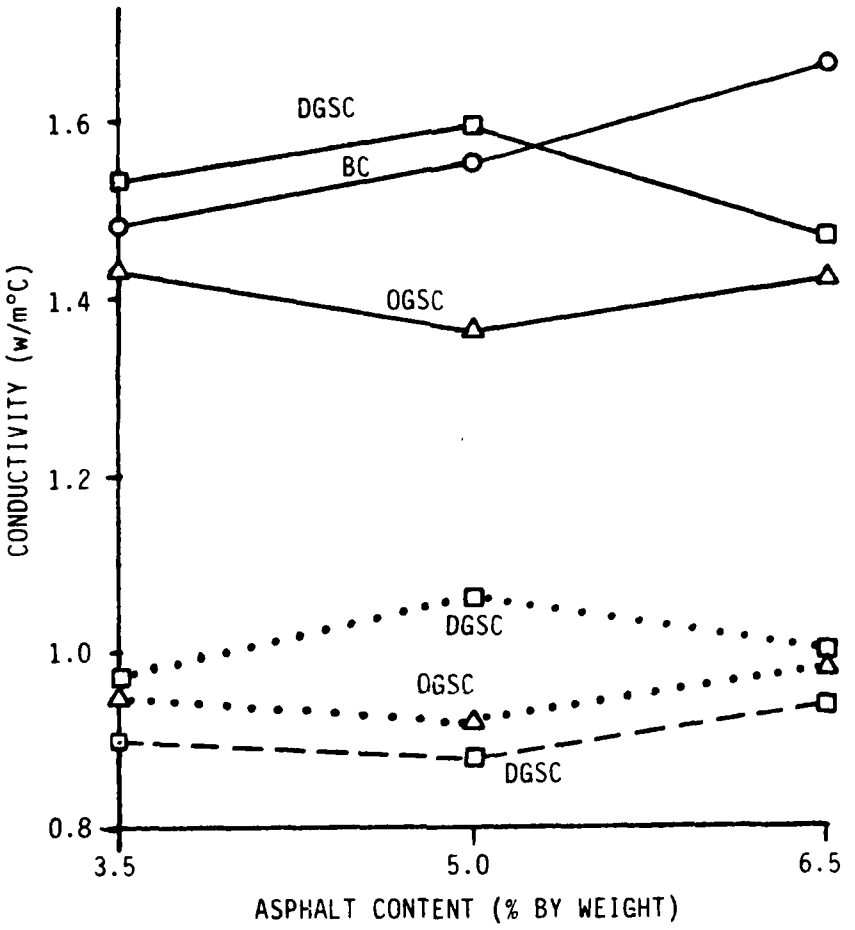

Legend

○ BC - Base Course
△ OGSC - Open Graded Surface Course
□ DGSC - Dense Graded Surface Course

——— Limestone Aggregate
— — — Lightweight Aggregate
····· Granite-gneiss Aggregate

Figure I-10. Thermal Conductivity as a Function of Asphalt Content for the Six Aggregate Mixes.

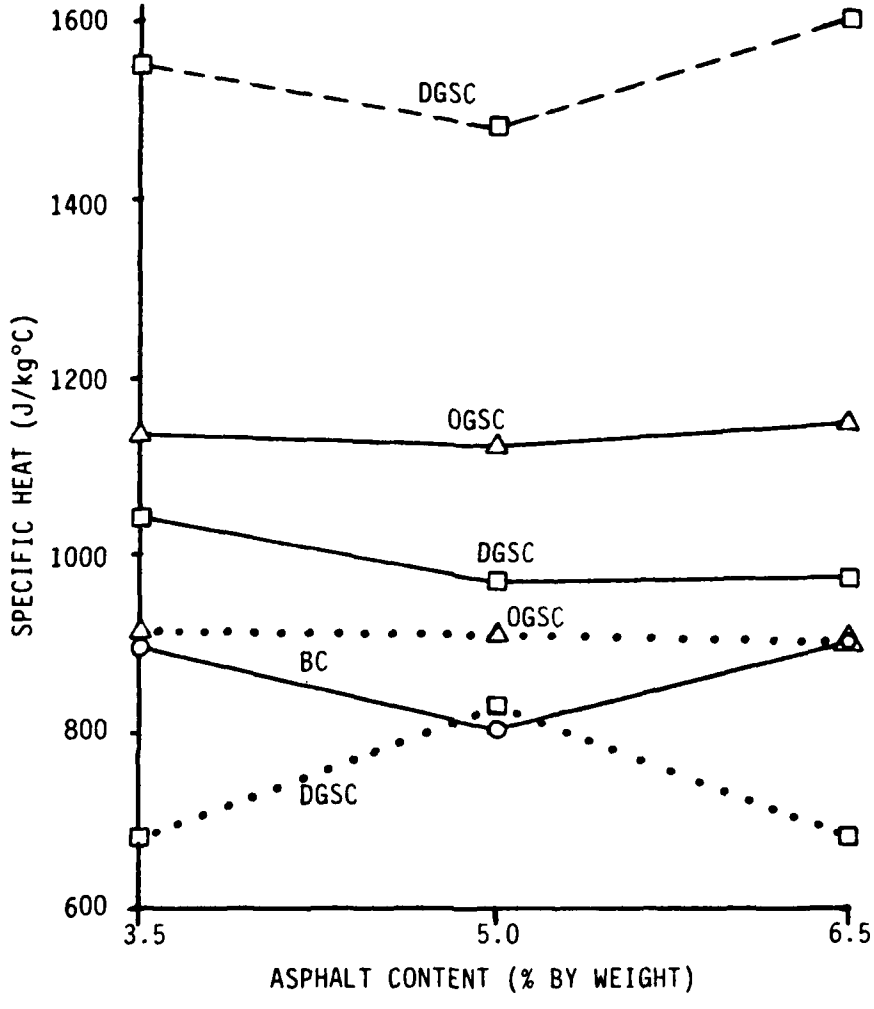

Legend

- ○ BC - Base Course
- △ OGSC - Open Graded Surface Course
- □ DGSC - Dense Graded Surface Course

——— Limestone Aggregate
– – – Lightweight Aggregate
····· Granite-gneiss Aggregate

Figure I-11. Specific Heat as a Function of Asphalt Content for the Six Aggregate Mixes.

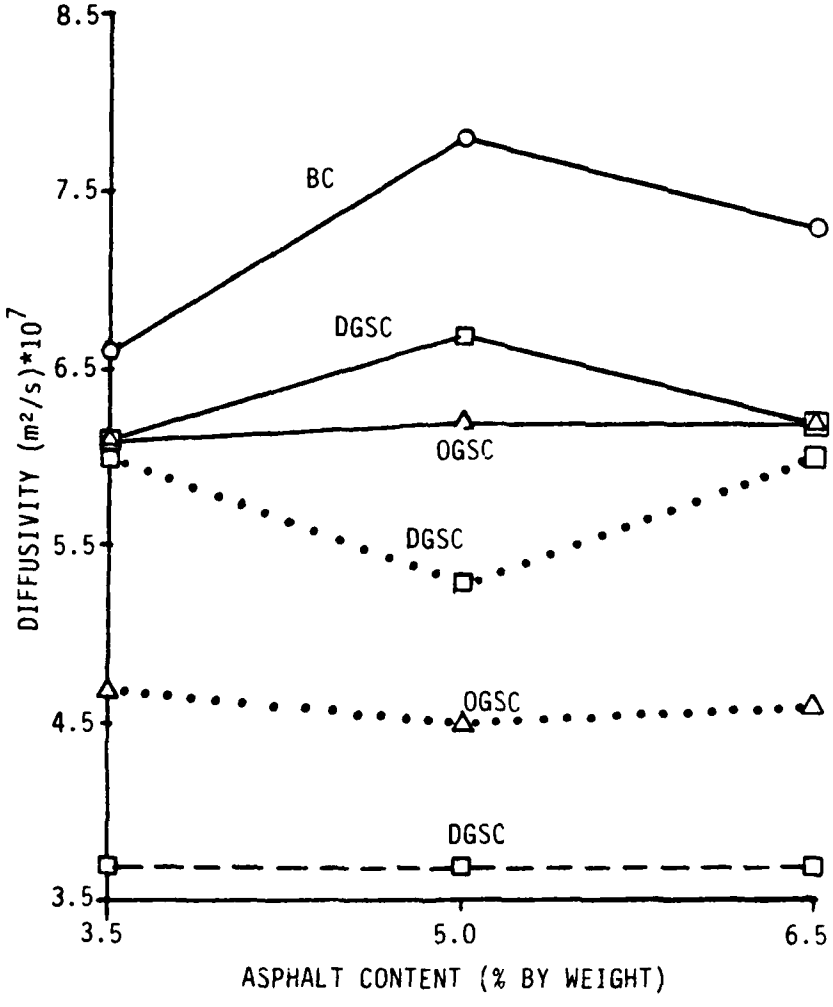

Legend

- ○ BC - Base Course
- △ OGSC - Open Graded Surface Course
- □ DGSC - Dense Graded Surface Course

——— Limestone Aggregate
– – – Lightweight Aggregate
····· Granite-gneiss Aggregate

Figure I-12. Thermal Diffusivity as a Function of Asphalt Content for the Six Aggregate Mixes.

Table I-4. Summary of Physical and Thermal Properties of the Six Aggregate Mixes.

Aggregate type and Gradation	% Asphalt	PROPERTIES (average of 4 or 5 samples) ρ (Mg/m³)	k (w/m°C)	c (J/kg°C)	α ($m^2/s*10^{-7}$)
Limestone					
DGSC	3.5	2.41	1.53	1040	6.1
	5.0	2.47	1.59	968	6.7
	6.5	2.47	1.47	970	6.2
OGSC	3.5	2.10	1.43	1135	6.1
	5.0	2.12	1.36	1120	6.2
	6.5	2.23	1.42	1145	6.2
BC	3.5	2.50	1.48	900	6.6
	5.0	2.51	1.55	802	7.8
	6.5	2.48	1.66	900	7.3
Granite-gneiss					
DGSC	3.5	2.37	0.97	682	6.0
	5.0	2.46	1.06	828	5.3
	6.5	2.45	1.00	677	6.0
OGSC	3.5	2.21	0.95	908	4.7
	5.0	2.25	0.92	907	4.5
	6.5	2.28	0.98	900	4.6
Expanded Shale					
DGSC	3.5	1.58	0.90	1550	3.7
	5.0	1.62	0.88	1480	3.7
	6.5	1.63	0.94	1600	3.7

LEGEND

DGSC - Dense Graded Surface Course
OGSC - Open Graded Surface Course
BC - Base Course

graded surface course mixes. This is to be expected because (1) as shown in Table I-2, the thermal conductivity of granite-gneiss is less than that of limestone (10% to 18% less), and (2) the density of the granite-gneiss mix is slightly (1%) less than that of the limestone mix (Figure I-9).

The thermal conductivity of the limestone base course mix increased with asphalt content over the entire range of asphalt content (3.5% to 6.5%) at which samples were tested. This behavior was observed despite the fact that the density of the base course mix changed little with asphalt content. It is believed that this is due to the fact that most of the heat transferred through this mix is through the larger aggregate (up to 38 mm), and that after the mineral aggregate voids are filled, the asphalt thickness around the larger particles is not increased substantially. The continuous increase in k with asphalt content may suggest a rearrangement of the mineral structure such that although the mean distance between particles has increased (as suggested by a slight decrease in density), the nearest proximity points of individual aggregates may have decreased.

The open graded surface course mix with both the limestone and the granite-gneiss aggregate experienced first a decrease then an increase in thermal conductivity as the asphalt content was increased from 3.5% to 6.5%. This can be explained by recognizing that there are two opposing effects of adding asphalt to a uniform aggregate size. The first, as mentioned previously, is to replace air in the mineral aggregate voids with asphalt. This would tend to increase the conductivity of the mix--as seen in both of the open graded mixes as the asphalt content is increased from 5.0% to 6.5% (Figure I-10). Secondly, and working counter to the first effect, is the influence of increasing the asphalt coating around the particles as the asphalt content is increased. Since the particles are moved farther apart by the less conductive asphalt, the conductivity of the mix would be reduced--as seen in both of the open graded mixes as

the asphalt content is increased from 3.5% to 5.0% (Figure I-10). The increase in asphalt coating thickness as asphalt content increases would be greater in the open graded surface course mix than in the other aggregate mixes studied because of the smaller specific surface (surface area per unit volume) of the open graded mix. The specific surface of the open graded surface course mix is about 40% of that of the dense graded surface course mix.

The granite-gneiss open graded mix had thermal conductivity values about 30% less than that of the limestone open graded mix. This lower value is the result of the lower conductivity of the granite-gneiss mineral (See Table I-2).

The thermal conductivity of the dense graded surface course mix with the lightweight aggregate was about 40% less than that of the dense graded mix having limestone aggregate and about 11% less than that of the dense graded mix having granite-gneiss aggregate. This mix consisted (by weight) of 25% expanded shale (from 5 mm to 13 mm size), 30% limestone aggregate and filler, and 45% river sand (quartz). The expanded shale controlled the conductivity of the mix and the asphalt content had little effect on the conductivity (Figure I-10). It is postulated that the air trapped in the expanded shale is an important limiting factor controlling the conductivity of this mix.

Since the specific heat of asphalt is much higher than that of air, limestone, granite-gneiss, and shale (Tables I-1 and I-2) it was expected that as the asphalt content of the mixes was increased from 3.5% to 6.5%, there would be a corresponding increase in the specific heat of the mixes. However, the specific heat of the mixes is more dependent on the aggregate gradation and mineralogy than the asphalt content (Figure I-11). Based on these data, it seems that an average value of c for each mix, independent of asphalt content, could be used.

The average specific heat of the lightweight aggregate mixes was much higher than the limestone aggregate mixes. This is primarily due to the decrease in

density of the expanded shale.

It is interesting to note that the product ρc of the lightweight mixes and of both dense and open graded surface course limestone mixes is very nearly the same ($2.5*10^6$ J/m^3°C). This may indicate that the specific heat is dependent upon the density for these mixes. This product for the limestone aggregate base course mix is about 13% less, while the product for both granite-gneiss mixes is about 24% less.

The diffusivity-asphalt content relationship for each of the mixes is shown in Figure I-12. For the open graded surface course mixes (limestone and granite-gneiss aggregates), α is essentially independent of asphalt content; for the limestone base course mix and the limestone and granite-gneiss dense graded surface course mixes, the diffusivity varied about 12% over the range of asphalt contents used in the mixes. The values shown in Figure I-12 for the limestone and granite-gneiss mixes are well within the range reported by others (Table I-1). Due to the lower thermal conductivity values, the mixes made with the granite-gneiss aggregate had diffusivity values less than that of the comparable mixes made with limestone aggregate. The granite-gneiss dense graded surface course mix had diffusivity values about 9% less than the limestone dense graded mix, while the diffusivity of the granite-gneiss open graded mix was about 25% less than that of the limestone open graded mix. The diffusivity of the dense graded surface course using lightweight aggregate was much less than that of the dense graded limestone mix and was found to be independent of asphalt content. Since the product ρc for the lightweight mixes is similar to that of the limestone mixes, the reduction in α is due to the smaller thermal conductivity of the lightweight mixes (Figure I-10).

CHAPTER I-F RESULTS OF PROPERTY ANALYSIS OF FIELD SPECIMENS

This chapter presents the physical and thermal analyses of the asphaltic

concrete pavement cores taken from Myrtle Beach and Loring Air Force Bases. These bases were selected due to their geographical extremes (South Carolina and northern Maine) which would insure different asphaltic concrete pavement mix designs.

Seven 10.2 cm diameter cores were drilled at different locations on both the Myrtle Beach and Loring Bases. The top six centimeters of each core was sliced with a rock saw to make three disks about two centimeters thick each. The density of each disk was determined according to ASTM D1188, and thermocouple recessing grooves were sawn into one surface of each disk. The thermal properties of each disk were then obtained by the procedure described previously (Chapter I-C).

One of the three disks from each core was used in an asphalt extraction test, ASTM D2172-81, to determine the amount of asphalt cement present in the different pavements. Also a grain size analysis was conducted on the aggregate remaining from each of the extraction tests.

A summary of the result of the thermal and physical analyses of the field pavement samples is shown in Figures I-13 and I-14 and Tables I-5, I-6, and I-7. In the analysis of the data, the mean and standard deviation of the density (ρ), percent asphalt by weight, diffusivity (α), conductivity (k), and the specific heat (c) are calculated to indicate the average values and the variations, respectively (Table I-5). Tables I-6 and I-7 show the thermal and physical properties of the three groups of similar pavements from Myrtle Beach and Loring Air Force Bases. A group is defined as samples from locations on the base with similar histories, features, and pavement thicknesses. The features and history of Loring Group A are very well defined since all the pavements in this group were resurfaced in the summer of 1982. The Myrtle Beach Group and Loring Group B each have similar histories but the features and pavement thicknesses are not as closely matched as Loring Group A.

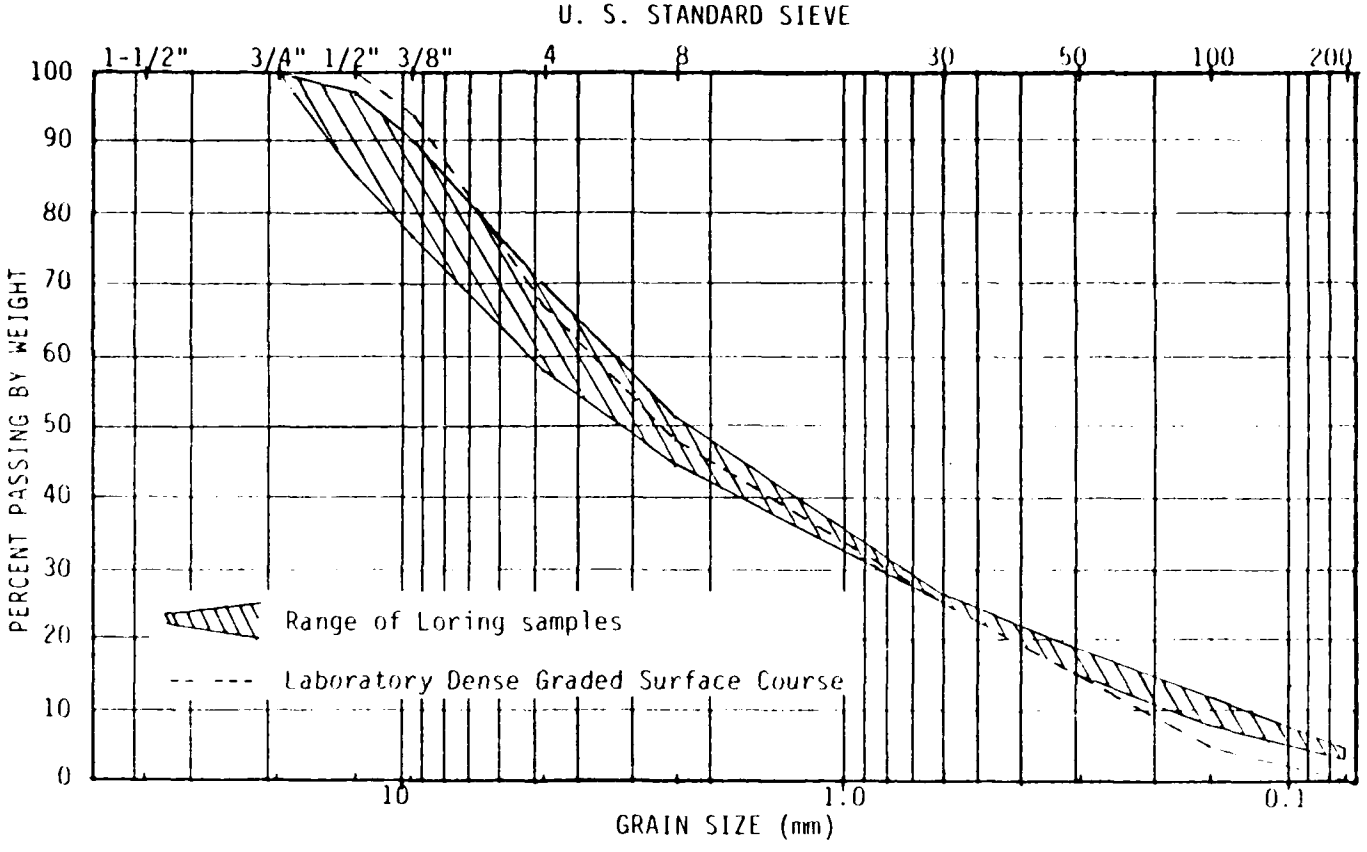

Figure I-13. Range of Grain Size Distributions for the Loring Samples.

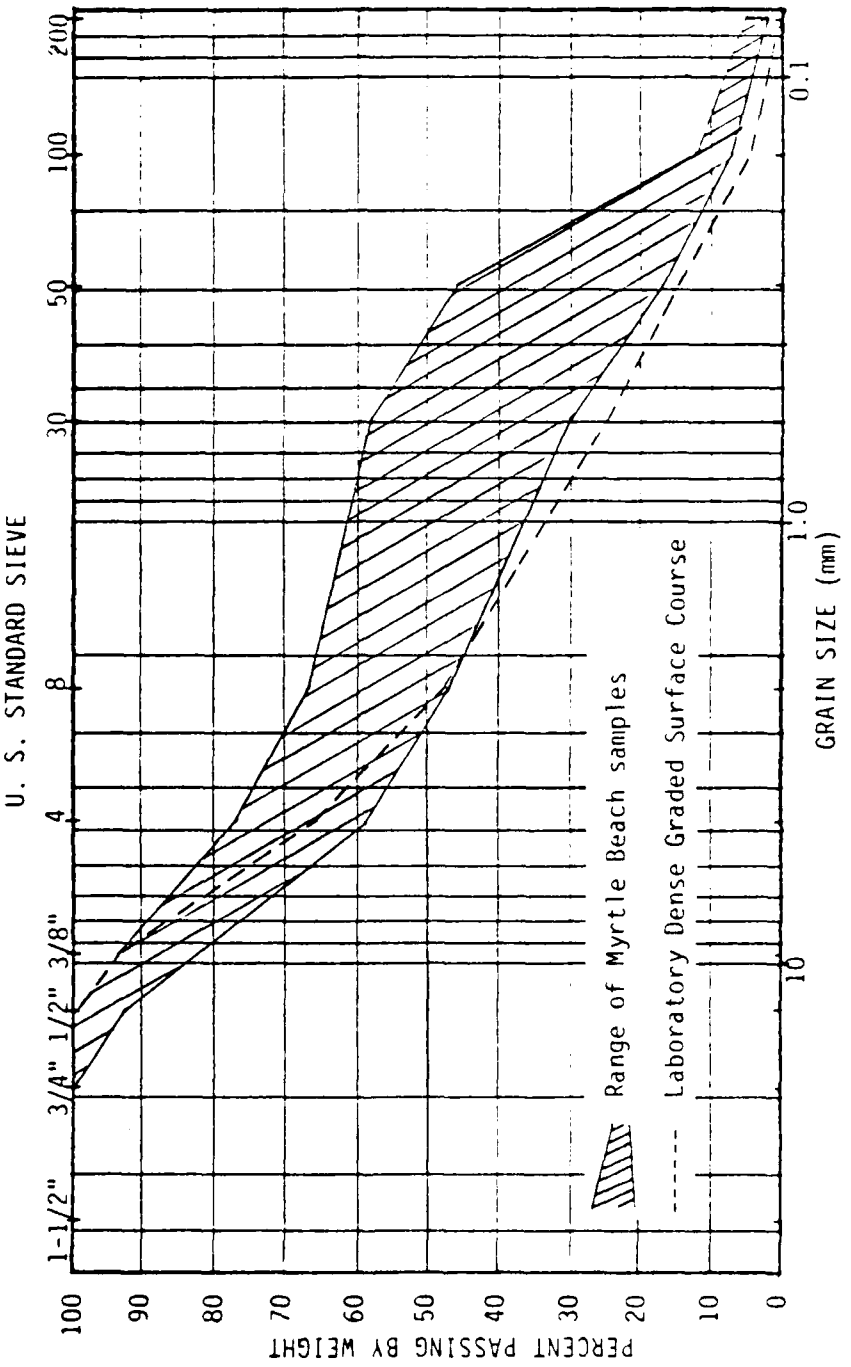

Figure I-14. Range of Grain Size Distributions for the Myrtle Beach Samples.

Table I-5. Summary of Physical and Thermal Properties of Myrtle Beach (M) and Loring (L) Air Force Base Field Samples.

ID#	ρ (Mg/m^3)	% Asphalt	PROPERTIES (average of 3 samples) k (w/m°C)	c (J/kg°C)	α (m^2/s*10^{-7})
M1	2.26	4.8	0.80	425	8.4
M2	2.25	4.6	0.71	412	7.6
M3	2.22	8.0	0.93	500	6.3
M4	2.28	8.0	0.82	561	6.4
M5	2.27	6.7	0.93	572	7.2
M6	2.22	6.7	0.63	445	6.5
M7	2.37	6.7	0.67	423	6.9
Mean	2.27	6.5	0.78	477	7.0
S.D.	0.05	1.4	0.12	68	0.8
L1	2.41	8.9	0.68	501	5.5
L2	2.38	8.9	0.80	636	5.3
L3	2.32	8.9	0.83	651	5.6
L6	2.38	8.5	0.81	629	5.4
L7	2.49	5.7	0.90	763	5.0
L8	2.45	7.0	0.80	556	5.9
L9	2.42	7.0	0.82	595	5.7
Mean	2.41	7.8	0.81	618	5.5
S.D.	0.05	1.3	0.07	82	0.3

Table I-6. Summary of Physical and Thermal Properties of Myrtle Beach Group.

ID#	ρ (Mg/m^3)	% Asphalt	PROPERTIES (average of 3 samples) k (w/m°C)	c (J/kg°C)	α (m^2/s*10^{-7})
M3	2.22	8.0	0.93	500	6.3
M4	2.28	8.0	0.82	561	6.4
M7	2 37	6.7	0.67	423	6.9
Mean	2.29	7.6	0.81	495	6.5
S.D.	0.08	0.7	0.13	69	0.3

Table I-7. Summary of Physical and Thermal Properties of Loring Group A and Group B.

ID#	ρ (Mg/m^3)	% Asphalt	PROPERTIES (average of 3 samples) k (w/m°C)	c (J/kg°C)	α (m^2/s*10^{-7})
Group A					
L1	2.41	8.9	0.68	501	5.5
L2	2.38	8.9	0.80	636	5.3
L3	2.32	8.9	0.83	651	5.6
L4	2.38	8.5	0.81	629	5.4
Mean	2.37	8.8	0.78	604	5.5
S.D.	0.04	0.2	0.07	69	0.1
Group B					
L7	2.49	5.7	0.90	763	5.0
L8	2.45	7.0	0.80	556	5.9
L9	2.42	7.0	0.82	595	5.7
Mean	2.45	6.6	0.84	638	5.5
S.D.	0.04	0.7	0.05	110	0.5

The extraction test results indicate a range of asphalt contents from 4.6% to 8.0% (Table I-5). The Myrtle Beach samples have an average asphalt content of about 6.5%, while the Loring samples have a higher average of 7.8%. The course aggregate in the Myrtle Beach samples is granite, and the fine aggregate is quartz sand. The Loring pavement aggregate is composed of a mixture of slate and basalt (10) as both the coarse and fine aggregate.

Grain size distributions are shown in Figures I-13 and I-14. The dashed line on each of the figures is the grain size distribution curve for the dense graded surface course mix which was presented in Chapter I-D. The range of grain sizes from the Loring samples very closely resembles the laboratory dense graded surface course curve (Figure I-13). The Myrtle Beach samples contain a higher percentage of fine aggregate (sand size) than the laboratory dense graded surface course mix (Figure I-14).

The density of each mix is shown in Table I-5. The samples from Myrtle Beach have densities averaging about 6% less than the samples from Loring. The mean density of each of the three groups (Tables I-6 and I-7) is within 2% of the mean of their parent data sets (Table I-5).

The thermal conductivity of each mix is shown in Table I-5. Each value represents the average of three samples. The mean value of each data set is very nearly the same, with the Loring set having a slightly higher average of thermal conductivity. This is probably due to the lower conductivity of the quartz sand fine aggregate present in the Myrtle Beach pavements (see Table I-2). There is less variation in the Loring samples as shown by the smaller standard deviation value. The Myrtle Beach Group (Table I-6) has a mean thermal conductivity value about 4% higher that the mean conductivity of all the Myrtle Beach data (Table I-5). The Loring Groups have mean conductivity values of 4% less (Group A) and 4% greater (Group B) than the mean conductivity of all the Loring data (see Tables I-5 and I-7).

The average specific heat values (shown in Table I-5) for the Myrtle Beach samples are much less than the average values of the Loring samples (about 22% less). This is due to the higher specific heat of the Loring slate-basalt aggregate than that of the granite and quartz aggregate in the Myrtle Beach pavements (See Table I-2). The mean specific heat values of each of the three groups (Tables I-6 and I-7) are within 4% of the mean specific heat value of their parent data sets (Table I-5).

The average thermal diffusivity (Table I-5) of the Loring samples is much (21%) less than that of the Myrtle Beach samples since both the density and the specific heat of the Loring samples have higher values. The mean diffusivity of both of the Loring Groups (Table I-7) is the same as that of the entire Loring data set, while the mean diffusivity of the Myrtle Beach Group (Table I-6) is 7% less than that of all the Myrtle Beach data.

Since the uncertainty of each of the measured thermal properties is about 5.5% (see Appendix I-B), it can be said that each group's mean thermal property values (Tables I-6 and I-7) is essentially the same as its parent data set (Table I-5), i.e. the uncertainty of the measured values is greater than the variation of the mean values. Also, the mean conductivity of each of the Loring and Myrtle Beach data sets (Table I-5) is essentially the same, since the percent difference between the two mean values is less than the percent uncertainty (Appendix I-B). However, the mean specific heat and diffusivity of the Loring and Myrtle Beach data sets are quite different due to the different densities and aggregate types.

PART II

A NUMERICAL MODEL OF THE HEATING PROCESS FOR ASPHALTIC CONCRETE PAVEMENT

CHAPTER II-A INTRODUCTION

The process of heating an asphalt pavement prior to its removal has several inherent problems that have not yet been adequately resolved. Foremost among these problems is the inadvertent depletion of plasticizing agents in the asphalt. These volatile components are driven off when the temperature of the asphalt exceeds a threshold value of approximately 505 (°K) during the heating process. This loss of plasticizing agents is harmful since it is known to promote early aging of asphaltic pavements. Since the heating is usually accomplished with fossil fuel-fired heaters, the chemical reaction of certain combustion products with the asphalt also presents a problem. These and other problems associated with the heating of asphalt pavements have motivated the construction of the analytical model of the heating process presented in this report.

CHAPTER II-B. A TYPICAL STRATEGY FOR HEATING ASPHALTIC PAVEMENT PRIOR TO REMOVAL OF A SURFACE LAYER

As stated above, the pavement must be heated to its removal depth in order to reduce its shearing strength. Specifically, the object of this heating process is to raise the temperature of the entire layer of pavement to be removed to above a minimum desirable temperature for removal ($T_{REMOVAL} \cong 363°K$) without exceeding the maximum allowable temperature of 505°K anywhere in the pavement.

For economic reasons, the heating process must be completed as rapidly as possible. Due to the extremely low thermal diffusivity of asphaltic pavement, however, a typical pavement heater is capable of raising the surface temperature of the pavement to above the maximum allowable value (505°K) long before the temperature at the removal depth has reached the minimum desirable temperature for removal (363°K). Thus, some paving contractors have adopted a simple strat-

egy for heating asphaltic pavement that may be summarized in the following steps:

1) The pavement is heated until the maximum allowable temperature is reached at the upper surface.
2) Heating is then discontinued and the surface is insulated for an arbitrarily specified period of time during which the surface temperature decreases due to the diffusion of thermal energy into the interior of the pavement by conduction.
3) The insulation is removed from the surface and the heating is begun again. This heating-insulation cycle is repeated until the temperature reaches the desired value (363°K) at the depth which is to be removed.

The analytical model of the pavement heating process presented in this report is based on the heating strategy described above.

CHAPTER II-C. A DETAILED DESCRIPTION OF ASPHALTIC PAVEMENT

An asphaltic pavement is composed of solid, semisolid, or gaseous phases. The solid, or aggregate, phase typically consists of sand, gravel, crushed stone, slag and mineral filler. The semi-solid phase is a viscoelastic asphaltic material which is derived from petroleum and which may have widely varying properties. Approximately 5% of the mixture by weight is composed of the asphaltic material which serves to bind together the aggregate. The gaseous phase is composed of the air which fills the voids. Water in either vapor or liquid form may also occupy these voids.

A typical asphaltic pavement is constructed of three layers, or "courses", as shown in Figure II-1. The uppermost, or "wearing", course is a well-compacted, hot-rolled asphaltic mix which has a very low permeability to water, while the lowest, or "base", course may have a high percentage of voids that are easily penetrated by water. The middle, or "binder," course is usually of an intermediate composition. Measurements of the thermophysical properties of asphaltic

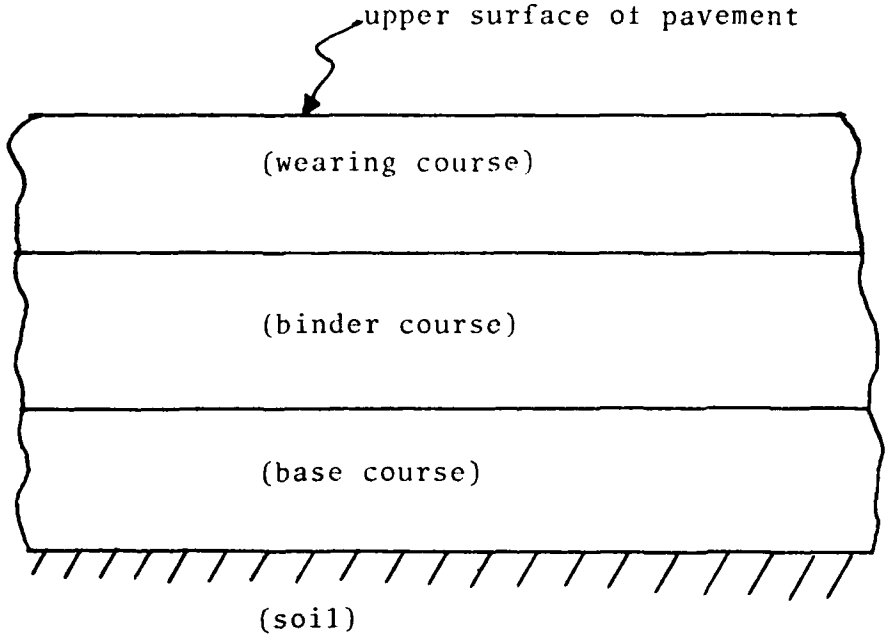

Figure II-1. Typical Structure Of Asphalt Pavement

concrete have been reported by Kavianipour and Beck (19) and in Part I of this report.

CHAPTER II-D. ANALYSIS OF THE HEATING PROCESS

Problem Statement

It is desired to develop an analytical model of the transient heat transfer that occurs during the heating of an asphaltic pavement by the combined action of convection and radiation at the upper surface of the wearing course.

Modeling the Composite Pavement as a Homogeneous Body

The heat transfer within the pavement is entirely by conduction. Since the pavement is composed of three courses, each with different thermophysical properties, it would seem that the pavement should be modeled as a three-layer composite body. The variations between the properties of the three courses are relatively small, however, which suggests that the pavement might be adequately described by modeling it as a homogeneous body. Thus, an analytical study was performed to justify the use of this approximation. This study, which is described in detail in Appendix II-A, shows that the errors incurred by modeling a three-layer asphaltic pavement as a homogeneous (one-layer) body are negligibly small. Therefore, the analytical model of the asphaltic pavement heating process presented in this report is based on the assumption that an actual three-layer pavement may be accurately modeled as a homogeneous body.

The Analytical Model

A schematic of the idealized heater-pavement system being analyzed is shown in Figure II-2. The analytical model of this system is based on the following assumptions:

(1) The three-course composite pavement may be accurately modeled as a homogeneous (one-layer) body with constant thermal properties.

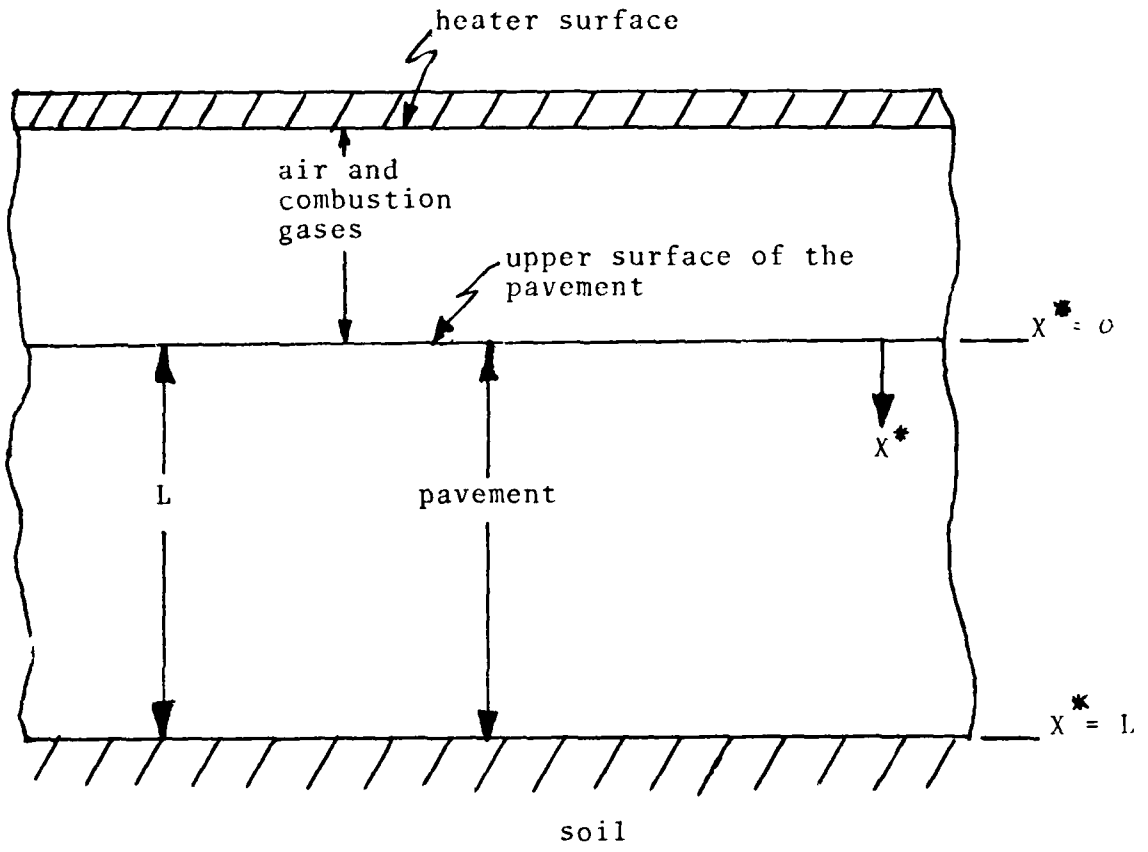

Figure II-2. Idealized Heater-Pavement System

(2) The heat transfer within the pavement takes place entirely by transient, one-dimensional conduction.

(3) The heat transfers along the upper surface of the wearing course, the combusion gases, and the bottom surface of the heater occur by combined radiation and convection.

Note: The role of convection in the overall heat transfer process at the upper surface of the pavement is currently not well-understood. Several models depicting the possible contributions of convection to this heat transfer process are briefly discussed in Appendix II-B.

(4) The radiative exchange between the upper surface of the pavement and the lower surface of the heater is the same as the radiative exchange between two infinite, parallel gray planes. (The gap between these two planes is assumed to be filled with a nonparticipating medium since the degree of participation of the hot combustion gases in the radiative exchange is also presently not well understood.)

(5) The temperature at the bottom surface of the pavement remains constant and is equal to the soil temperature.

(6) The initial temperature distribution in the pavement is known and the heating process is initiated by exposing the upper surface of the pavement to the lower surface of the heater (as shown in Figure II-2).

The above assumptions yield the following governing equation for the transient conduction in the pavement along with its initial and boundary conditions:

$$\frac{\partial T^*}{\partial t^*} = \frac{\alpha^2 T^*}{\partial x^{*2}} \quad (0 \leq x^* \leq L) \tag{1a}$$

$$T^*(x^*,0) = T_0^*(x^*) \quad (0 \leq x^* \leq L) \tag{1b}$$

$$T^*(L,t^*) = T^*_{soil} \quad (= \text{constant}) \tag{1c}$$

$$\left\{ \frac{\sigma}{\frac{1}{\varepsilon_s} + \frac{1}{\varepsilon_H} - 1} \right\} [T^{*4}_H - T^{*4}(0,t^*)] + h_c[T^*_R - T^*(o,t^*)]$$

$$= -k \left. \frac{\partial T^*}{\partial x^*} \right|_{x^*} = 0 \tag{1d}$$

where:

T^* ≡ pavement temperature

x^* ≡ spatial coordinate in the pavement

t^* ≡ time

L ≡ overall thickness of the pavement

T^*_{soil} ≡ temperature at the bottom surface of the pavement

T^*_H ≡ heater surface temperature

T^*_R ≡ an appropriate reference temperature for the convective heat transfer

h_c ≡ convective heat transfer coefficient

α ≡ thermal diffusivity of the pavement

k ≡ thermal conductivity of the pavement

ε_s ≡ emissivity of the upper surface of the pavement

ε_H ≡ emissivity of the heater surface

σ ≡ Stefan Boltzman constant = $(5.6697 * 10^{-8}) \left(\frac{w}{m^2 - {}^oK^4}\right)$

The transient conduction problem defined by equations (1a)-(1d) is non-linear because of the radiation boundary condition at the upper surface. The

use of a so-called "radiation heat transfer coefficient" to linearize this boundary condition is inappropriate in this problem because of the large temperature differences between the pavement and heater surfaces. Thus, the problem will be solved numerically using finite difference techniques.

Formulation of the Numerical Model

For the purposes of the numerical model, the pavement is represented by (M + 1) nodes as shown in Figure II-3. The two surface nodes (nodes 1 and M + 1) each represent a layer of pavement with a thickness of $\Delta x^*/2$ (where $\Delta x^* = L/M$), while the (M - 1) interior nodes each represent a layer of pavement of thickness Δx^*. Since the temperature at the bottom of the slab is assumed to be a given constant (T^*_{soil}), the temperature of the (M + 1)-th node is known. Thus, only M equations must be written to determine the temperatures of the remaining nodes (nodes 1 through M).

An energy balance on the i-th interior node gives

$$\begin{pmatrix}\text{Rate of conduction}\\ \text{heat transfer to}\\ \text{node i}\end{pmatrix} = \begin{pmatrix}\text{Rate of conduction}\\ \text{heat transfer}\\ \text{from node i}\end{pmatrix} + \begin{pmatrix}\text{Rate of change of}\\ \text{thermal energy stored}\\ \text{in node i}\end{pmatrix}$$

or

$$-kA\left[\frac{T^*_{i-1} - T^*_i}{x^*_i - x^*_i}\right] = -kA\left[\frac{T^*_i - T^*_{i+1}}{x^*_i - x^*_{i+1}}\right] + [\rho c A \ \Delta x^*]\ \frac{dT^*_i}{dt^*}$$

which reduces to

$$\frac{dT^*_i}{dt^*} = \frac{\alpha}{(\Delta x^*)^2}\ [T^*_{i-1} - 2T^*_i + T^*_{i+1}] \qquad (2 \le i \le M) \qquad (1a)$$

where:

$\alpha = \frac{k}{\rho c}$ = thermal diffusivity of the pavement

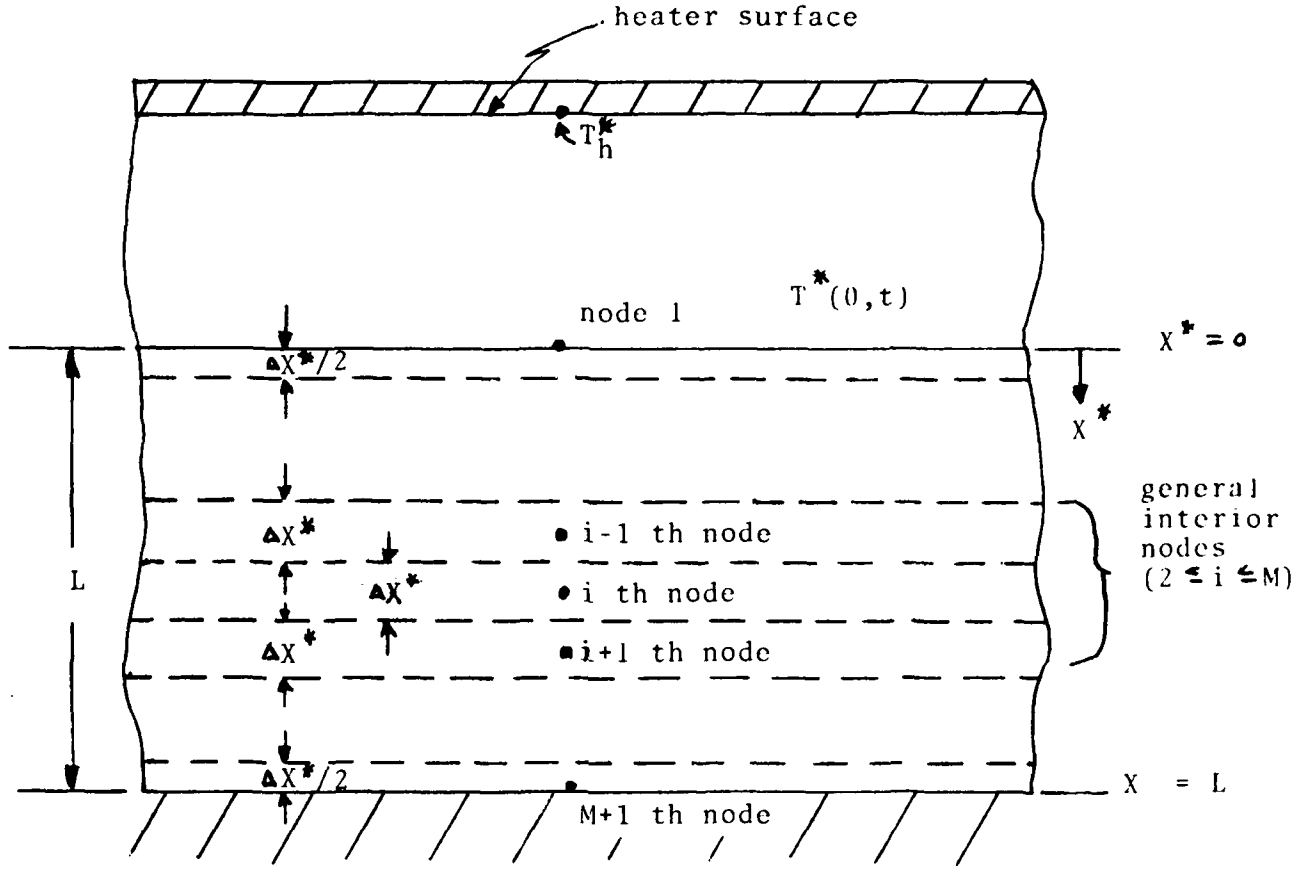

Figure II -3. Nodal Representation Of The Pavement For The Finite-Difference Model

Similarly, an energy balance for node 1 (the node at the upper surface of the pavement) while the pavement is being heated gives:

$$\begin{pmatrix}\text{Rate of radiation heat}\\ \text{transfer to node 1}\end{pmatrix} + \begin{pmatrix}\text{Rate of convection heat}\\ \text{transfer to node 1}\end{pmatrix}$$

$$= \begin{pmatrix}\text{Rate of radiation}\\ \text{heat transfer}\\ \text{from node 1}\end{pmatrix} + \begin{pmatrix}\text{Rate of conduction}\\ \text{heat transfer}\\ \text{from node 1}\end{pmatrix} + \begin{pmatrix}\text{Rate of change of}\\ \text{thermal energy}\\ \text{stored in node 1}\end{pmatrix}$$

or,

$$\sigma\, \gamma_{H-1}\, (T_H^{*4} - T_i^{*4}) + h_c\, (T_R^* - T_i^*) = - k \left[\frac{T_1^* - T_2^*}{x_1^* - x_2^*}\right]$$

$$+ \frac{\rho c A \Delta x^*}{2} \frac{dT_i^*}{dt^*}$$

which reduces to

$$\frac{dT_1^*}{dt^*} = \frac{2}{\rho c \Delta x^*} \left[\sigma\, \gamma_{H-1}\, (T_H^{*4} - T_1^{*4}) + h_c\, (T_R^* - T_1^*)\right.$$

$$\left. - \frac{(k)}{\Delta x^*} (T_1^* - T_2^*)\right] \qquad (1b)$$

where:

γ_{H-1} ≡ radiation heat transfer modulus that accounts for the emissivities and relative geometries of the pavement and heater surfaces

$$\left(= \frac{1}{1/\varepsilon_s + 1/\varepsilon_H - 1}\right)$$

$$(x_1^* - x_2^*) = - (\Delta x^*)$$

Note: The numerical model must be capable of computing the transient

temperature distributions in the pavement during both the heating and insulation periods of the cyclic process described earlier in this report. Thus, an energy balance on node 1 while the surface is insulated gives

$$\begin{bmatrix}\text{Rate of conduction}\\ \text{heat transfer from}\\ \text{node 1}\end{bmatrix} + \begin{bmatrix}\text{Rate of change of}\\ \text{thermal energy}\\ \text{stored in node 1}\end{bmatrix} = 0$$

or,

$$- k\left[\frac{T_1^* - T_2^*}{x_1^* - x_2^*}\right] + \frac{\rho c \Delta x^*}{2}\ \frac{dT_1^*}{dt^*} = 0$$

which reduces to:

$$\frac{dT_1^*}{dt^*} = - \frac{2\alpha}{(\Delta x^*)^2}\ [T_1^* - T_2^*] \qquad (1c)$$

The initial condition is given by specifying the initial temperature

$$T_i^* = C_i^* \qquad \text{for } [1 \leq i \leq (M + 1)] \text{ at } t^* = 0 \qquad (1d)$$

at each nodal point (where C_i^* is an appropriate set of constants). Finally, the boundary condition at the bottom surface of the pavement is given by

$$T_{M+1}^* = T_{soil}^* \qquad (\text{for } t^* > 0). \qquad (1e)$$

In summary, the numerical model (written in terms of physical variables) consists of equations (1a) through (1e). These equations contain a number of independent parameters (i.e., α, h_c, T_H^*, ε_s, ε_H, ...). As in all heat transfer problems, it is convenient to reduce the number of independent parameters

enhances our physical understanding of the solution, but also greatly reduces the number of computations required to complete a parametric study of the problem by presenting the solutions in their most general forms. Thus, the following set of nondimensional variables are introduced

$$T \equiv \frac{T^*}{T^*_{REM}}, \qquad x \equiv \frac{x^*}{L}, \qquad t \equiv \frac{t^*}{(L^2/\alpha)}$$

where:

$T^*_{REM} \equiv$ the minimum temperature to which the pavement must be heated at the depth to which it is to be removed x^*_{REM}, before the removal can take place ($\cong 363^oK$)

Note:

(1) The temperature must be nondimensionalized as shown above instead of in the usual manner; that is, by letting

$$T \equiv \frac{T - T_{REF}}{(\Delta T)_{REF}}$$

because of the nonlinear radiation boundary condition.

(2) T^*_{REM} was chosen as the temperature scale because it is the only temperature in the entire problem with a constant value.

Substituting the nondimensional variables in equations (1a) through (1e) yields the following set of equations which comprise the nondimensional form of the numerical model.

$$\frac{dT_i}{dt} = \frac{1}{(\Delta x)^2} [T_{i-1} - 2\,T_i + T_{i+1}] \qquad (2 \leq i \leq M) \qquad (2a)$$

$$\frac{dT_1}{dt} = \frac{2}{\Delta x} \left[(A)\,(T_H^4 - T_1^4) + (Bi)(T_R - T_1) - \left(\frac{1}{\Delta x}\right)(T_1 - T_2)\right] \qquad (2b)$$

$$\frac{dT_1}{dt} = -\left[\frac{2}{(\Delta x)^2}\right]\,[T_1 - T_2] \qquad (2c)$$

$$T_i = C_i \quad \text{for } [1 \leq i \leq (M + 1)] \text{ at } t = 0 \qquad (2d)$$

$$T_{m+1} = T_{soil} \quad (\text{for } t > 0) \qquad (2e)$$

where:

$$A \equiv \frac{\sigma L\, \gamma_{H-1}\, T^{*3}_{REM}}{k} = \frac{\sigma L\, T^{*3}_{REM}}{k\left(\frac{1}{\varepsilon_H} + \frac{1}{\varepsilon_s} - 1\right)} = \text{radiation-conduction parameter}$$

$$Bi \equiv \frac{h_c L}{k} = \text{Biot number}$$

$$T_H \equiv \frac{T^*_H}{T^*_{REM}} = \text{dimensionless heater temperature}$$

$$T_R \equiv \frac{T^*_R}{T^*_{REM}} = \text{dimensionless reference temperature for convection}$$

Implementation of the Numerical Model

The nondimensional form of the numerical model given by equations (2a)-(2e) was programmed for execution on a digital computer. This program incorporates the heating technique described earlier in this report; that is, the heating is begun and continues until either the surface temperature exceeds a maximum allowable value

$$(T_1)_{MAX} = \frac{(T_1^*)_{MAX}}{T^*_{REM}}$$

or the temperature at

$$x_{REM} = \frac{x^*_{REM}}{L}$$ reaches the value required for

removal [$T_{REM} = 1$], at which time the process is terminated. If the temperature at x_{REM} has not reached the desired value of $T_{REM} = 1$ when T_1 reaches $(T_1)_{MAX}$, the heating is terminated and the upper surface is insulated for an arbitrarily specified period of time,

$$t_{INSUL} \equiv \frac{t^*_{INSUL}}{(L^2/\alpha)}$$

This cycle is repeated until $T = T_{REM} = 1$ *at* x_{REM}. *Thus, specifying the values* of the eight dimensionless parameters A, Bi, T_H, T_R, T_{REM}, x_{REM}, $(T_1)_{MAX}$ and t_{INSUL}, along with the initial temperature distribution, completely specifies the problem.

The solution of the numerical model employs a simple, explict finite difference technique. A brief description of this technique and the reasons for its selection are given in Appendix II-C. A listing of the resulting FORTRAN code, HEAT1, is given in Appendix II-D.

CHAPTER II-E. PRESENTATION OF RESULTS FOR THE "NOMINAL" HEATING PROCESS IN THE PRESENT INVESTIGATION

To illustrate some typical output from the HEAT1 code, representative temperature histories and distributions for the "nominal" heating case in this investigation are presented here in graphical form. The nominal heating case is defined by the values of the eight dimensionless parameters shown in Table

II-1. Note that this case assumes the surface of the pavement is heated by radiation alone and that the initial temperature distribution in the pavement is uniform.

Figure II-4 shows the surface and removal depth temperature histories for the nominal heating case. The monontonically rising surface temperature clearly shows that no insulation periods are required for the nominal case. The heater temperature is low enough that thermal energy can diffuse into the pavement by conduction fast enough to raise the temperature at the removal depth to its required value (= 1.0) before the surface temperature exceeds the maximum allowable value (= 1.394) in the pavement. The Fourier number at the end of the heating period is ($13.4 * 10^{-3}$), which corresponds to a heating time of 31.5 min.

Figure II-5 shows the dimensionless temperature profiles in the pavement at different dimensionless times during the heating period. These profiles dramatically illustrate the exceptionally low value of the thermal diffusivity of asphalt. At the end of the heating period (31.5 min), thermal energy from the surface heating has diffused through only about 40% of the total thickness of the pavement.

$$A = \left[\frac{\sigma L \ T^{*3}_{REM}}{k(\frac{1}{\varepsilon_H} + \frac{1}{\varepsilon_s} - 1)} \right] = 0.289$$

$$Bi = \frac{h_c L}{K} = 0 \text{ (No convection, radiative heating only)}$$

$$T_H = \frac{T^*_H}{T^*_{REM}} - = 1.854$$

$$T_R = T_H = 1.854$$

$$T_{REM} = \frac{T^*_{REM}}{T^*_{REM}} = 1.0$$

$$t_{INSUL} = \frac{t^{*\alpha}_{INSUL}}{L^2} = (2.131 * 10^{-3})$$

$$x_{REM} = \frac{x^*_{REM}}{L} = 0.833$$

$$T_{MAX} = \frac{T^*_{MAX}}{T^*_{REM}} = 1.391$$

$$T_i = C_i = T_{soil} = \frac{T^*_{soil}}{T^*_{REM}} = 0.807 \qquad \text{For } [1 \leq i \leq (M + 1)].$$

Note: The nominal heating case assumes a uniform initial temperature distribution.

Table II-1. Values of the Nondimensional Parameters in the Heat1 Code for the Nominal Heating Case

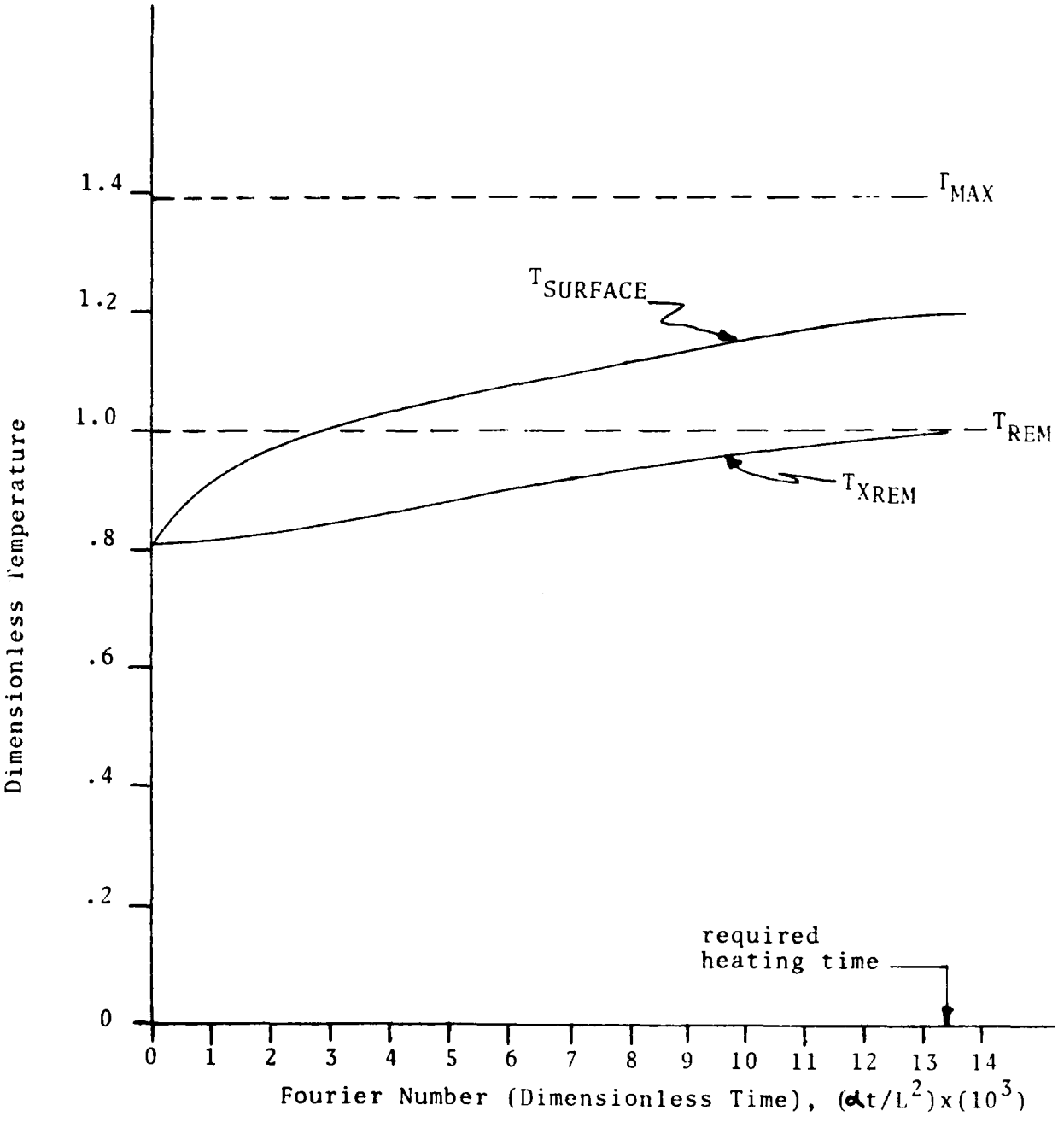

Figure II-4. Surface And Removal Depth Temperature Histories For The Nominal Heating Case

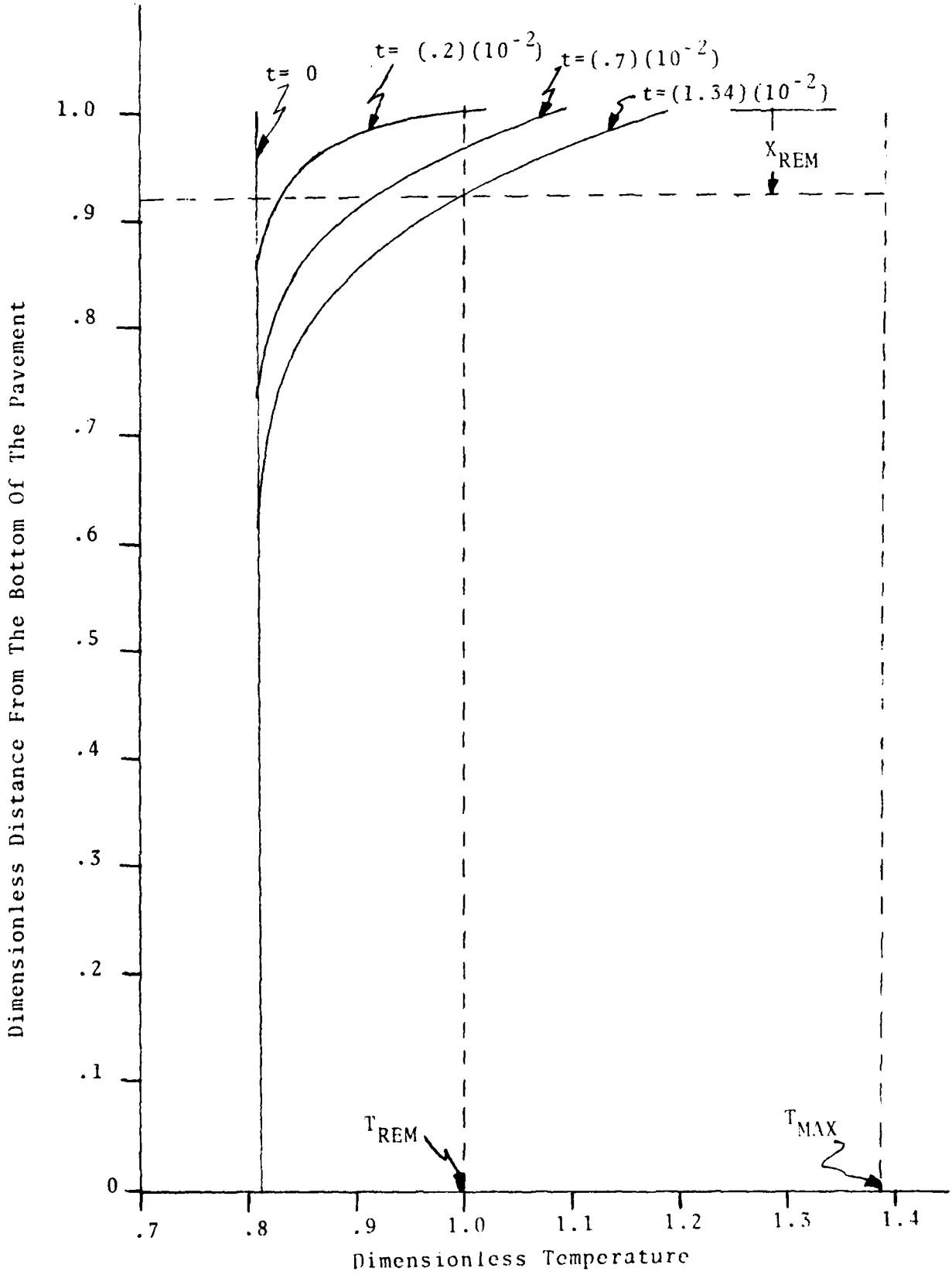

Figure II-5. Dimensionless Temperature Profiles In The Pavement For The Nominal Heating Case

PART III

VALIDATION OF THE

THERMAL MODEL

CHAPTER III-A INTRODUCTION

To acquire the data needed validate the thermal model of asphaltic pavement, field tests were conducted at two U. S. Air Force Bases -- Myrtle Beach Air Force Base (AFB) in South Carolina and Loring AFB in northern Maine. This part of the research effort provides a description of the heater tests and comments on the validity of the thermal model. The field tests involved heating the asphaltic concrete pavement using a propane fired field heater and measuring temperatures at various depths within the pavement as a function of time. To determine the validity of the model presented in Part II, the thermal properties of the appropriate field sample (See Chapter I-F; emissivity values for steel and asphalt were assumed) were used in the numerical model of the heating process along with pertinent field heater characteristics to predict the temporal-spatial temperature history of an in-service asphaltic concrete pavement at the site the sample was obtained. The predicted temperature-time history at various depths in the pavement was then compared to the temperatures measured at a particular site during a field test. Good agreement between observed (measured) and predicted temperature data would establish the validity of the model. This part of the research effort provides a description of the heater tests and comments on the validity of the thermal model.

CHAPTER III-B DESCRIPTION OF FIELD HEATER TESTS AND DISCUSSION OF RESULTS

Seven sites were selected at each Base, and 15.2 cm cores were drilled vertically through the pavement at each site. From inside the core hole, four lateral holes (0.32 cm in diameter) and about 5 cm long were drilled horizontally into the pavement which provided thermocouple placement at depths within the pavement varying from about 0.5 cm to about 5.6 cm (See Figure III-1). The

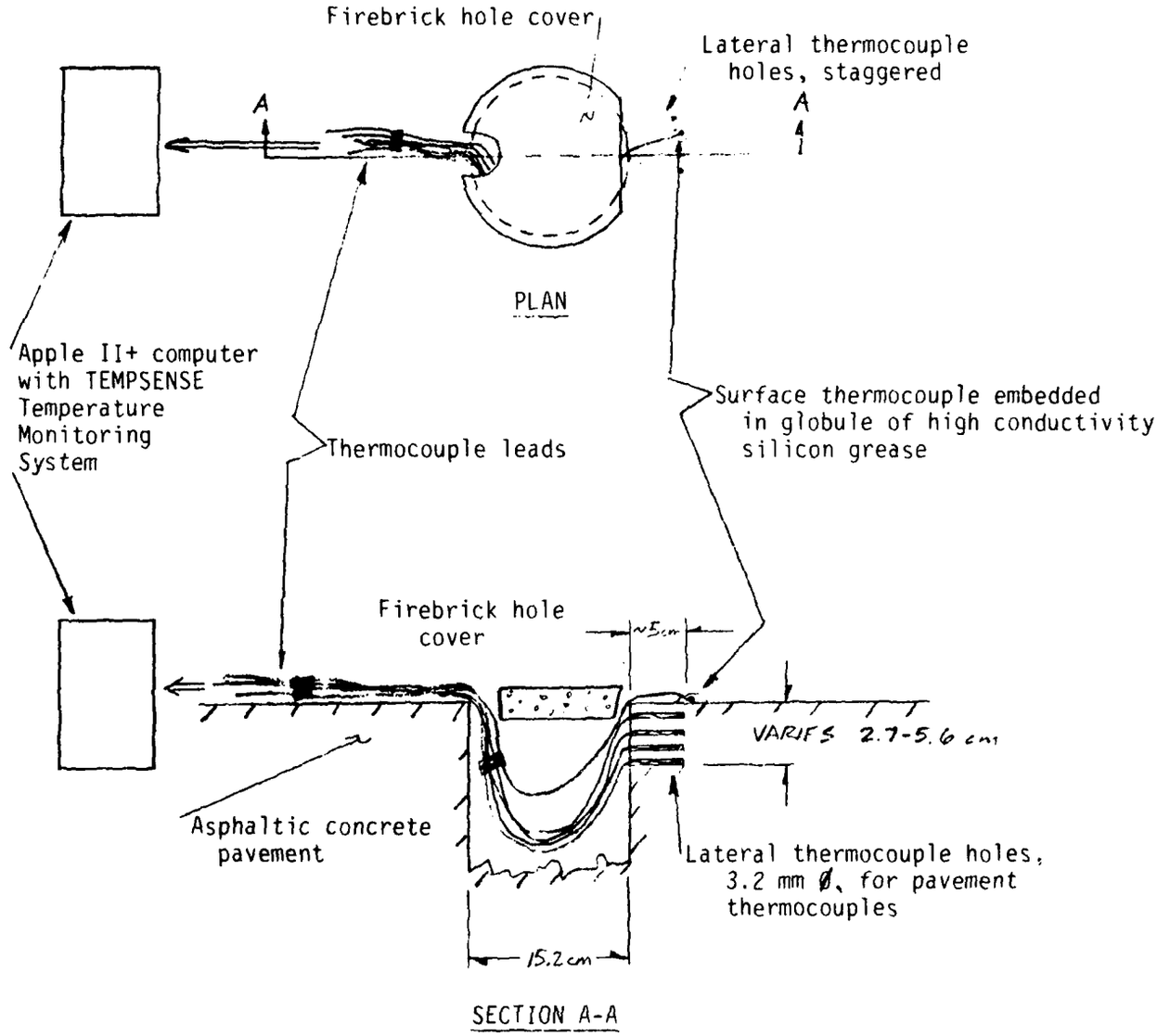

Figure III-1. Plan and Section View of a Typical Test Hole

lateral holes were filled with high conductivity silicon grease (Omegatherm 201 from Omega Engineering, Inc.), and a 24 AWG cooper-constantan thermocouple was inserted into each lateral hole. At the pavement surface, a 24 AWG copper-constantan thermocouple was embedded in a globule of high conductivity silicon grease. These five thermocouples (and a sixth which was attached to the heater) led to the same temperature measuring system (Apple II+ computer and TEMPSENSE software) used in the thermal property analysis described in Chapter I-C.

A schematic of the field heater is shown in Figure III-2. The heater was manufactured by Aeroil Products Co., Inc. of New Jersey and is designed to be used in pavement pothole patching. Although it was understood that with this heater the surface heating of asphaltic pavement could be modeled as a purely radiation process (26), test data indicated that convective cooling around the edges of the heater was an important characteristic and therefore was incorporated in the model. A 20 AWG chromel-alumel heater thermocouple was mounted between the two center heater tubes at the same height as the bottom of the heater tubes (See Figure III-1). It was found later that this location gave temperature readings that were not representative of the temperature of the burner tubes. Heater temperatures were corrected as described below.

Heater tests were carried out with thermocouples attached to different points on the heater. Since the temperature of the burner tubes was important in the analysis, a correlation was established between the burner tube temperature and the temperature at a point between the center heater tubes. The field heater temperature data were then corrected using the adjusted temperature. This adjustment was critical in the analysis because the radiant heat delivered to the pavement surface is a function of the fourth power of the heater temperature (T_H^4) and small errors in T_H would lead to very large errors in the analysis.

The Myrtle Beach field tests were run in March, 1983. The coastal winds

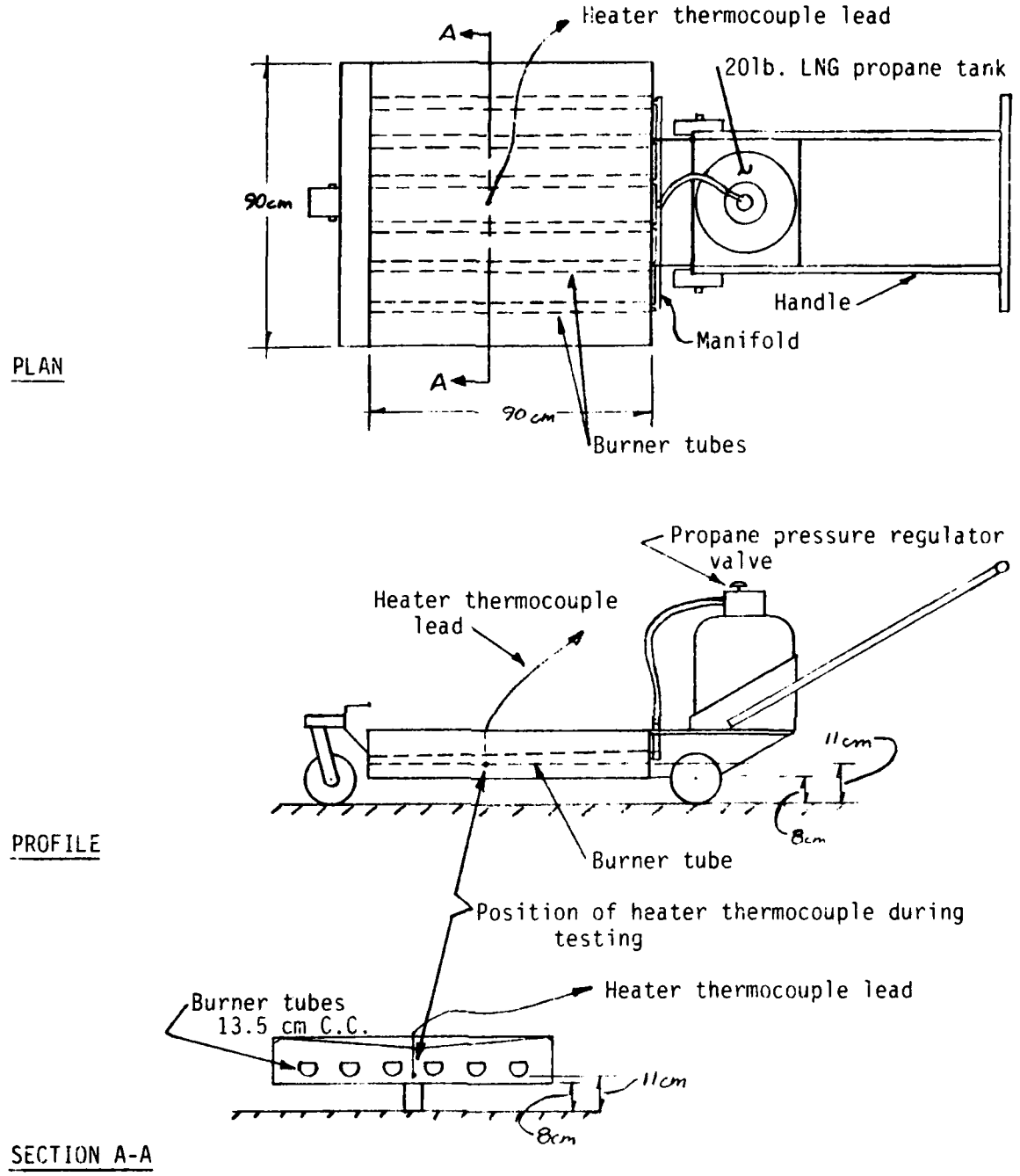

Figure III-2. Plan, Profile, and Section View of Field Heater.

prevailing at the time disturbed the temperature patterns of the air between the heater and the pavement surface and all the heat generated by the heater was not delivered to the pavement surface beneath the heater. Thus, for a given heater temperature, the temperature of the pavement surface fluctuated widely with the wind velocity (both speed and direction). Hence, the temperature data were considered to be unreliable and no meaningful analysis could be carried out on the Myrtle Beach data.

The problem was solved at Loring Air Force Base when these tests were run in June, 1983 by erecting a corrugated steel fence (wind fence) about 3 m square and about 0.8 m high around the heater and the test hole. That the wind fence was very effective in reducing the wind velocity between the heater and the pavement surface was shown by the less variable pavement surface and heater temperature data.

A typical test proceeded as follows:

- A 15.2 cm diameter core and lateral thermocouple holes were drilled.
- The thermocouple hole depths were measured and recorded.
- The wind fence was set up to enclose the test hole and the heater.
- An asbestos board was placed underneath the heater to prevent scoring the pavement while the heater was reaching steady state.
- The thermocouple holes were filled with high conductivity silicon grease and the four subsurface thermocouples were inserted.
- The surface thermocouple was embedded in a globule of high conductivity silicon grease.
- A firebrick hole cover was placed over the core hole to prevent heat from entering through the open core hole.
- The heater was lit and the desired heater temperature (T_H) was set by adjusting the propane pressure (the propane pressure only approximately related to the heater temperature).

- When the heater had reached steady state, the temperature measurements were begun to acquire the initial temperature profile of the pavement.
- The heater was then centered over the core hole and temperature measurements were continued for the predetermined duration of test.

Two types of tests were conducted at Loring AFB. One was a "slow" test characterized by low heater temperatures (around 300°C) and a long exposure time (around 25 minutes), and the other was a "quick" test characterized by high heater temperatures (around 600°C) and a shorter exposure time (1-3 minutes). During the "slow" tests, the heater propane pressure was adjusted such that the surface temperature of the pavement did not rise above about 230°C (close to the flash point of asphalt). For the "quick" tests the heater was removed when the pavement surface reached about 230°C. Temperatures were recorded every 20 seconds in the "slow" test and every 3 seconds in the "quick" test.

Figure III-3 shows the comparison of predicted and observed temperatures for one of the slow tests carried out at Loring Air Force Base. The predicted temperatures are very close to the measured temperatures at points beneath the pavement surface throughout the duration of the test. However, the computer code consistently overestimated the measured temperature at the pavement surface. It is believed that this was due to conduction losses of the thermocouple leads at the pavement surface. Sparrow (27) indicates that it is not possible to estimate the magnitude of the temperature error due to conduction losses with any precision. However, the error is in the direction that was predicted by the numerical model, i.e. the true surface temperature is higher than measured.

The observed and predicted temperatures at the typical removal depth (25 mm) are very close. In this test with a heater temperature of 525°C the removal

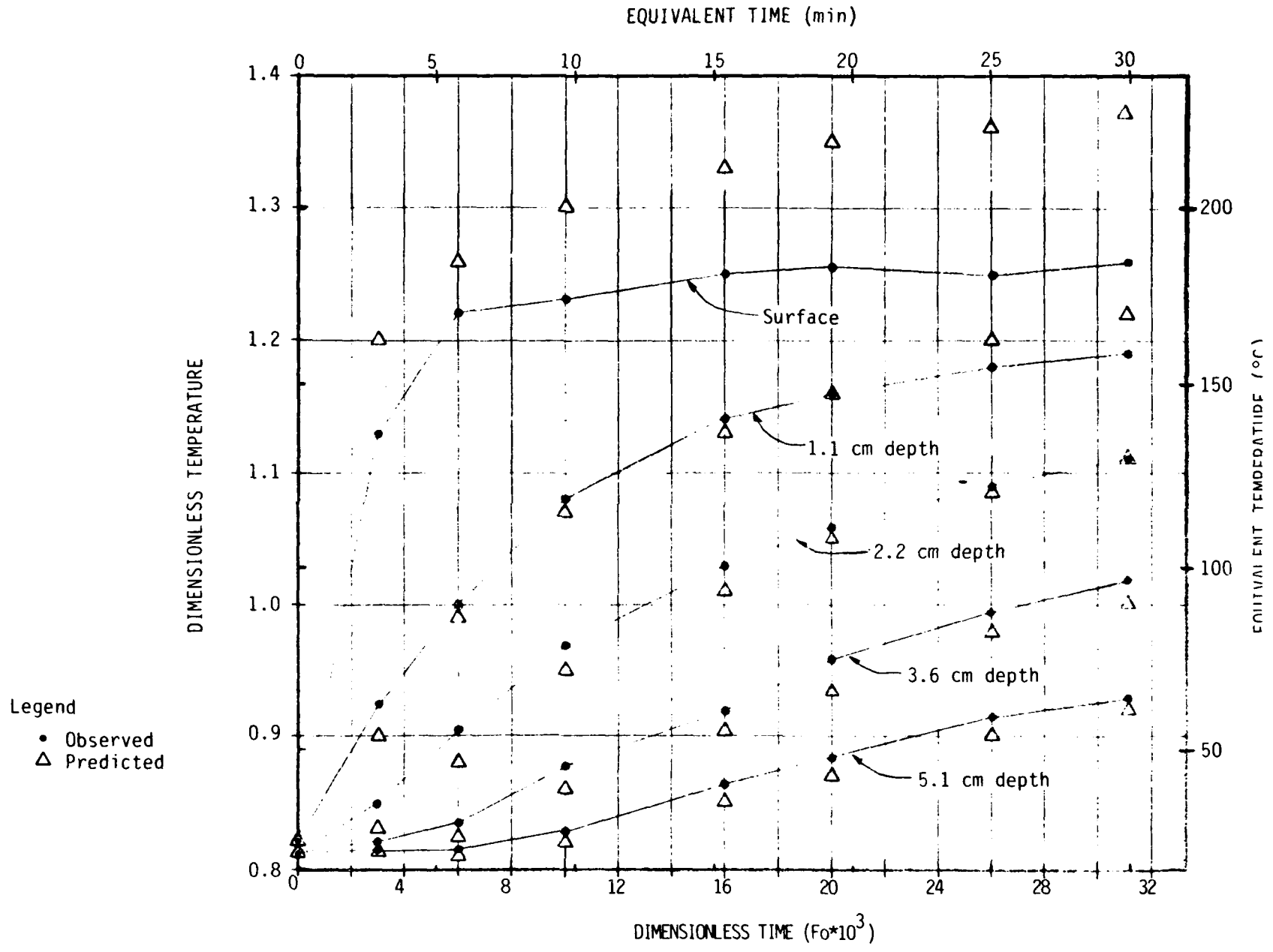

Figure III-3. Measured and Predicted Spatial-Temperature History for a Slow Test.

temperature (90°C) is not reached at the typical 25 mm removal depth for about 13.5 minutes.

Figure III-4 shows observed and predicted temperature histories for a quick test. Again, the predicted surface temperatures were higher than observed because of conduction losses as discussed above. The model did an excellent job of predicting the subsurface temperatures.

The close agreement between observed and predicted temperatures lends credibility to the numerical model and indicates that the model can be used with confidence to predicted in situ temperature due to surface heating by fossil fuel heaters.

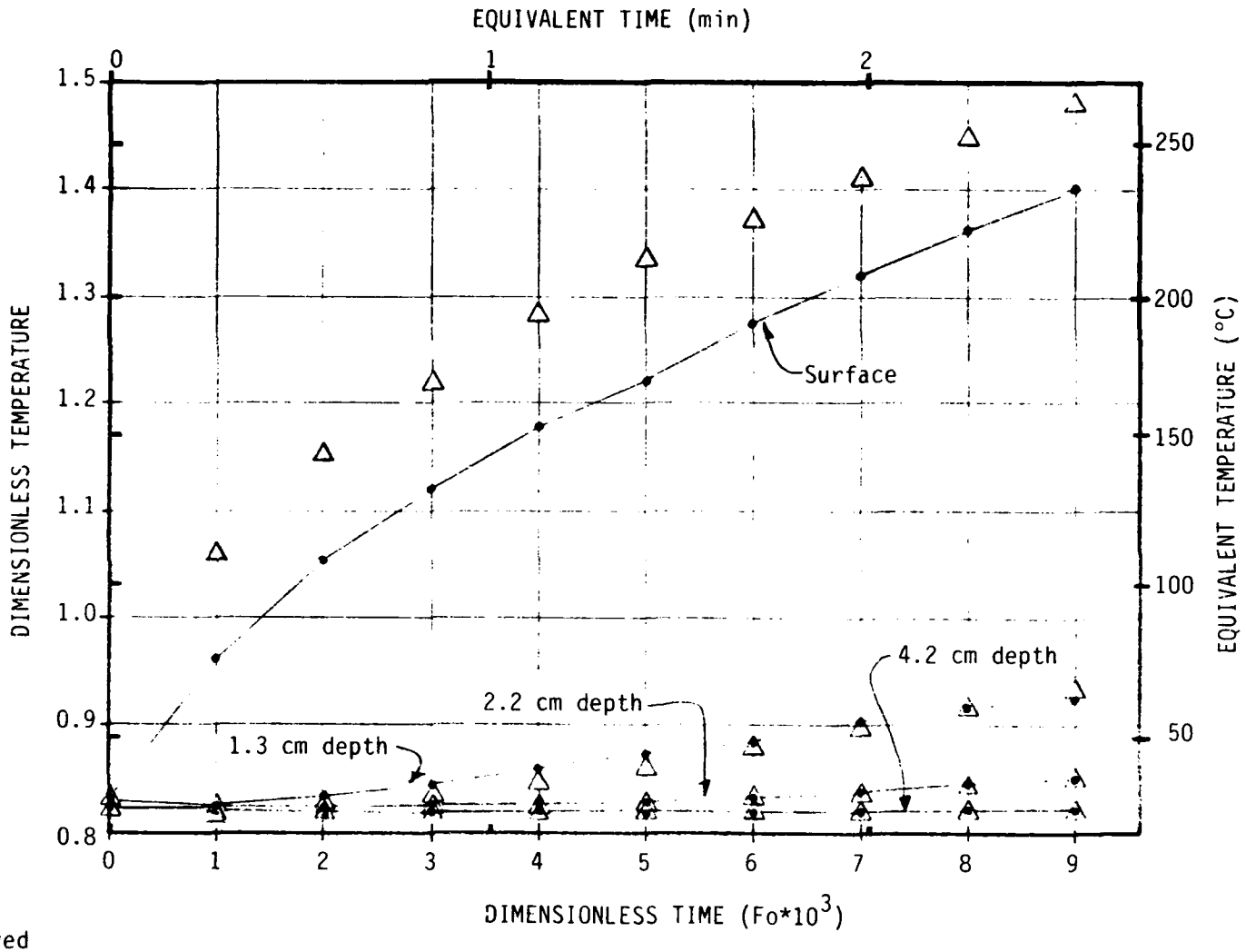

Figure III-4. Measured and Predicted Spatial-Temperature History for a Quick Test.

PART IV

A PARAMETRIC STUDY OF THE HEATING PROCESS FOR ASPHALTIC CONCRETE PAVEMENT

CHAPTER IV-A INTRODUCTION

Preliminary Remarks

Part IV presents a parametric study of the heating process for asphaltic concrete pavement using the HEAT1 code. A detailed description and a complete listing of this code appear in Part II and Appendix II-D, respectively.

A Typical Strategy for Heating Asphaltic Pavement Prior to Removal of a Surface Layer.

The HEAT1 code models the thermal aspects of a recycling process for asphaltic concrete pavement. Specifically, the code models that phase of the recycling process during which a pavement is heated at its upper surface by a fossil fuel-fired heater prior to removal of the upper part of the pavement by mechanical means. The object of the heating process is to reduce the shearing strength of the entire layer of pavement to be removed by raising the temperature of this layer to above a minimum desirable temperature for removal ($T_{removal} \cong 363°K$) without exceeding a maximum allowable temperature ($\cong 505°K$) anywhere in the pavement.

For economic reasons, the heating process must be completed as rapidly as possible. Due to the extremely low thermal diffusivity of asphaltic concrete (See Chapters I-E and I-F) however, a typical pavement heater is capable of raising the surface temperature of the pavement to above the maximum allowable value (505°K) long before the temperature at the removal depth has reached the minimum desirable temperature for removal (363°K). Thus, some contractors have adopted a strategy for heating asphaltic pavement that may be summarized in the following steps:

(1) The pavement is heated until the maximum allowable temperature is reached at the upper surface.

(2) Heating is then discontinued and the surface is insulated for an arbitrarily specified period of time during which the surface temperature deceases due to the diffusion of thermal energy into the interior of the pavement by conduction.

(3) The insulation is removed from the surface and the heating is begun again.

Ideally, this heating insulation cycle is repeated until the temperature reaches the desired value (363°K) at the depth which is to be removed. From a practical standpoint, however, a heating process that requires more than two heating-insulation cycles would be highly undesirable for use in the field by a contractor.

CHAPTER IV-B DESCRIPTION OF THE PARAMETRIC STUDY

Preliminary Remarks

HEAT1 uses a finite-difference technique to perform numerical solutions of the analytical model which governs the heat transfer process in an asphaltic concrete pavement. The analytical model has been recast in nondimensional form, thereby reducing the number of parameters from fourteen to nine. Thus, the parametric study of the heating process consists of:

(1) defining a "nominal heating case"; that is, selecting a set of nominal values for the nine dimensionless parameters in the model;

(2) determining the solution of the problem for the nominal heating case;

(3) systematically varying the values of the parameters in the model to determine their effects on the heating process (specifically, the effects of these variations on the required heating time);

(4) providing physical interpretations of the numerical results;

(5) and identifying (whenever possible) combinations of the dimensionless parameters that result in relatively short heating times.

Note: This is a parametric study, not an optimization study. No attempt has been made to identify an optimum set of the dimensionless parameters which would yield an absolute minimum heating time.

Discussion of the Dimensionless Parameters

The fourteen parameters in the dimensional analytical model of the heating process are defined below:

$h_c \equiv$ convective heat transfer coefficient

$k \equiv$ thermal conductivity of the pavement

$L \equiv$ overall thickness of the pavement

$t^*_{INSUL} \equiv$ duration of the insulation period for the upper surface of the pavement

$T^*_H \equiv$ heater surface temperature

$T^*_{MAX} \equiv$ maximum allowable temperature in the pavement

$T^*_R \equiv$ an appropriate reference temperature for the convective heat transfer

$T^*_{REM} \equiv$ temperature to which the pavement must be heated at the depth to which it is to be removed (x^*_{REM})

$T^*_{SOIL} \equiv$ temperature at the bottom surface of the pavement

$x^*_{REM} \equiv$ depth of pavement which is to be removed

$\alpha \equiv$ thermal diffusivity of the pavement

$\varepsilon_H \equiv$ emissivity of the heater surface

$\varepsilon_S \equiv$ emissivity of the upper surface of the pavement

$\sigma \equiv$ Stefan-Boltzman constant

AD-A141 691 A STUDY OF THERMAL PROPERTIES AND THE HEATING PROCESS IN ASPHALTIC CONCRETE(U) TENNESSEE UNIV KNOXVILLE DEPT OF CIVIL ENGINEERING W H HIGHTER ET AL. FEB 84 2/2

UNCLASSIFIED AFOSR-TR-84-0432 AFOSR-82-0250 F/G 11/2 NL

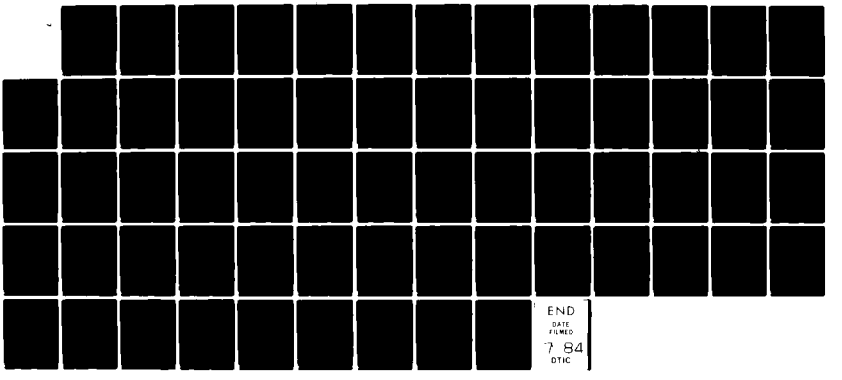

END
DATE FILMED
7 84
DTIC

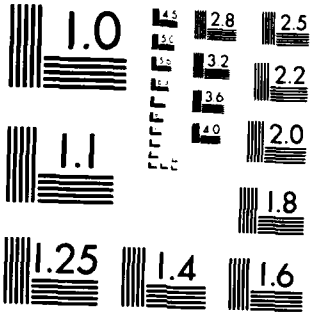

The minimum, maximum, and nominal values of the fourteen dimensional parameters are shown in Table IV-1. The data in Table IV-1 show that the values of the parmeters T^*_{MAX}, T^*_{REM}, x^*_{REM}, and σ remain constant throughout the parametric study and that the value of the reference temperature for convective heat transfer (T^*_R) is assumed to be equal to the heater surface temperature (T^*_H). Also, note that the nominal heating case assumes that the heat transfer at the upper surface of the pavement is by radiation alone (no convective heat transfer). Finally, it should be mentioned at this point that the entire parametric study (with two exceptions to be discussed later) was performed under the assumption of a uniform initial temperature profile in the pavement ($T^*_{INITIAL} = T^*_{SOIL}$).

When the analytical model is recast in nondimensional form, the fourteen dimensional parameters defined above are combined to give the nine dimensionless parameters shown below:

$$A \equiv \frac{\sigma L T^{*3}_{REM}}{k\left(\frac{1}{\varepsilon_H} + \frac{1}{\varepsilon_S} - 1\right)} = \text{radiation - conduction parameter} = \frac{\text{(thermal conductance for radiation heat transfer)}}{\text{(thermal conductance for conduction heat transfer)}}$$

$$Bi \equiv \frac{h_c L}{k} = \text{Biot number} = \frac{\text{(thermal conductance for convection heat transfer)}}{\text{(thermal conductance for conduction heat transfer)}}$$

$$t_{INSUL} \equiv \frac{t^*_{INSUL}}{(L^2/\alpha)} = \text{dimensionless duration of the insulation period for the upper surface of the pavement}$$

$$T_H \equiv \frac{T^*_H}{T^*_{REM}} = \text{dimensionless heater temperature}$$

$$T_{MAX} \equiv \frac{T^*_{MAX}}{T^*_{REM}} \quad (= 1.391) = \text{dimensionless maximum allowable temperature in the pavement}$$

DIMENSIONAL PARAMETER	MINIMUM VALUE	MAXIMUM VALUE	NOMINAL VALUE
h_c, $\left(\frac{W}{M^2\text{-}^\circ K}\right)$	0	300	0
k, $\left(\frac{W}{M\text{-}^\circ K}\right)$	0.9	1.65	1.2
L, (M)	0.254	0.381	0.3048
t^*_{INSUL}, (Sec)	60	300	300
T^*_H, ($^\circ$K)	573.16	1253.16	673.16
T^*_{MAX}, ($^\circ$K)	505	505	505
T^*_R, ($^\circ$K)	573.16	1253.16	673.16
T^*_{REM}, ($^\circ$K)	363.16	363.16	363.16
T^*_{SOIL}, ($^\circ$K)	273.16	310.94	293.16
x^*_{REM}, (M)	0.0254	0.0254	0.0254
α, $\left(\frac{M^2}{Sec}\right)$	3.7×10^{-7}	1×10^{-6}	6.6×10^{-7}
ε_H, (-)	0.3	0.58	0.44
ε_S, (-)	0.75	0.95	0.9
σ, $\left(\frac{W}{M^2\text{-}^\circ K^4}\right)$	5.6697×10^{-8}	5.6697×10^{-8}	5.6697×10^{-8}

TABLE IV-1. Summary of the Minimum, Maximum, and Nominal Values of the Fourteen Parameters in the Dimensional Model of the Heating Process.

$$T_R \equiv \frac{T^*_R}{T^*_{REM}}$$ = dimensionless reference temperature for convective heat transfer

$$T_{REM} \equiv \frac{T^*_{REM}}{T^*_{REM}}$$ = dimensionless temperature to which the pavement must be heated at the depth to which it is to be removed (X_{REM})

$$T_{SOIL} \equiv \frac{T^*_{SOIL}}{T^*_{REM}}$$ = dimensionless temperature at the bottom of the pavement (the initial dimensionless temperature throughout the pavement)

$$X_{REM} \equiv \frac{X^*_{REM}}{L}$$ = dimensionless depth of the pavement which is to be removed.

The minimum, maximum, and nominal values of the nine dimensionless parameters are given in Table IV-2. These values were computed using the data in Table IV-1 and are the values used to perform the parametric study.

Selection of the Dimensionless Spatial and Time Increments

The finite-difference solution of the heating process performed by the HEAT1 code requires the selection of dimensionless spatial and time increments. On the basis of a number of trial runs, the following values were chosen for these quantities:

(dimensionless spatial increment) = $\Delta x = .01$ (101 nodal points)

(dimensionless time increment) = $\Delta t = 10^{-6}$

The entire parametric study was performed using these values.

DIMENSIONLESS PARAMETER	MINIMUM VALUE	MAXIMUM VALUE	NOMINAL VALUE
A	0.114	0.647	0.289
Bi	0	127	0
t_{INSUL}	1.529×10^{-4}	2.131×10^{-3}	2.131×10^{-3}
T_H	1.578	3.451	1.854
T_{MAX}	1.391	1.391	1.391
T_R	1.578	3.451	1.854
T_{REM}	1.0	1.0	1.0
T_{SOIL}	0.752	0.856	0.807
x_{REM}	0.0667	0.1	0.0833

TABLE IV-2. Minimum, Maximum, and Nominal Values of the Nine Dimensionless Parameters used to Perform the Parametric Study.

CHAPTER IV-C RESULTS OF THE PARAMETRIC STUDY

The Nominal Heating Case

The nominal heating case is defined by the nominal values of the nine dimensionless parameters listed in Table IV-2. Representative temperature histories and distributions are presented here in graphical form. Figure IV-1 shows the surface and removal depth temperature histories. The monotonically rising surface temperature clearly shows that no insulation periods are required for the nominal case. The heater temperature is low enough that thermal energy can diffuse into the pavement by conduction fast enough to raise the temperature at the removal depth to its required value (=1.0) before the surface temperature exceeds the maximum allowable value (=1.391) in the pavement. The Fourier number at the end of the heating period is (13.4×10^{-3}), which corresponds to a heating time of 31.5 (min). From a practical point of view, this is an unacceptably long heating period.

Figure IV-2 shows the dimensionless temperature profiles in the pavement at different dimensionless times during the heating period. These profiles dramatically illustrate the exceptionally low value of the thermal diffusivity of asphalt. At the end of the heating period (31.5 min), thermal energy from the surface heating has diffused through only about 40% of the total thickness of the pavement.

The Effect Of Initial Pavement Temperature On Heating Time

Figure IV-3 shows the effect of the initial pavement temperature (T_{SOIL}) on the heating time for an otherwise nominal case. The minimum value of T_{SOIL} (0.752) yields a dimensionless heating time of (17.89×10^{-3}), or 42.05 min.; while the maximum value of T_{SOIL} (0.856) requires a heating time of (9.822 x

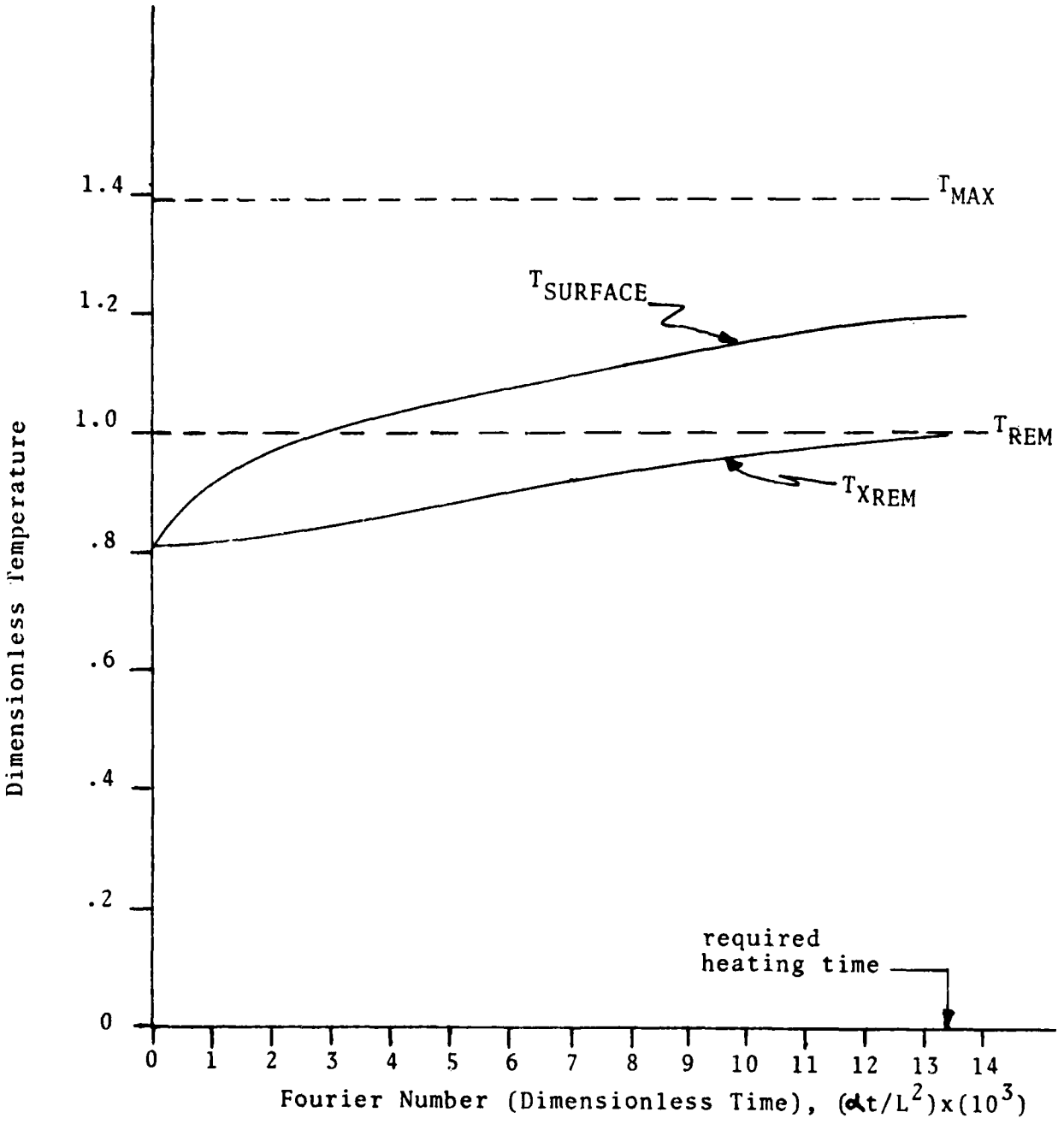

Figure IV-1. Surface And Removal Depth Temperature Histories For The Nominal Heating Case

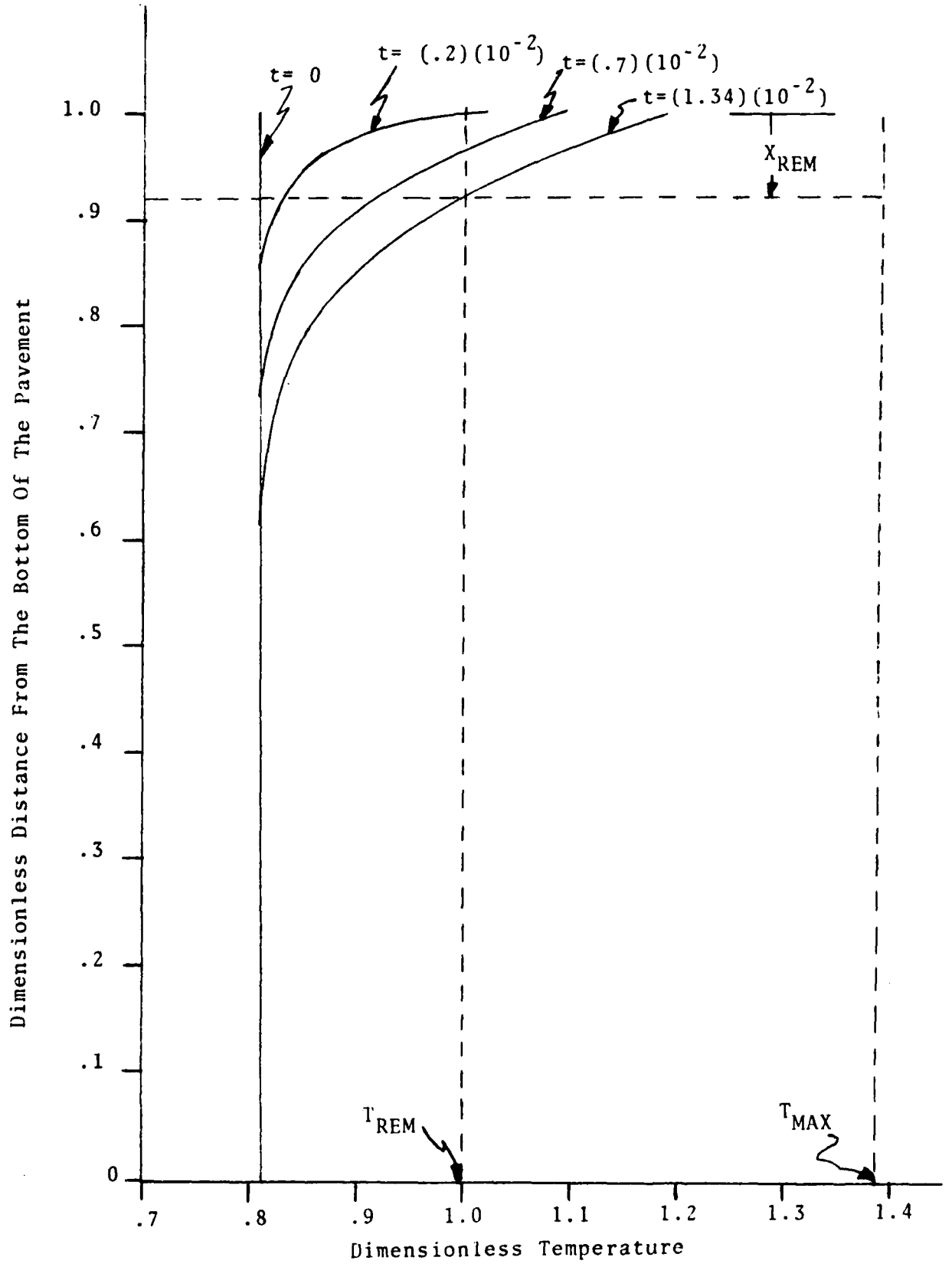

Figure IV-2. Dimensionless Temperature Profiles In The Pavement For The Nominal Heating Case

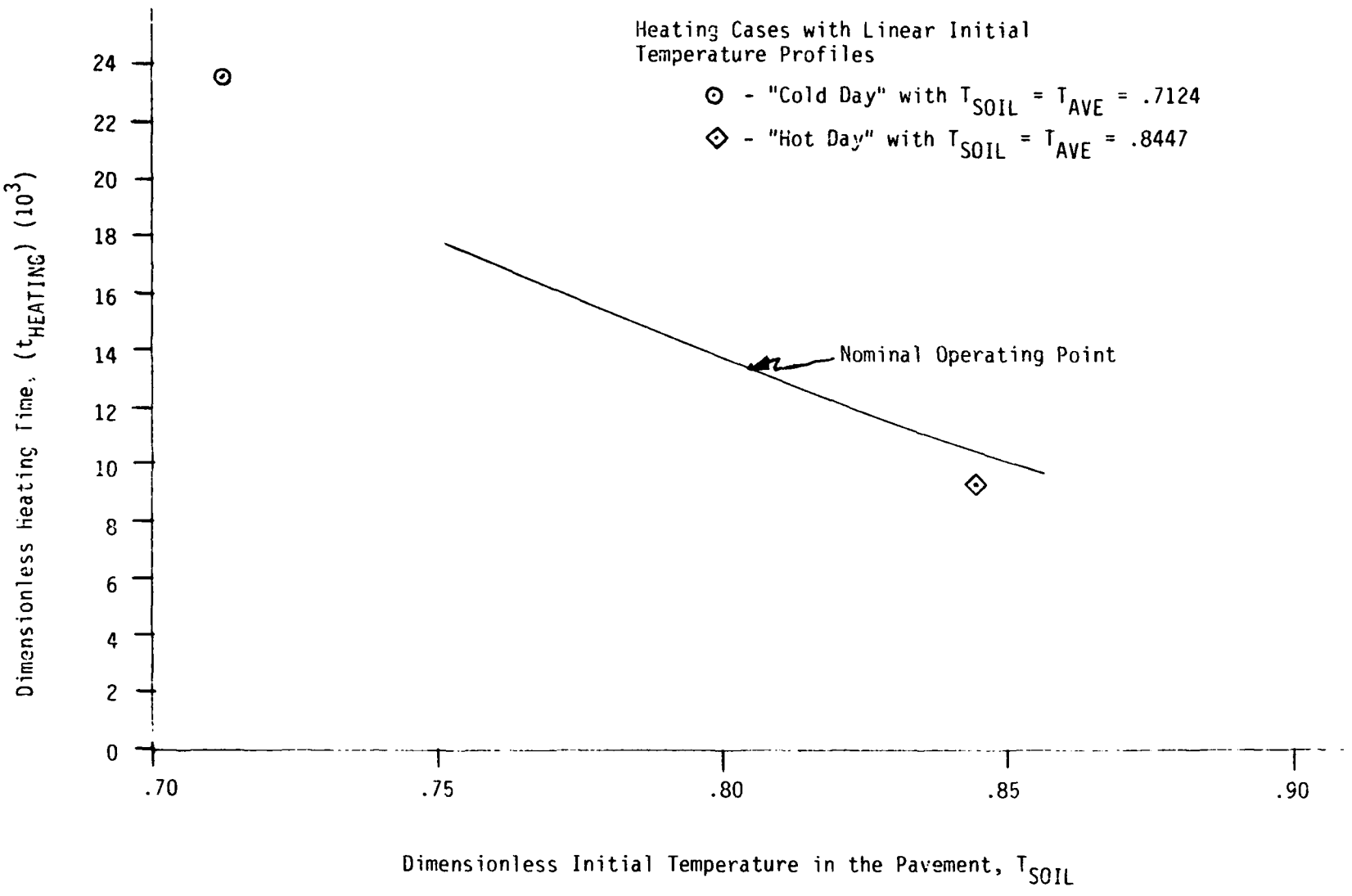

Figure IV-3. The Effect of Initial Pavement Temperature on Heating Time

10^{-3}), or 23.08 min. Comparing these times with the nominal heating time of (13.4×10^{-3}), or 31.5 min., shows as expected, that initial temperatures lower or higher than the nominal initial value (0.807) significantly increase or decrease, respectively, the required heating time. Note, however, that even the minimum heating time of 23.08 min. is unacceptable large.

All of the above calculations were made by assuming a uniform initial temperature distribution in the pavement. It is well-known, however, that the initial temperature distribution in an actual pavement is nonuniform, although the general functional form of this distribution is unknown. Thus, in order to assess the validity of performing the parametric study with a uniform initial temperature distribution, two heating cases were computed using nonuniform (linnear) initial temperature profiles. These profiles, which are specified in the HEAT1 code, are based on soil and surface temperatures representative of typical "hot" and "cold" days. The results of these two cases are also displayed in Figure IV-3. The plotting of these two points is based on the assumption that the appropriate values of T_{SOIL} are given by the average of the soil and surface temperatures for each profile. The heating time for the linear initial temperature profile for a hot day is seen to be less than the heating time for a uniform initial temperature distribution with the same value of T_{SOIL} (0.8447). This arises from the fact that the initial temperatures in the layer to be removed are higher than $T_{SOIL} = 0.8447$ for the hot day case with a linear initial temperature profile. Analogous reasoning can be used to explain why the data point for the cold day heating case lies above the (extrapolated) heating time versus initial temperature curve. These calculations clearly indicate that the heating times computed by assuming uniform initial temperature profiles are highly representative of the heating times that would result from the (more complicated) computations based on more realistic nonuniform initial temperature

profiles. Thus, all subsequent calculations in the parametric study are based on the assumption of uniform initial temperature profiles.

The Effects Of Heater Temperature and the Duration Of the Insulation Period on Heating Time

The heating time is shown as a function of the heater temperature (T_H) in Figure IV-4. The parameter in Figure IV-4 is the duration of the insulation period, t_{INSUL}, which assumes its maximum value (2.131×10^{-3}), an intermediate value (1.2×10^{-3}), and its minimum value (0.1529×10^{-3}). The other seven dimensionless parameters retain their nominal values during this portion of the parametric study.

Figure IV-4 clearly shows that, for any given value of t_{INSUL}, the heating time - heater temperature curve is a U-shaped curve which is concave upward. Thus, there are two values of the heater temperature which correspond to any given value of the heating time. The entire curve for a given value of t_{INSUL} is composed of two distinct branches: a "left-hand branch" for $T_H < 2.257$ and a "right-hand branch" for $T_H > 2.257$. As shown in Figure IV-4, the left-hand branch is independent of the value of t_{INSUL}. This branch, which represents the locus of all those operating points for which no insulation periods are required, includes the nominal operating point. Thus, for all of the operating points on the left-hand branch of the curve the thermal processes in the pavement are qualitatively the same as those for the nominal point, which are portrayed in Figures IV-1 and IV-2. For all such cases the temperature at the removal depth reaches the desired value for removal, T_{REM}, before the surface temperature reaches the maximum allowable value in the pavement, T_{MAX}. Therefore, when operating on the left-hand branch of the curve, the heating time can always be reduced by increasing the heater temperature. Such reductions are possible, of course, because increases in the heater temperature result in allow-

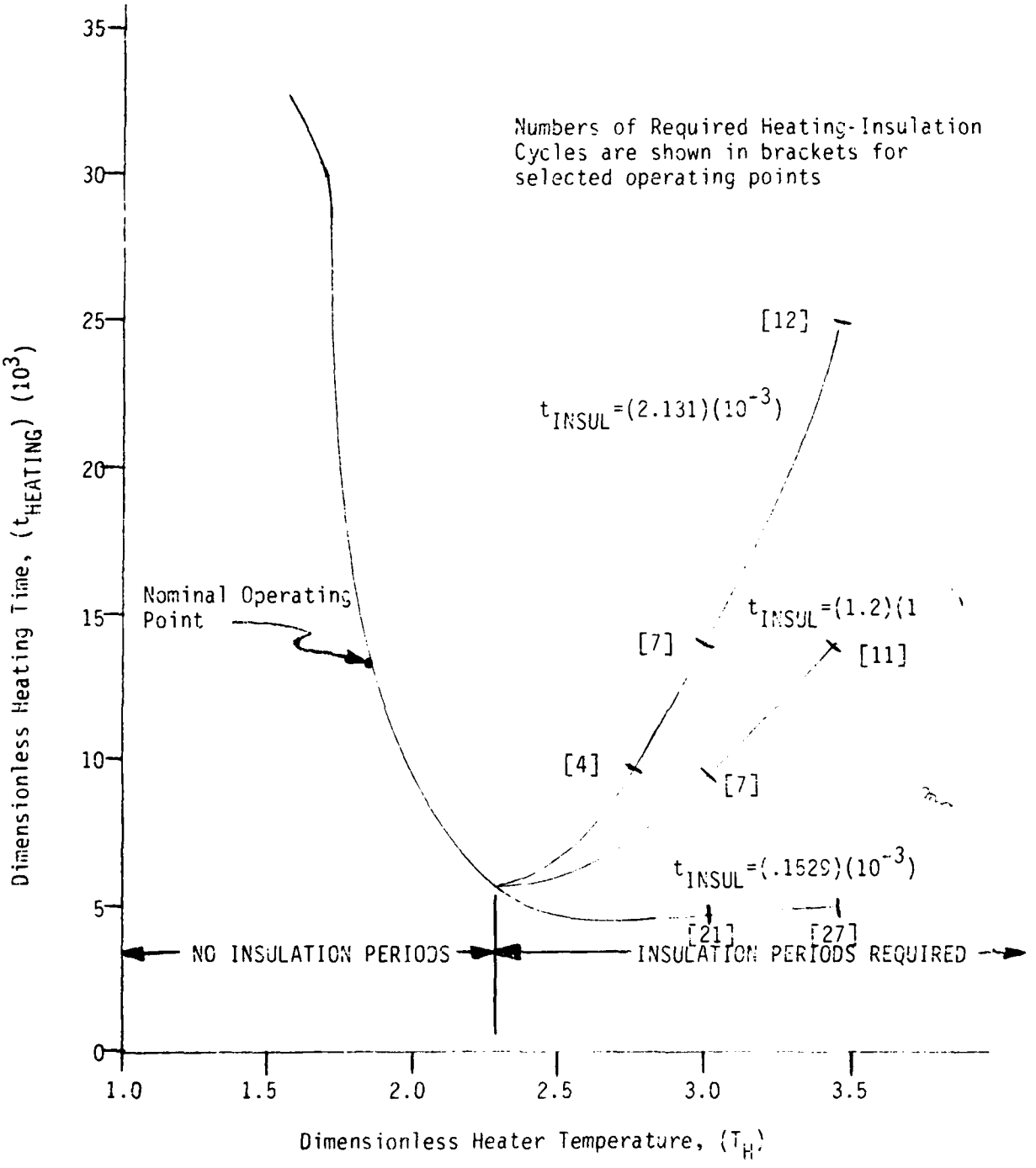

Figure IV-4. The Effect of Heater Temperature on Heating Time

able increases in the surface temperature. These increases in the surface temperature steepen the time-averaged temperature gradient which serves as the potential for the transfer of thermal energy by conduction in the pavement. This behavior continues until T_H reaches a value of 2.257, which corresponds to the minimum heating time of 5.947×10^{-3} for which no insulation periods are required. At this point, the surface temperature reaches T_{MAX} at exactly the same instant as the temperature at the removal depth reaches T_{REM}. Any further increases in T_H cause the surface temperature to reach T_{MAX} before the temperature at the removal depth reaches T_{REM}, thereby necessitating the use of at least one insulation period. Thus, the right-hand branch of the heating time versus heater temperature curve corresponds to the locus of all those operating points for which one or more insulation periods are required. The numbers of heating-insulation cycles for a selected group of such operating points are displayed in Figure IV-4.

At first glance, the right-hand branch of the curve exhibits a rather unexpected behavior; that is, increases in heater temperature result in corresponding increases in the required heating time. Qualitatively this behavior is independent of the value of t_{INSUL}; however, as may be seen in Figure IV-4, the magnitude of these increases in heating time is a strong function of t_{INSUL}. Thus two important features of the right-hand branch of the curve must be explained: (1) the qualitative effects of t_{INSUL} on the heating time for a given heater temperature, and (2) the relative independence of the heating time on the heater temperature for small values of t_{INSUL}.

As shown in Figure IV-4, when t_{INSUL} assumes its largest possible value (2.131×10^{-3}), the heating time varies over a wide range of values as a function of the heater temperature. This trend for a large value of t_{INSUL} is easily explained with the aid of Figure IV-5, which is a plot of the surface and removal depth temperature histories for a heater temperature of 2.75 and

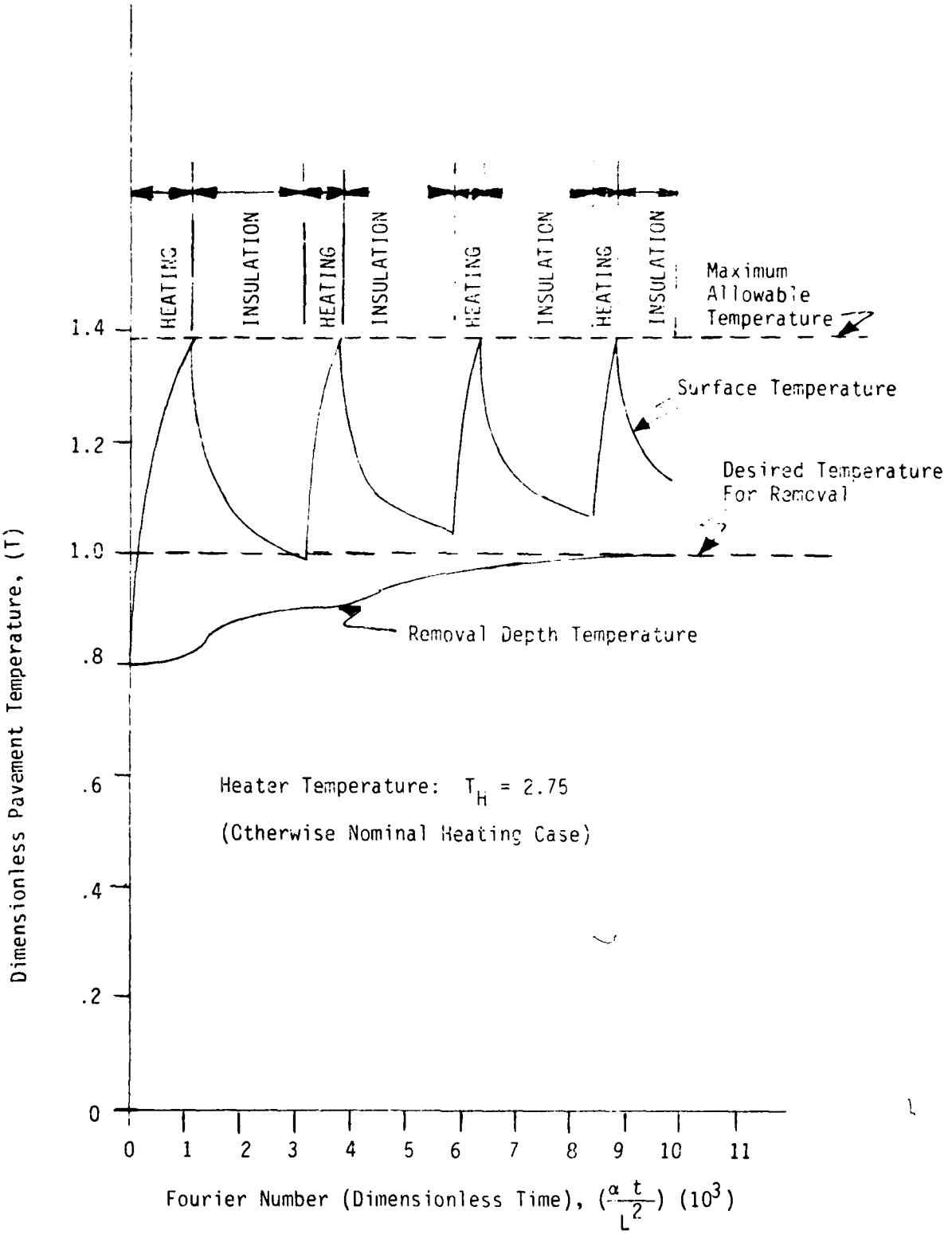

Figure IV-5. Surface and Removal Depth Temperature Histories for a Typical Case Requiring Multiple Heating - Insulation Cycles - Nominal Insulation Period

$t_{INSUL} = 2.131 \times 10^{-3}$. At heater temperatures greater than 2.257, the surface temperature rises quickly and reaches T_{MAX} before the temperature at the removal depth reaches T_{REM}. As may be seen in Figure IV-5, this initiates an insulation period of a duration which is significantly longer than that of a typical heating period. During each of these "long" insulation periods, thermal energy diffuses into the interior regions of the pavement by conduction; however, the flow of additional thermal energy into the pavement at its upper surface is delayed until the end of the insulation period. Thus, the net effect of employing a long insulation period is to markedly flatten out the temperature gradient in the pavement. This reduces the time-averaged rate of conduction heat transfer into the interior of the pavement and thereby increases the required heating time.

In contrast to this behavior for a large value of t_{INSUL}, Figure IV-4 reveals that the behavior of the right-hand branch is qualitatively different for small values of t_{INSUL}. This difference in behavior may be best explained in terms of an optimal (minimum time) heating process. In this idealized optimal heating process the initial heater temperature would be so large that the surface temperature would rise to T_{MAX} in a very short period of time; however, this would not initiate an insulation period. Instead, the heater temperature would be reduced in a manner such that the surface temperature was maintained at a constant value of T_{MAX} until the temperature at the removal depth had risen to T_{REM}. This process would result in the maximum possible time-averaged temperature gradient in the pavement and, therefore, in the minimum possible heating time. (The absolute minimum heating time would be obtained in the limiting case of the optimal heating process which corresponds to a step change in the surface temperature from T_{SOIL} to T_{MAX}. Under otherwise nominal conditions, the required heating time in this limit is (3.66×10^{-3}); or approximately 8.6 minutes). Implementation of the optimal heating process obviously requires the use

of a variable temperature heater; however, this is forbidden by the scope of the present study. It is possible, though, to operate a constant temperature heater such that the deviation of the actual surface temperature history from the optimal surface temperature history is arbitraily small. This can be accomplished by decreasing the duration of the insulation period, t_{INSUL}. For a very small value of t_{INSUL} there is only a slight decrease in the surface temperature from T_{MAX} during an insulation period, after which the heater quickly raises this temperature back to T_{MAX}.

Thus, in the limit of t_{INSUL} approaching zero the surface temperature oscillates in a very narrow band of temperatures with an upper bound of T_{MAX}. The width of this band can always be made less than any desired value by choosing a small enough value of t_{INSUL}. Since the duration of a typical heating period also approaches zero in the limit of t_{INSUL} approaching zero, the surface temperature history very closely approximates the optimal surface temperature history which accounts for the low heating times for small values of t_{INSUL}. Furthermore, the difference between the surface temperature at the end of an insulation period and T_{MAX} approaches zero as t_{INSUL} approaches zero. Since this temperature difference is small and the value of T_H is relatively large, the duration of the ensuing heating period will be essentially independent of the value of T_H. Thus, since t_{INSUL} is a fixed value, the required heating time will be a weak function of the heater temperature.

The behavior described above for small values of t_{INSUL} is portrayed in Figures IV-4 and IV-6. In Figure IV-4 the right-hand branch of the heating time versus heater temperature curve for the minimum value of t_{INSUL} (0.1529×10^{-3}) exhibits the expected relatively low values of the heating time and the weak dependence of the heating time on heater temperature. Figure IV-6 is a plot of the surface and removal depth temperature histories for a heater temperature of 2.75 and the shortest possible insulation period (0.1529×10^{-3}). [Recall that

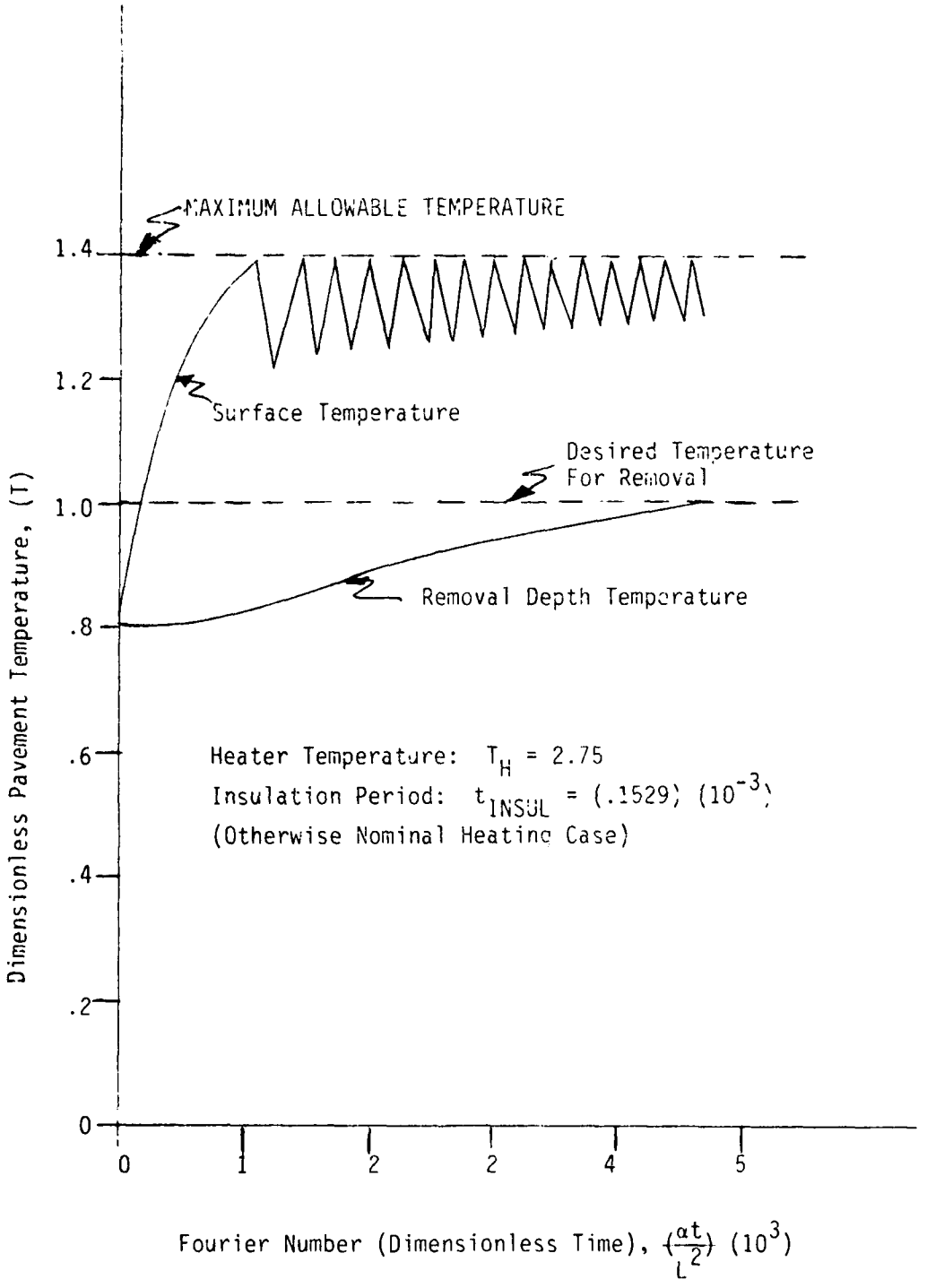

Figure IV-6. Surface and Removal Depth Temperature histories for a Typical Case Requiring Multiple Heating-Insulation Cycles-Minimum Insulation Period

Figure IV-5 is a plot of these same temperature histories for T_H = 2.75 and the maximum value of t_{INSUL} (2.131×10^{-3})]. Figures IV-4, IV-5, and IV-6 illustrate the effect of t_{INSUL} on the heating time, which is reduced from (9.845×10^{-3}) to (4.688×10^{-3}) as t_{INSUL} decreases from its maximum value of (2.131×10^{-3}) to its minimum value (0.1529×10^{-3}) at a heater temperature of 2.75. Figures IV-5 and IV-6 also portray the approach of the surface temperature history to the optimum surface temperature history in the limit of t_{INSUL} approaching zero as described above.

The forgoing discussions might lead to the erroneous conclusion that the best heating process for an asphaltic concrete pavement is one which employes a heater temperature greater than 2.257 and the smallest possible value of t_{INSUL}. In the present study this would reduce the heating time from the minimum value required for no insulation periods (13.4×10^{-3}) to the minimum value of (4.688×10^{-3}) corresponding to a heater temperature of 2.75 at the smallest possible value of t_{INSUL} (0.1529×10^{-3}), a reduction of 65 percent. As shown in Figure IV-6, however, the number of heating-insulation cycles [14] required to achieve this reduction is unacceptably large for practical implementation.

Based on the above discussion, the following conclusions may now be made:

(1) The minimum possible heating time may be achieved with heater temperatures greater than 2.257 and with the minimum value of t_{INSUL}.

(2) This is not a practical mode of operation, however, since the number of heating-insulation cycles is prohibitively large.

(3) The use of the "heating-insulation cycle strategy" by paving contractors should be discontinued since it is not a practical technique.

(4) Paving contractors who wish to employ surface heating techniques should operate their heaters at the maximum possible temperature (2.257 in this

study) below which no heating-insulation cycles are required.

Note: This recommendation is based on the assumption of no convective heat transfer. As will be shown, a more economical (lower than 2.257) heater temperature may be employed if there is some convective heating at the upper surface of the pavement.

The Effect of the Biot Number on the Heating Time

The Biot number, which is defined by the expression ($h_c L/k$), may be interpreted physically as the ratio of the thermal conductance for convective heat transfer to the thermal conductance for conduction heat transfer. For the nominal heating case all of the heat transfer at the upper surface of the pavement is assumed to take place by radiation. Thus, the Biot number for this case is identically equal to zero. As the Biot number increases from zero, the net rate of heat transfer to the pavement (radiation plus convection) increases due to the increase in convection heat transfer with no corresponding increase in the heater temperature. Therefore, qualitatively, an increase in the Biot number should have the same effect on the required heating time as an increase in the heater temperature. This behavior is, indeed, displayed in Figure IV-7, which shows the required heating time as a function of the Biot number for an otherwise nominal heating case. The characteristic U-shaped curve may be interpreted in the same manner as the heating time versus heater temperature curve (Figure IV-4). Of special interest here is the left-hand branch of the curve which corresponds to the locus of all those operating points for which no heating-insulation cycles are required. When operating on this branch, increases in the Biot number result in decreases in the required heating time. This behavior persists up to a Biot number of 10, which corresponds to a dimensionless heating time of (4.694×10^{-3}), or 11.75 minutes under nominal conditions.

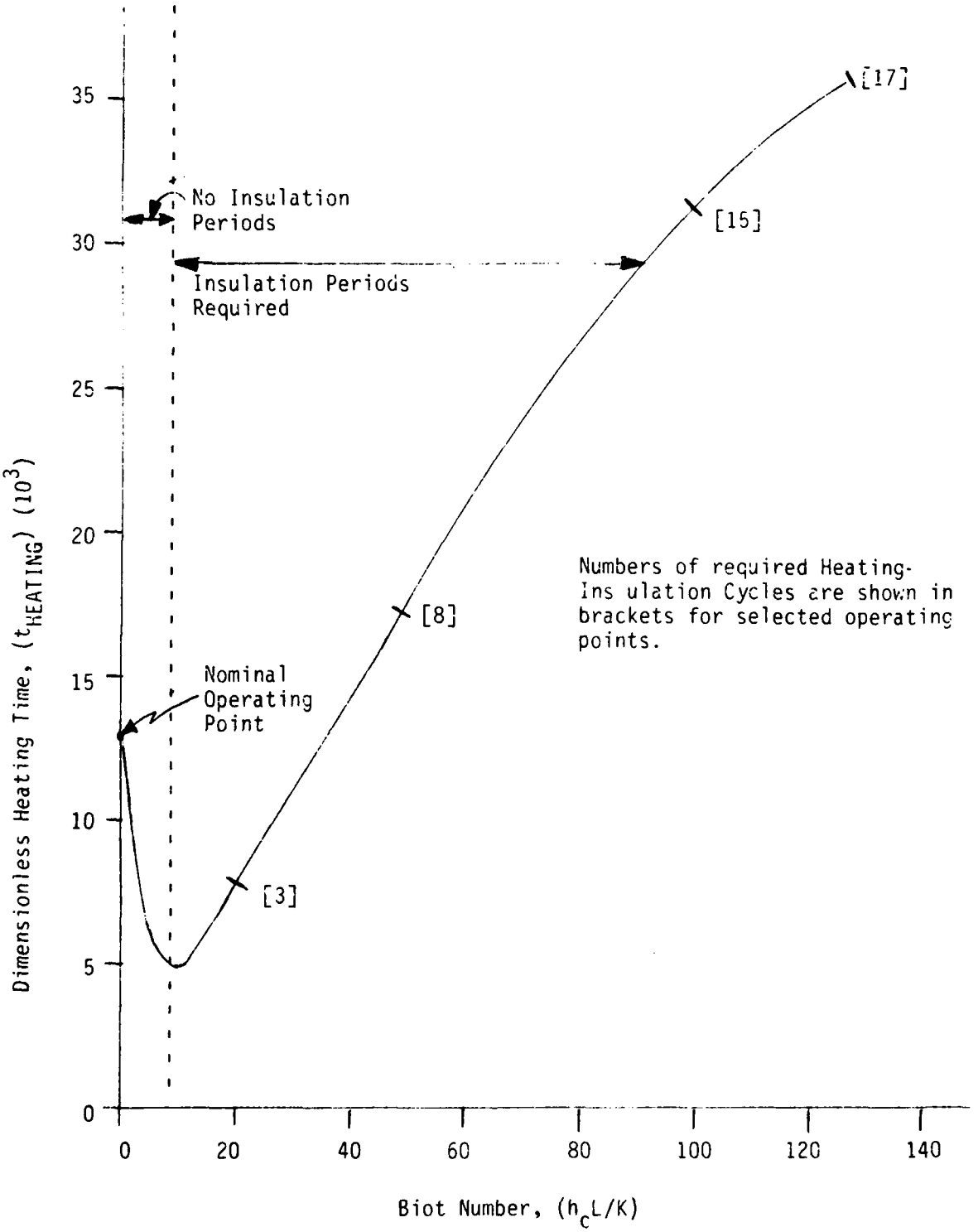

Figure IV-7. The Effect of Convective Heating on Heating Time

Since heater fuel consumption is directly proportional to some function of the heater temperature, it is always desirable to operate the heater at the lowest possible temperature. Thus, an important result may now be found by noting that the minimum heating time of (4.964×10^{-3}) for an off-nominal Biot number of 10 was computed for a nominal heater temperature of 1.854. This time corresponds to a 16.6% reduction from the minimum heating time of (5.947×10^{-3}) computed for a nominal value (zero) of the Biot number and an off-nominal heater temperature of 2.257.

Therefore, we may conclude that:

(1) The use of convective heating is desirable.

(2) Operating points on the right-hand branch of the heating time versus Biot number curve are always impractical.

The first conclusion is, of course, based on the fact that the minimum heating time may be reduced to (4.964×10^{-3}) by employing convective heating such that the Biot number is 10. (Additional information on the desirability of convective, as opposed to radative, heating will be included in the following section). The second conclusion follows since operating points on the right-hand branch of the curve correspond to longer than minimum heating times and require prohibitively large number of heating-insulation cycles as shown in Figure IV-7.

The Effect of the Radiation-Conduction Parameter ("A") on the Heating Time

Figure IV-8 displays the effect of the radiation-conduction parameter, which is defined by the expression:

$$A = \frac{\sigma L T^{*3}_{REM}}{k(1/\varepsilon_H + 1/\varepsilon_S - 1)}$$

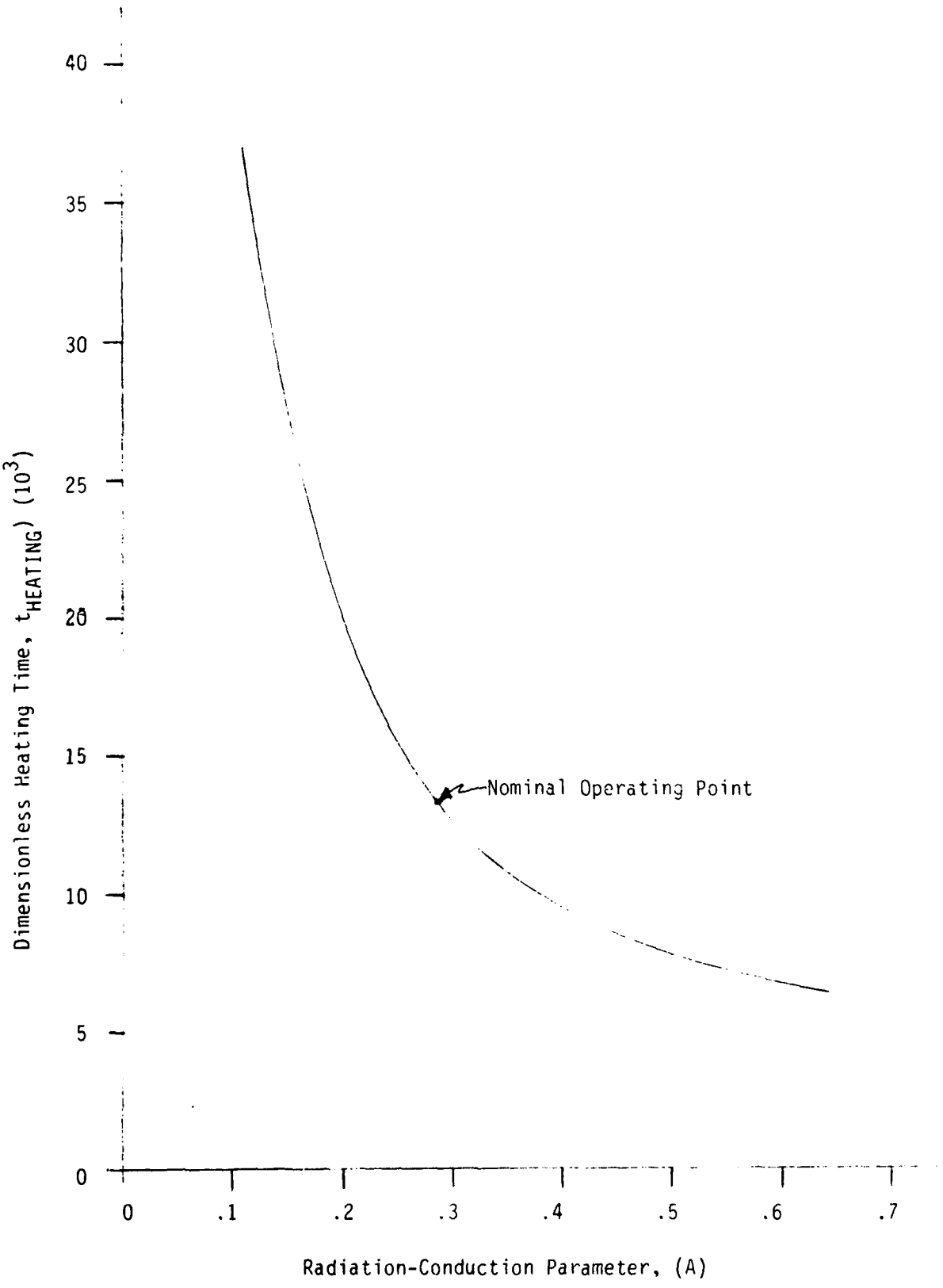

Figure IV-8. The Effect of the Radiation-Conduction Parameter on Heating Time

on the heating time for an otherwise nominal heating case. This parameter may be interpreted physically as the ratio of the thermal conductance for radiation heat transfer to the thermal conductance for conduction heat transfer.

Over the range of values of A considered in the present study (0.114 - 0.647), the heating time is seen to be a monotonically decreasing function of A. Since the Biot number is equal to zero for the nominal heating case (no convective heat transfer) and the parameter A is always less than unity, the behavior exhibited in Figure IV-8 clearly indicates that the heating process with no convection is "radiation controlled". Thus, the overall rate of transfer of thermal energy from the heater to the inner regions of the pavement is limited in this case by the radiative heat transfer process at the upper surface of the pavement, rather than by the diffusion of thermal energy by conduction in the pavement. Therefore, when A increases (meaning that the thermal conductance for radiation increases relative to the thermal conductance for conduction) there should be a corresponding decrease in the heating time as shown in Figure IV-8. Given the extremely low thermal diffusivity of asphaltic concrete, this is an interesting and, perhaps, unexpected result which suggests that the use of a thermal radiation heater is a rather inefficient technique for this application.

A deeper understanding of the above result and the result of the previous section can be obtained by examining the relative importance of the radiative and convective heat transfer process for the otherwise nominal case for which the Biot number is 10. Keeping in mind the physical interpretations of the Biot number (Bi) and the radiation-conduction parameter (A), we have for this case:

$$\frac{Bi}{A} = \frac{h_c}{\dfrac{\sigma T^{*3}_{REM}}{(1/\varepsilon_S + 1/\varepsilon_H - 1)}} = \frac{\text{thermal conductance for convection heat transfer}}{\text{thermal conductance for radiation heat transfer}}$$

$$\text{or,} \quad \frac{Bi}{A} = \frac{10}{.289} = 34.6;$$

that is, the thermal conductance for convective heat transfer is approximately 35 times greater than the thermal conductance for radiation heat transfer. This suggests that a convection heater, rather than a thermal radiation heater, should be used for the surface heating of asphaltic concrete pavements. Finally, since the radiative heating is essentially negligible with respect to the convective heating for this case, the physical interpretation of the Biot number as the ratio of the thermal conductance for convection to the thermal conductance for conduction shows that, when convection heating dominates radiative heating, the overall heat transfer process is "diffusion limited". This means that the overall rate of transfer of thermal energy from the heater to the inner regions of the pavement is controlled by the diffusion of thermal energy by conduction in the pavement.

The Effect of Removal Depth on Heating Time

The effect of removal depth on heating is displayed in Figure IV-9 for an otherwise nominal case. As expected, this plot simply shows that increasing the removal depth increases the required heating time.

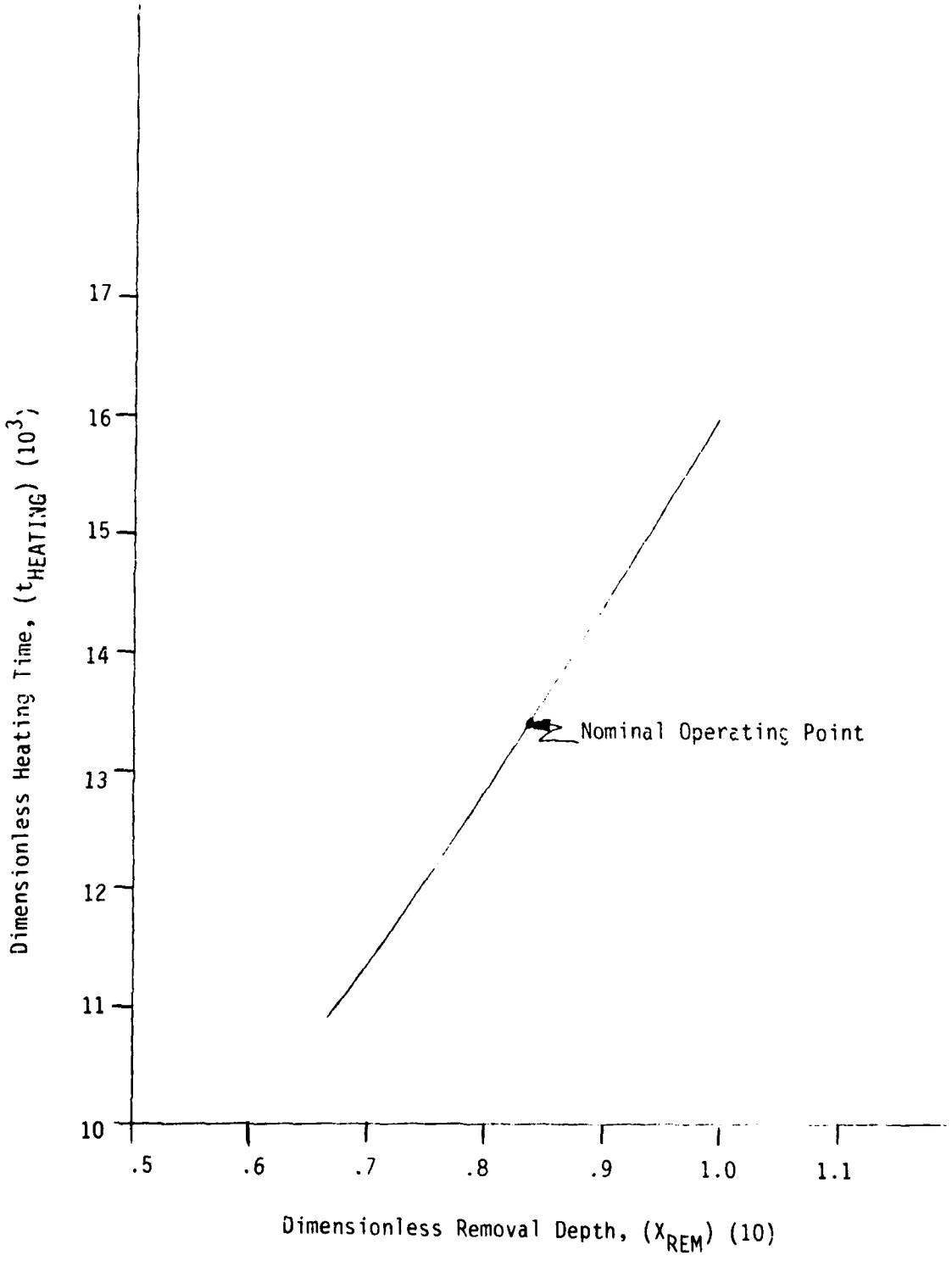

Figure IV-9. The Effect of Removal Depth on Heating Time

PART V

SUMMARY OF RESULTS

AND CONCLUSIONS

CHAPTER V-A SUMMARY OF PART I-THERMAL PROPERTIES

As a result of the research described Part I, the following results and conclusions can be stated:

1. In analyzing heat transfer in asphaltic concrete pavement having limestone or granite-gneiss aggregate, this study indicates that an average value of specific heat and an average value of diffusivity can be used which are independent of asphalt content but depend on the aggregate gradation and type. The conductivity used in analysis must take into account the asphalt content in addition to the aggregate type and gradation.

2. Both aggregate type and gradation have a greater effect on the thermal properties of asphaltic concrete pavement than does the percentage of asphalt present in the mix.

3. There are two opposing mechanisms that influence the thermal conductivity of an asphaltic concrete mix as the asphalt content is increased. On one hand the replacement of air in the voids by asphalt tends to increase the conductivity of the mix because the conductivity of asphalt is much higher than that of air; on the other hand the additional asphalt increases the thickness of the coating around aggregates which tends to decrease the conductivity of the mix because the conductivity of asphalt is much less than that of the aggregate. The dominant mechanism depends on the asphalt content and the mix properties such as the largest particle sizes present, the gradation, and the specific surface.

4. For a given aggregate type, as the percentage of air voids in an asphaltic concrete is increased, the thermal conductivity of the mix will decrease

because the thermal conductivity of air is less than that of asphalt or aggregate. Also, entrapped air in the aggregate particles tends to decrease the thermal conductivity of the mix.

5. The specific heat capacity of the six laboratory mixes tested did not vary systematically as the asphalt content was increased. The specific heat is more dependent on the aggregate gradation and mineralogy than the asphalt content. Based on these data, it seems that an average value of c for each mix, independent of asphalt content, could be used.

6. The thermal diffusivity of the open graded surface course mixes (limestone and granite-gneiss aggregates) is essentially independent of asphalt content; the diffusivity of the limestone base course mix and the limestone and granite-gneiss dense graded surface course mixes varied about 12% over the range of asphalt contents used in the mixes. The diffusivity of the dense graded surface course mix having lightweight aggregate is much less than that of the dense graded limestone mix and is essentially independent of asphalt content.

7. The thermal and physical properties analyses of the field specimens from Myrtle Beach and Loring Air Force Bases indicate no relationship between the properties tested (ρ, k, c, and α) and asphalt content. There is a relationship between the thermal properties (k, c, and α) and the aggregate type present in the samples. The average (of 21 samples) thermal conductivity of the Loring samples is slightly higher that that of the Myrtle Beach samples due to the lower conductivity of the quartz sand fine aggregate present in the Myrtle Beach pavement. The average specific heat of the Myrtle Beach samples is much less than that of the Loring samples,

because the Loring slate-basalt aggregate has higher specific heat than the Myrtle Beach granite and quartz sand aggregate.

8. The thermal properties (k, c, and α) of asphaltic pavement samples can be determined with about 5.8% or less uncertainty by using the apparatus and procedure described in Chapter I-C and Appendix I-A.

CHAPTER V-B SUMMARY OF PART II - NUMERICAL MODEL

As a result of the research performed in Part II, the following conclusions and results can be summarized:

1. The errors incurred by modeling the process of heat transfer through a three layer asphaltic concrete pavement as that of the transfer of heat through a one-layer (homogeneous) body are negligibly small.

2. The nondimensional form of the numerical model was programmed for execution on a digital computer. In the program, heating is begun and continues until either the surface temperature reaches a maximum allowable value (flash point of asphalt), or the temperature at the prescribed removal depth attains a desired value, at which time the process is terminated. If the temperature at the removal depth has not reached the desired value before the maximum allowable surface temperature is reached, the heating is terminated and the surface of the pavement in insulated for a specified period of time and the cycle is repeated until the desired temperature at the removal depth is obtained.

3. A "nominal" heating case was described in which (a) typical values of the parameters in the model were assumed; (b) the surface of the pavement was assumed to be heated by radiation alone (no convection) and; (c) the initial temperature distribution in the pavement was assumed to be uniform.

4. The analysis showed that for the nominal heating case no insulation periods were required i.e., the heater temperature was low enough that thermal energy could diffuse into the pavement by conduction fast enough to raise the temperature at the prescribed removal depth to its required value before the surface temperature exceeded its maximum allowable value. For the nominal case, the required heating time was an unacceptably long 31.5 minutes.

5. Because of the very low diffusivity of asphaltic concrete, for the heating time of 31.5 minutes in the nominal case, only the upper 40% of the total thickness of the pavement experienced an increase in temperature due to the surface heating.

CHAPTER V-C SUMMARY OF PART III - VALIDATION OF THE MODEL

As a result of comparing measured pavement temperature histories from field tests carried out at Myrtle Beach and Loring Air Force Bases and histories predicted for these tests by the thermal model, the following points can be made:

1. The results of the tests carried out at Myrtle Beach Air Force Base in March of 1983 were considered to be unreliable because the coastal winds prevailing at the time disturbed the temperature patterns in the air between the heater and pavement surface. Because of the wind gusts, unpredictable convective cooling of the pavement surface occurred and surface temperatures as well as heater temperatures fluctuated widely. Thus no meaningful analysis of these tests could be made.

2. The wind problem was alleviated during the field tests carried out at Loring Air Force Base in June of 1983 by erecting a corrugated steel "wind" fence about 3m square and 0.8m high around each test site.

3. Analyses of the Loring test data indicated that the analytical model consistently predicted higher temperature at the pavement surface than were measured by thermocouples. This was to be expected due to conduction cooling of the thermocouples beads. The error introduced in the measurements could not be calculated but the error analysis is in the right direction i.e. it indicates that the measured surface temperatures were lower than what actually existed.

4. Comparison of the predicted and measured temperature histories for points in the pavement below the surface indicated that the model did a fair to excellent job in predicting temperature histories. Generally, the predicted-measured temperature data matched more closely as the depth from the pavement surface increased. At the typical removal depth of 2.5 cm, the computer model predicted the temperature time data extremely well.

5. Although the commercially available heater used in the study was purported to be a radiant heater, test data tend to support the belief that convective cooling around the edges of the heater was an important characteristic and should be incorporated in the analysis.

CHAPTER V-D SUMMARY OF PART IV - PARAMETRIC STUDY

In the parametric study a nominal heating case was defined and the solution of the problem was obtained as described previously. Then the values of the parameter in the model were systematically varied to determine their effects on the heating process. As a result of this part of the study, the following conclusions and results can be stated:

1. The initial temperature of the pavement significantly affects the required heating time. Also, it was found that the heating time computed by assum-

ing uniform initial pavement temperature profiles was an excellent approximation of the heating time resulting from a more realistic nonuniform initial temperature profile.

2. The heating time - heater temperature curve was found to be a U-shaped curve which is concave upward. The bottom of the curve defines the minimum heating time corresponding to the heater temperature at which the surface temperature reaches its maximum allowable value at the same time the desired removal temperature is reached at the prescribed removal depth.

3. For heater temperatures greater than that corresponding to the bottom of the U-shaped curve, the surface temperature reaches its maximum allowable value before the removal temperature is reached at the removal depth. Thus, insulation periods are required in this (the right hand) part of the curve.

4. In the left hand part of the curve the heating time can be decreased by increasing the heater temperature. In this part of the heating time - heater temperature curve, the removal temperature is reached at the removal depth before the surface temperature reaches its maximum allowable value and no insulation periods are required.

5. The analysis indicated that heating times could be decreased below the value corresponding to "no insulation" only if many heating - insulation cycles of very short duration were used. Since this is not a practical alternative to use in the field, an important finding of this research is that "soaking" or insulation periods should not be used in heating asphaltic pavements. The best strategy is to use the maximum temperature below which no heating - insulation cycles are required.

6. Some convection in addition to radiant heat transfer from the heater to the pavement surface is desirable because it decreases the minimum required heating time. Alternatively, for a given heating time, the required heater temperature can be reduced if some convection heat transfer occurs. The minimum heating time with no insulation cycles corresponded to a Biot number of 10.

7. It was found that if there were no convective heat transfer, the overall rate of transfer of thermal energy from the heater to the inner regions of the pavement is limited by the radiative heat transfer process at the surface of the pavement rather than by diffusion of thermal energy by conduction in the pavement. This suggests that use of a radiative heater is a rather inefficient technique for heating pavements even though the diffusivity of asphaltic concrete is small.

8. Further analysis suggested that a combined convection-thermal radiation heater, rather than a thermal radiation heater alone, should be used for the surface heating of asphaltic concrete pavement.

REFERENCES

REFERENCES

1. ASHRAE Handbook & Product Directory, 1977 Fundamentals, Chapter 22, Design Heat Transmission Coefficients, Published by the American Society of Heating, Refrigerating, and Air-Conditioning Engineers, Inc., New York, 1978, pp. 22.1-22.28.

2. Aldrich, H. P., Jr., "Frost Penetration Below Highway and Airport Pavements," Highway Research Board Bulletin No. 135, 1956, pp. 124-149.

3. Barber, E. S., "Calculation of Maximum Pavement Temperature from Weather Reports," Highway Research Board Bulletin No. 168, 1957, pp. 1-8.

4. Beck, J. V., and Al-Araji, S., "Investigation of a New Simple Transient Method of Thermal Property Measurement," Journal of Heat Transfer, ASME, February 1974, pp. 59-64.

5. Birch, F., "Thermal Conductivity and Diffusivity," Section 17 of Handbook of Physical Constants, Edited by Birch, F., Schairer, J. F., and Spicer, H. C., Geologic Society of America Special Papers Number 36, 1942, pp. 243-265.

6. Brown, A. I., and Marcro, S. M., Introduction to Heat Transfer, Third Edition, McGraw-Hill Book Company, 1958, 332 pp.

7. Carlson, H., and Kersten, M. S., "Calculating Depth of Freezing and Thawing Under Pavements," Highway Research Bulletin No. 71, 1953, pp. 81-98.

8. Carmichael, T., Boyer, R. E., and Hokanson, L. D., "Modeling Heater Techniques for In-Place Recycling of Asphalt Pavements," Proceedings of the Association of Asphalt Paving Technologists, Vol. 46, 1977, pp. 526-540.

9. Carslaw, H. S., Jaeger, J. C. Conduction Heat In Solids, Oxford University Press, 1959.

10. Chesterman, C. W., The Audubon Society Field Guide to North American Rocks and Minerals, Published by Alfred A. Knopf, Inc., 1978, 850 pp.

11. Christison, J. T., and Henderson, K. O., "Response of Asphalt Pavements to Low Temperature Climatic Environments," Proceedings of the Third International Conference on the Structural Design of Asphalt Pavements, Vol. I, September 1972, pp. 41-52.

12. Corlew, J. S., and Dickson, P. F.,"Methods for Calculating Temperature Profiles of Hot-Mix Asphalt Concrete as Related to the Construction of Asphalt Pavements," Proceedings of the Association of Asphalt Paving Technologists, Vol. 37, 1968, pp. 101-140.

13. Corlew, J. S., and Dickson, P. F., "Cold Weather Paving of Thin Lifts of Hot-Mixed Asphalt on Preheated Asphalt Base," Highway Research Record, No. 385, 1972, pp. 1-6.

14. Cragoe, C. S., "Thermal Properties of Petroleum Products," Micellaneous Publication No. 97, U. S. National Bureau of Standards, November 9, 1929, 48 pp.

15. Dempsey, B. J., and Thompson, M. R., "A Heat Transfer Model for Evaluating Frost Action and Temperature-Related Effects in Multilayered Pavement Systems," Highway Research Record No. 342, 1970, pp. 39-56.

16. Frenzel, B. G., Dickson, P. F., and Corlew, J. S., "Computer Analysis for Modification of Base Enviromental Conditions to Permit Cold Weather Paving," Proceedings of the Association of Asphalt Paving Technologists, Vol. 40, 1971.

17. Gebhart, B., Heat Transfer, Second Edition, McGraw-Hill Book Company, 1971, 596 pp.

18. Goranson, R. W., "Heat Capacity; Heat of Fusion," Section 16 of the Handbook of Physical Constants, Edited by Birch, F., Schairer, J. F., and Spicer, H. C., Geological Society of America Special Papers Number 36, 1942, pp. 223-242.

19. Kavianipour, A., and Beck, J. V., "Thermal Property Estimation Utilizing the LaPlace Transform With Application to Asphaltic Pavement," International Journal of Heat and Mass Transfer, Vol. 20, No. 3, March 1977, pp. 259-266.

20. Kline, S. J., and McClintock, "Describing Uncertainties in Single-Sample Experiments, Mechanical Engineering, January 1953, p. 3.

21. Marks, L. S., Editor, Mechanical Engineers Handbook, Section 4--Heat, Fifth Edition, McGraw-Hill Book Company, 1951, pp. 273-392.

22. O'Blenis, J. D., "Thermal Properties of West Virginia Highway Materials," M. S. Thesis, Civil Engineering Department, West Virginia University.

23. Rumney, T. N., and Jimenez, R. A., "Pavement Temperatures in the Southwest," Highway Research Record No. 361, 1971, pp. 1-13.

24. Saal, R. N. J., "Physical Properties of Asphaltic Bitumen. 2. Surface Phenomena, Thermal and Electrical Properties, Etc," Chapter III in The Properties of Asphaltic Bitumen, Pfeiffer, J. Ph., Editor, Elsevier Publishing Company, Inc, 1950, 285 pp.

25. Southgate, H. F., and Deen, R. C., "Temperature Distribution Within Asphaltic Pavement and Its Relationship to Pavement Deflection," Highway Research Record No 291, 1969, pp. 116-128.

26. Spall, M., "Developing a Thermal Model For Asphaltic Concrete," M. S. Thesis, Department of Mechanical and Industrial Engineering, Clarkson College of Technology, Potsdam, New York, 1982, 68 pp.

27. Sparrow, E. M., "Error Estimates in Temperature Measurements," in Measurements in Heat Transfer, Eckert, E. R. G. and Goldstein, R. J., Editors, Second Edition, McGraw-hill, 1976, 642 pp.

28. Straub, A. L., Schenk, H. L., Jr., and Przybycien, F. E., "Bituminous Pavement Temperature Related to Climate," Highway Research Record No. 256, 1968, pp. 53-77.

29. Warme, P. K., TEMPSENSE Temperature Monitoring Package, Interactive Microware, Inc., 1982, 13 pp.

30. Wolfe, R. K., and Colony, D. C., "Asphalt Cooling Rates: A Computer Simulation Study," Report No. OHIO-DOT-07-06, Ohio Department of Transportation, October 1976, 91 pp.

31. Wolfe, R. K., Heath, G. L., and Colony, D. C., "University of Toledo Time Temperature Model Laboratory and Field Validation," Report No. FHWA/OH-80/006, Ohio Department of Transportation, April 1980, 56 pp.

32. Yoder, E. J., and Witczak, M. W., Principles of Pavement Design, Second Edition, John Wiley and Sons Inc., 1975, 711 pp.

APPENDIXES

APPENDIX I-A

TEMPERATURE MEASURING SYSTEM

The TEMPSENSE Temperature Monitoring System marketed by Interactive Microware (29) in conjunction with an Apple II+ 48K computer was used to collect temperature and time data. This Appendix provides a brief description of the TEMPSENSE system and of the hardware used in collecting the data.

The hardware provided with the TEMPSENSE system includes an ADALAB data acquisition interface card, an ADA-MUX 8-channel multiplexer, and an ADA-AMP variable-gain instrumentation amplifier. The voltage from each thermocouple goes first through the multiplexer, which is a switching device, then to the amplifier where the voltage is amplified. The amplified voltage is then routed to the analog to digital converter on the ADALAB interface card. Interpolation tables for many types of thermocouples are stored in the software.

Copper-constantan thermocouples of size 30 AWG were used to determine the temperature at the top of the pavement sample (T_t), while size 24 AWG thermocouples were used for the bottom of the pavement sample (T_b). The TEMPSENSE software guides the user through adjustment of the amplifier, calibration of the thermocouples using an ice bath and another known temperature bath, and selection of the cold junction compensation method. A solid state sensor was used to measure the temperature of the cold junction (multiplexer terminal).

After the amplifier is properly adjusted and the thermocouples are calibrated, temperature measurements may be taken. The TEMPSENSE program prompts the user for the frequency of sampling (up to 3 samples per second) and the number of measurements to be averaged for each reading. Then, the total duration of sampling and the name of the disk file is selected. The time of each measurement is listed on the screen, along with the temperature measured by each thermocouple. When the storage buffer is full, the data are automatically

stored on a floppy disk, and measurements continue until the end of the pre-selected duration time. The data are automatically stored in binary form, but the program allows the user to change the binary file to a text file which may be more compatible to some users.

APPENDIX I-B

UNCERTAINTY ANALYSIS

This section presents the precision of each type of measurement (e.g. length, temperature, etc.) and an uncertainty analysis of each of the thermal properties (as suggested by Kline and McClintock, Ref. 20) using the apparatus and procedure described in Chapter I-C. Also included is an analysis of the amount of heat loss from the calorimeter and from the sample holder. The results are summarized in Figure I-B1.

Figure I-B1 shows a schematic drawing of the calorimeter and the sample holder. A steady-state, one-dimensional heat transfer analysis was conducted to determine the approximate amount of heat loss from the calorimeter and the sample holder. The thermal properties of the insulating materials were obtained from References 1 and 21. The analysis shows a heat loss of about 10.7 watts from the calorimeter and about 2.0 watts from the sample holder. For a typical test duration of about 25 minutes, the total heat loss is about 15,910 J from the calorimeter and about 3,010 J from the sample holder.

The percentage of uncertainty of each of the thermal properties was determined in the following manner:

1. An actual test data set was chosen (because of its similarity to several other test data) to represent a typical test data set.
2. The uncertainty of each of the primary experimental measurements is specificed (called w_a, w_b,..., w_n, where the subscript refers to the measurement and w is the uncertainty of that measurement).
3. Each thermal property equation (Equations 7, 8, and 9 of Chapter I-C) is partially differentiated with respect to each of the primary experimental measurements ($\frac{\partial X}{\partial a}$, $\frac{\partial X}{\partial b}$,..., $\frac{\partial X}{\partial n}$, where X is the thermal property equation and a, b,...,n refer to the measurement).

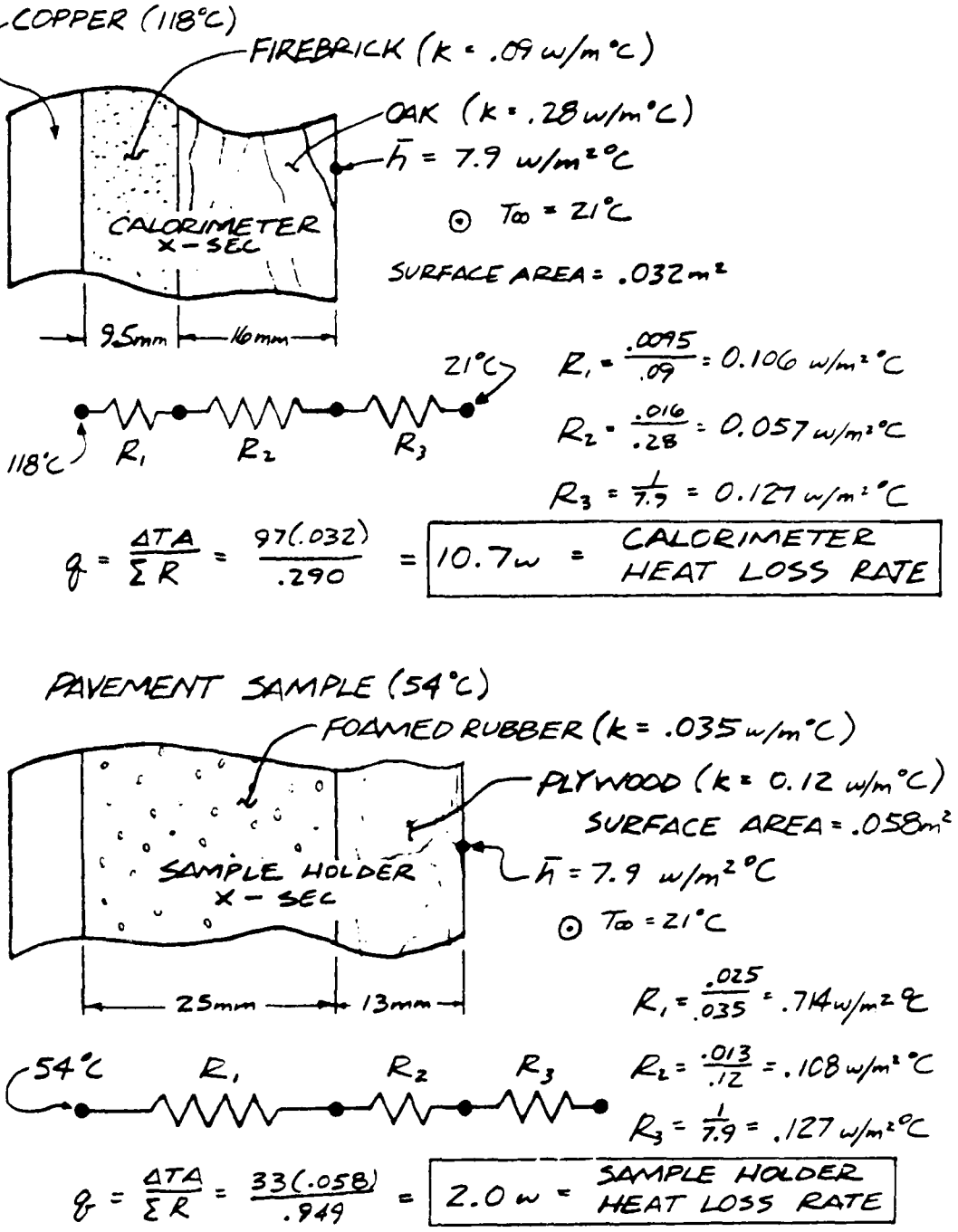

Figure I-B1. Calculations of Potential Heat Loss from the Calorimeter and from the Sample Holder.

4. Kline and McClintock (20) have shown that the uncertainty (w_x) of each of the thermal properties can be determined by the following equation:

$$w_x = [(\frac{\partial X}{\partial a} w_a)^2 + (\frac{\partial X}{\partial b} w_b)^2 + \ldots + (\frac{\partial X}{\partial n} w_n)^2]^{\frac{1}{2}} \qquad \text{(I-B1)}$$

where w_x = uncertainty of the value of equation X

w_n = uncertainty of the primary measurement n

$\frac{\partial X}{\partial n}$ = partial of equation X with respect to the primary measurement n

Using the actual data set and its uncertainties, Equation I-B1 can be solved for the uncertainty of each of the thermal properties (Table I-B1).

TABLE I-B1 SUMMARY OF RESULTS OF UNCERTAINTY ANALYSIS

MEASUREMENT	NOMINAL VALUE	UNCERTAINTY
L	0.0257 m	±0.0005 m
Q	$4.596*10^6$ J	$\pm 0.025*10^6$ J
T_f-T_i	59.44°C	±0.56°C
ρ	2.453 Mg/m^3	±0.016 Mg/m^3
$\int (T_t-T_b)$	10.02°C-hr	+0.56°C-hr

PROPERTY	PERCENT UNCERTAINTY
α	4.5
k	5.9
c	5.6

APPENDIX II-A

JUSTIFICATION FOR MODELING A THREE-LAYER ASPHALTIC CONCRETE PAVEMENT AS A HOMOGENEOUS BODY

OBJECTIVE

The objective of this sub-study is to justify the use of a homogeneous model of a three-layer asphaltic concrete pavement by demonstrating that the errors incurred in the approximation are negligibly small. This objective is accomplished by comparing a characteristic temperature history given by a simplified analytical model of the transient heat transfer in the actual composite pavement with the analogous temperature history given by a homogeneous model of the pavement and showing that these results are virtually identical.

ANALYSIS

In order to facilitate the comparison described above, the pavement is assumed to be a semi-infinite body initially at a uniform temperature, T_i. At time $t = 0$, the surface of the pavement is assumed to undergo a step change in temperature from T_i to T_s. (The surface temperature is maintained at T_s for all $t > 0$.) The transient conduction heat transfer is then computed using two different models of the pavement. First, the pavement is modeled as a composite body consisting of two different homogeneous, constant-property layers (representing the wearing and binder courses). The neglect of the base course and the use of a semi-infinite geometry are reasonable assumptions for the purposes of this side study because of the extremely low thermal diffusivity of asphaltic concrete and the relatively short heating times employed in a typical recycling process. Thus, the wearing course-binder course interface temperature history computed with the two-layer model is assumed to be representative of the actual interfacial temperature history in an asphaltic pavement during the heating

phase of a recycling process. Next, the pavement is modeled as a homogeneous, constant-property body. The temperature history at a distance from the surface in the homogeneous body equal to the interface distance in the two-layer body is then compared with the interface temperature history computed with the two-layer model. The deviations of the former temperature history from that in the two-layer body are assumed to be indicative of the errors incurred in modeling an actual composite pavement as a homogeneous body.

As outlined above, we first assume the pavement is a semi-infinite body occupying the half-space $x > -L$, as shown in Figure II-A1. The body is composed of two layers of different properties. In the region ($-L \leq x \leq 0$), the thermal conductivity, specific heat, density, and thermal diffusivity are given by k, c_1, ρ_1 and α_1, respectively. The temperature in this region is denoted by T_1 and the properties (k_1, c_1, ρ_1, α_1) are assumed to be constants. Similarly, in the region ($0 < x < \infty$) the properties are given by k_2, c_2, ρ_2 and α_2 and the temperature is denoted by T_2. It is also assumed that there is no contact resistance between the two layers in the pavement. Carslaw and Jaeger (9) show that the time-varying temperature distribution in material 2 (the binder course) is given by

$$\frac{T_2(x,t)}{T_s} = \frac{2}{\sigma + 1} \sum_{n=0}^{\infty} \left[\frac{\sigma - 1}{\sigma + 1}\right]^n \text{ERFC}\left[\frac{(2n+1) + \sqrt{\frac{\alpha_1}{\alpha_2}}\left(\frac{x}{L}\right)}{2\sqrt{Fo}}\right] \quad \text{(II-A1)}$$

where:

$$\sigma = \sqrt{\frac{k_2\rho_2c_2}{k_1\rho_1c_1}} \quad . \quad \text{(II-A2)}$$

$$Fo = \frac{\alpha_1 t}{L^2} = \text{Fourier number (dimensionless time)}$$

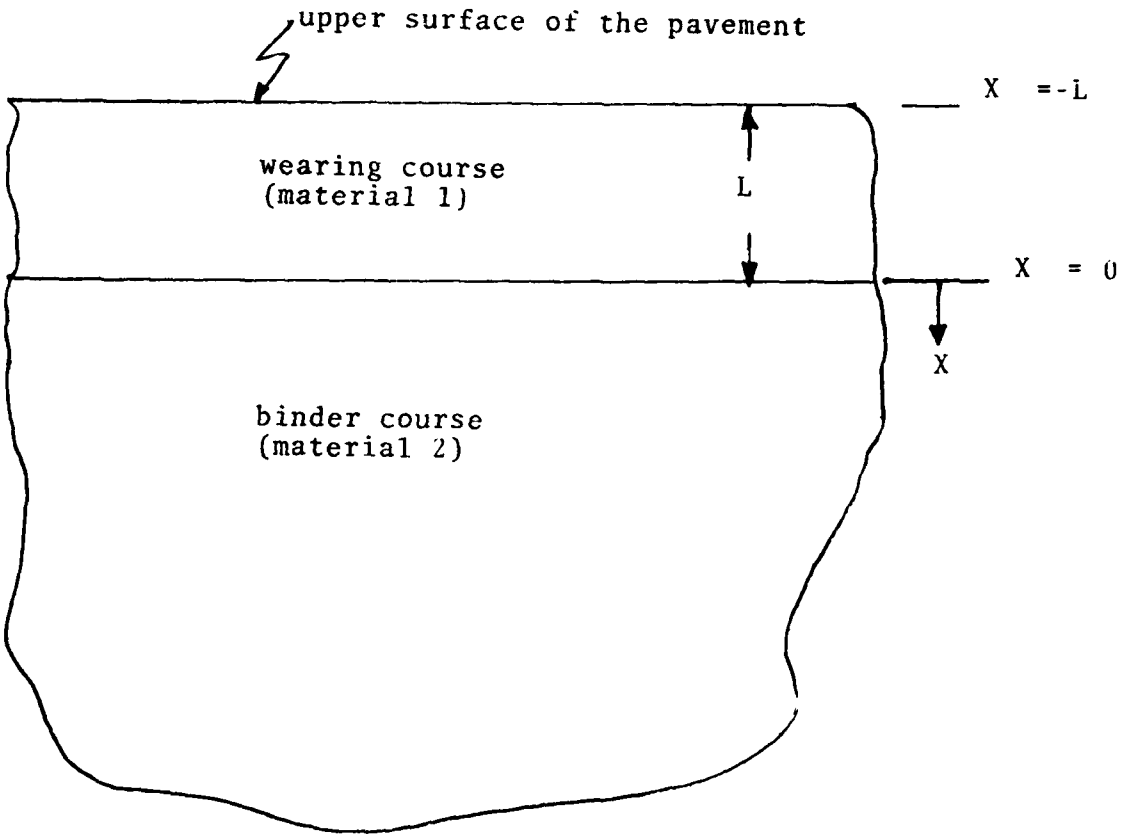

Figure II-A1. Pavement Geometry

Evaluating Equation (II-A1) at x = 0 yields the dimensionless temperature history at the interface between the wearing and binder courses as

$$\left[\frac{T_I\ (t)}{T_s}\right]_{2\ layer} = \frac{T_2(o,t)}{T_s} = \frac{2}{\sigma + 1} \sum_{n=0}^{\infty} \left(\frac{\sigma - 1}{\sigma + 1}\right)^n \text{ERFC}\ \frac{2n + 1}{2\sqrt{Fo}} \qquad \text{(II-A3)}$$

For a homogeneous body material 1 is identical to material 2, $\sigma = 1$, and equation (A3) reduces to:

$$\frac{T_I\ (t)}{T_s}_{HOMOG} = \text{ERFC}\ \frac{1}{2\sqrt{Fo}} \ . \qquad \text{(II-A4)}$$

This, of course, is just the classical result for the temperature history at a distance L from the surface of a semi-infinite homogeneous body that has undergone a step change in surface temperature.

Finally, we assume that

$$\begin{pmatrix}\text{\% error in modeling the}\\ \text{composite pavement as a}\\ \text{homogeneous body}\end{pmatrix} = \begin{pmatrix}\text{\% error in the interface}\\ \text{temperature history}\end{pmatrix} =$$

$$= \left\{\frac{\left(\frac{T_I}{T_s}\right)_{2\ LAYER} - \left(\frac{T_I}{T_s}\right)_{HOMOG}}{\left(\frac{T_I}{T_s}\right)_{2\ LAYER}}\right\} * 100\% \qquad \text{(II-A5)}$$

Equation (II-A5) was evaluated with the aid of a digital computer using Equations (II-A3) and (II-A4). The results are given in Figure II-A2 for a range of Fourier numbers (dimensionless heating times) that correspond to the range of actual heating times expected in recycling processes. The results are displayed for the parameter $\sigma = .9$ and 1.1. These values of σ correspond to $\pm$ 20% differences in the property group (ρCk) between the wearing and binder courses. Such differences are quite conservative and, therefore, the errors encountered in an

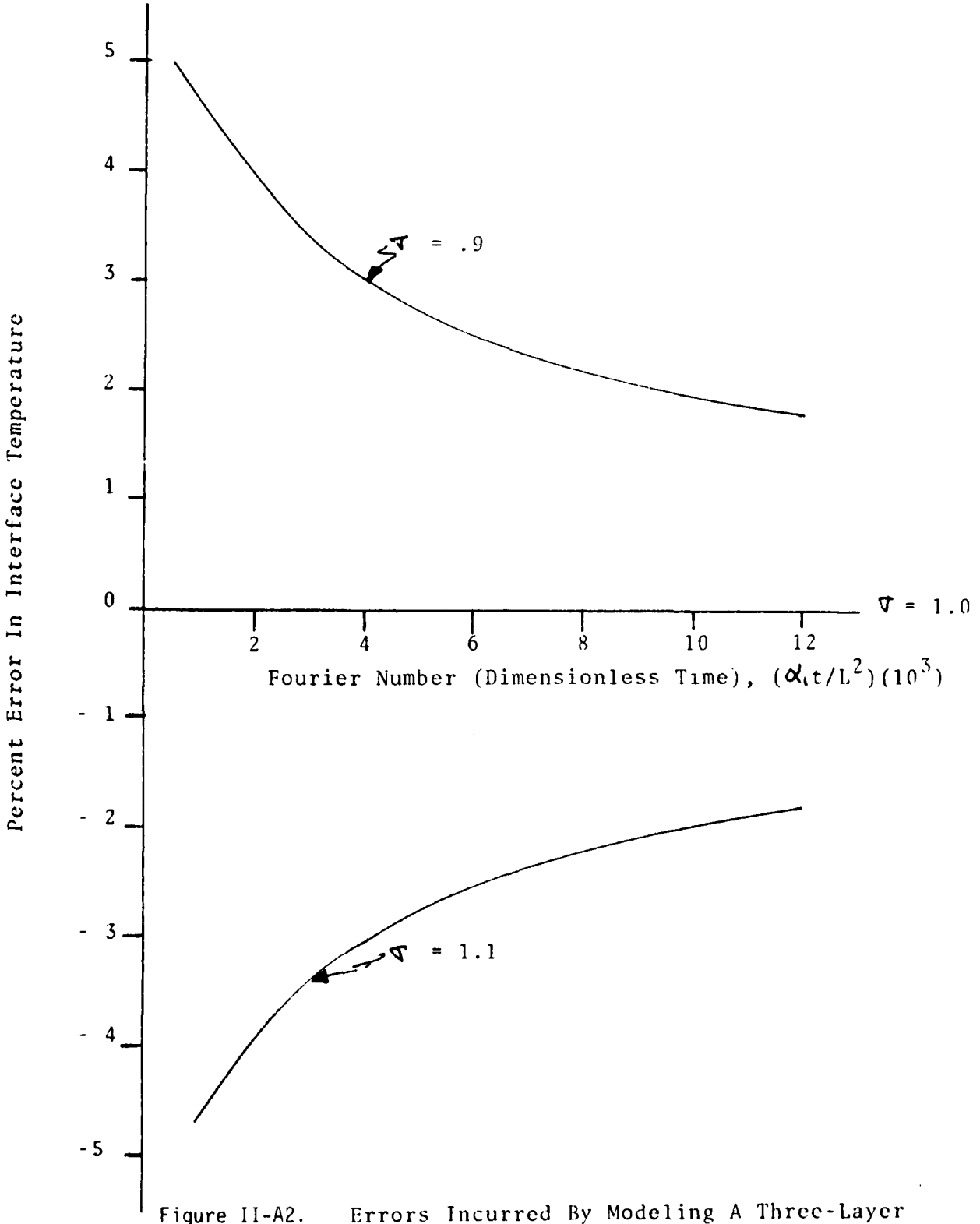

Figure II-A2. Errors Incurred By Modeling A Three-Layer Pavement As A Homogenous Body

actual heating process should be smaller than the limiting values computed with Equation (II-A5) using these values of σ. Figure II-A2 shows, however, that the maximum possible error is only 5%, with a time-average error much closer to 2% when the Fourier number ranges to its maximum possible value. In light of the many illdefined parameters that affect the heat transfer during a typical recycling process, such errors are assumed to be negligibly small. Thus, we may conclude that the transient heat transfer in the upper regions of a three-layer composite pavement may be adequately portrayed by modeling the pavement as a homogeneous body.

APPENDIX II-B

SOME ALTERNATIVE MODELS FOR THE COMBINED RADIATION-CONVECTION HEAT TRANSFER AT THE UPPER SURFACE OF THE PAVEMENT

As stated earlier in this report, the exact relative roles played by convection and radiation in the surface heating of asphaltic pavement are currently not well-understood. Investigators such as Spall (26) have claimed some degree of success in modeling the surface heating of asphaltic pavement as a purely radiative process, however, such minimal evidence is far from conclusive.

Three other possible models of the surface heating process as listed below:

Model 1 - Radiation and Forced Convective Heating

Heat transfer to the pavement surface is by radiation from the heater surface and by forced convection from the hot combustion gases (which are assumed to be in direct physical contact with the pavement).

Model 2 - Radiation and Forced Convective Cooling

Heat transfer to the pavement is by radiation from the heater surface. A forced convective flow of ambient air is assumed to be drawn in from the sides and thereby cool the pavement surface.

Model 3 Radiation and Combined Forced and Natural Convection

Heat transfer to the surface is by radiation from the heater surface. Natural and/or combined natural and forced convective flows of ambient air are assumed to cool the pavement.

APPENDIX II-C

DESCRIPTION OF THE FINITE-DIFFERENCE TECHNIQUE

The Euler method is an explicit technique that computes the temperature $(T_i^*)^{(v+1)}$ at the end of a time interval $\Delta t^* = (t^*)^{(v+1)} - (t^*)^{(v)}$ using the derivative evaluated at the beginning of the time interval, or

$$(T^*)^{(v+1)} = (T_i)^{(v)} + \frac{dT_i^*}{dt^*}^{(v)} (\Delta t^*) .$$

Rewriting this equation in terms of the nondimensional variables gives

$$T_i^{(v+1)} = T_i^{(v)} + \left(\frac{dT_i}{dt} \right)^{(v)} (\Delta t).$$

This method was chosen because of the extreme simplicity of its application. Although it is well-known that explicit methods are subject to unstable numerical oscillations, it is just as well-known that these methods are completely stable if a small enough time interval is employed in the calculations. The usual objection to explicit methods is that the small time intervals required to insure their stability increase the computational times with respect to implicit methods. This shortcoming of explicit methods is far outweighed in the present investigation by the ease of application of explicit techniques since the total computaional time required will be quite small, independent of the numerical technique.

APPENDIX II-D

LISTING OF HEAT1

```
C
C
C     ************************************************************************
C     ************************************************************************
C
C
C     PROGRAM HEAT1
C
C     WRITTEN BY DR. R.J. KRANE
C
C     DEPARTMENT OF MECHANICAL AND AEROSPACE ENGINEERING
C     UNIVERSITY OF TENNESSEE
C     KNOXVILLE , TENNESSEE
C
C
C     ************************************************************************
C     ************************************************************************
C
C
C     INTRODUCTION
C
C     THIS PROGRAM COMPUTES  THE TRANSIENT TEMPERATURE DISTRIBUTION
C     IN AN ASHALTIC PAVEMENT WHEN THE PAVEMENT IS HEATED AT ITS
C     UPPER SURFACE. HEAT TRANSFER AT THIS SURFACE IS ASSUMED TO TAKE
C     PLACE BY A COMBINATION OF BOTH RADIATION AND CONVECTION. THE
C     PROGRAM ALSO COMPUTES THE TRANSIENT TEMPERATURE DISTRIBUTION
C     IN THE PAVEMENT WHEN THE HEATING IS DISCONTINUED AND THE UPPER
C     SURFACE IS INSULATED.
C
C     ALL COMPUTATIONS ARE PERFORMED USING AN EXPLICIT FINITE
C     DIFFERENCE TECHNIQUE WHICH MODELS THE NONLINEAR (RADIATION)
C     BOUNDARY CONDITION ON THE UPPER SURFACE OF THE PAVEMENT. (THIS
C     BOUNDARY CONDITION HAS NOT BEEN LINEARIZED AS WAS DONE IN SOME
C     PREVIOUSLY WRITTEN CODES.)
```


Listing of Heat1

```
C
C
C     HEATING 'STRATEGY'
C
C     THIS PROGRAM MODELS AN ASHALTIC PAVEMENT HEATING STRATEGY THAT
C     MAY BE SUMMARIZED IN THE FOLLOWING STEPS :
C
C     (1) THE PAVEMENT IS HEATED UNTIL THE MAXIMUM ALLOWABLE
C         TEMPERATURE IS REACHED AT THE UPPER SURFACE.
C     (2) HEATING IS THEN DISCONTINUED AND THE SURFACE IS INSULATED
C         FOR AN ARBITRARILY SPECIFIED PERIOD OF TIME (DURING WHICH
C         THE SURFACE TEMPERATURE DECREASES DUE TO DIFFUSION OF
C         THERMAL ENERGY INTO THE INTERIOR OF THE PAVEMENT BY
C         CONDUCTION.)
C     (3) THE INSULATION IS REMOVED FROM THE SURFACE AND THE HEATING
C         IS BEGUN AGAIN.
C
C     THIS CYCLE IS AUTOMATICALLY REPEATED BY THE PROGRAM UNTIL THE
C     TEMPERATURE REACHES THE DESIRED VALUE AT THE DEPTH WHICH IS TO
C     BE SCRAPED OFF WHEN THE HEATING PROCESS IS TERMINATED.
C
C
C     ******************************************************************
C
C
      DIMENSION T(250), TP1(250), DTDT(250)
C
C
      DOUBLE PRECISION TIME, DTIME
C
C
C
C     LOAD DATA
C
```

Listing of Heat1 (cont'd)

```
C       PHYSICAL PARAMETERS
C
        A = .289
        BI = 0.0
        TH = 1.854
        TR = TH
        TSOIL = .807
        TINSUL = .002131
        XREM = .0833
C
C
C
C       PHYSICAL CONSTANTS
C
        TREM = 1.0
        TP1MAX = 1.391
C
C
C       OPERATIONAL CONSTANTS FOR THE PROGRAM
C
        M = 100
        DTIME = .000001
C
C       SWITCH :  = -1.0 (UPPER SURFACE IS BEING HEATED)
C                 =  1.0 (UPPER SURFACE IS INSULATED)
C
        SWITCH = -1.0
C
C       IOPT :  PRINT OPTION INDICATOR
C               IOPT = 1  PROGRAM PRINTS OUT TIME, T(1), TXREM AND THE
C                         ENTIRE TEMPERATURE PROFILE EVERY IMAX TIME
C                         STEPS  ('EXTENDED PRINTOUT')
C               IOPT = 2  PROGRAM PRINTS OUT TIME, T(1) AND TXREM EVERY
C                         IMAX TIME STEPS ('SHORT PRINTOUT')
C
        IOPT = 2
```

Listing of Heat1 (cont'd)

```
C
C
C     IMAX :  PROGRAM PRINTS OUT EVERY IMAX TIME STEPS
C
      IMAX = 200
C
C
C     INITIALIZE THE PRINT COUNTER
C
      IPRINT = 1
C
C
C     INITIALIZE THE INSULATION PERIOD COUNTER
C
      NINSUL = 0
C
C
C
C
C
C     INITIALIZE TIME
C
      TIME = 0.0
C
C
C     DIMENSIONLESS SPATIAL INCREMENT
C
      DELX = 1./FLOAT(M)
C
C
C
C     SELECT THE DESIRED INITIAL TEMPERATURE PROFILE
C
C
C         TIN = -1.0  : LINEAR INITIAL TEMPERATURE PROFILE
C                       FOR A 'COLD DAY'
```

Listing of Heat1 (cont'd)

```
C          TIN =  0.0   : UNIFORM INITIAL TEMPERATURE PROFILE
C
C          TIN =  1.0   : LINEAR INITIAL TEMPERATURE PROFILE
C                         FOR A 'HOT DAY'
C
      TIN = 0.0
C
C
      IF(TIN) 40, 41, 42
C
C     LINEAR INITIAL TEMPERATURE PROFILE FOR A 'COLD DAY'
C
   40 X = 0.0
      MP1 = M + 1
      DO 43 I=1, MP1, 1
      T(I) = .6726 + .0796 * X
   43 X = X + DELX
      TP1(MP1) = T(MP1)
      GO TO 45
C
C     UNIFORM INITIAL TEMPERATURE PROFILE
C
   41 MP1 = M + 1
      DO 1 I=1, MP1, 1
    1 T(I) = TSOIL
      TP1(MP1) = T(MP1)
      GO TO 45
C
C     LINEAR TEMPERATURE PROFILE FOR A 'HOT DAY'
C
   42 X = 0.0
      MP1 = M + 1
      DO 44 I=1, MP1 , 1
      T(I) = .8715 - .0535 * X
   44 X = X + DELX
      TP1(MP1) = T(MP1)
```


Listing of Heat1 (cont'd)

```
C
C     DETERMINE LOCATIONS OF NODES ON EITHER SIDE OF XREM
C
   45 X = 0.0
      DO 7 ICOUNT = 1, MP1, 1
      X = X + DELX
      IF(XREM.LE.X) GO TO 9
    7 CONTINUE
C
    9 XLOW = FLOAT(ICOUNT - 1) * DELX
      XHIGH = FLOAT(ICOUNT) * DELX
C
C     PRINT ALL LOAD DATA
C
      WRITE(5,25)
   25 FORMAT(///,3X,'LOAD DATA',//)
C
      WRITE(5,26) M
   26 FORMAT(3X,'M = ',I4)
C
      WRITE(5,27) A, BI
   27 FORMAT(3X,'A = ',E14.7,5X,'BI = ',E14.7)
C
      WRITE(5,28)  TR, TSOIL
   28 FORMAT(3X, 'TR = ',E14.7,5X, 'TSOIL = ', E14.7)
C
      WRITE(5,29) DTIME
   29 FORMAT(3X,'DTIME = ',D14.7)
C
      WRITE(5,30) TP1MAX, XREM
   30 FORMAT(3X,  'TP1MAX = ', E14.7, 5X,'XREM = ', E14.7)
C
      WRITE(5,31) TREM, TINSUL
   31 FORMAT(3X, 'TREM = ', E14.7,5X, 'TINSUL = ', E14.7)
C
      WRITE(5,32) SWITCH
   32 FORMAT(3X, 'SWITCH = ', E14.7)
```

Listing of Heat1 (cont'd)

```
C
      WRITE(5,33) IOPT
   33 FORMAT(3X,'IOPT = ', I2)
C
      WRITE(5,34) IMAX
   34 FORMAT(3X, 'IMAX = ', I4)
C
      WRITE(5,35) XLOW, XHIGH
   35 FORMAT(3X,'XLOW = ',E14.7, 5X, 'XHIGH = ', E14.7)
C
      WRITE(5,46) TIN
   46 FORMAT(3X, 'TIN = ', E14.7,//)
C
C
C
C
C
C
      IF(IOPT.GT.1) GO TO 16
C
C     PRINT OUT THE ENTIRE INITIAL TEMPERATURE PROFILE IN THE PAVEMENT
C
      X = 0.0
      DO 36 I=1, MP1,1
      TT = T(I)
      WRITE(5,37) X, TT
   37 FORMAT(3X,'X = ',E14.7, 5X, 'T = ', E14.7)
   36 X = X + DELX
C
      GO TO 16
C
   15 IPRINT = IPRINT + 1
C
C
C     RATE OF CHANGE OF SURFACE NODE TEMPERATURE
C
```


Listing of Heat1 (cont'd)

```
   16 IF(SWITCH.GT.0.0) GO TO 3
C
C     (HEATED SURFACE)
C
      DTDT(1) =(2./DELX)*(A*(TH**4-T(1)**4) + BI*(TR-T(1)))
     1 - (2./DELX**2) * (T(1) - T(2))
C
      GO TO 4
C
C     (INSULATED SURFACE)
C
    3 DTDT(1)= -(2./(DELX**2))*(T(1)-T(2))
C
C     RATES OF CHANGE OF INTERIOR NODE TEMPERATURES
C
    4 DO 5 I=2,M,1
    5 DTDT(I)=(1./DELX**2)*(T(I-1)-2.*T(I)+T(I+1))
C
C     NEW TEMPERATURES AT ALL NODES
C
C         NOTE : TEMPERATURE OF THE (M+1)TH NODE (NODE ON THE BOTTOM
C                SURFACE OF THE BASE COURSE) REMAINS EQUAL TO ITS
C                SPECIFIED VALUE, TSOIL.
C
      DO 6 I=1,M,1
    6 TP1(I) = T(I) + DTDT(I) * DTIME
C
C     NEW TEMPERATURE AT DEPTH TO WHICH THE PAVEMENT IS TO BE REMOVED
C
      TXREM = TP1(ICOUNT+1) + ((XREM-XHIGH)/(XLOW-XHIGH))*
     1  (TP1(ICOUNT)-TP1(ICOUNT+1))
C
C     CHECK TO DETERMINE IF THE TEMPERATURE (TXREM) AT THE DEPTH OF
C     PAVEMENT TO BE REMOVED (XREM) EQUALS ITS DESIRED VALUE (TREM)
C
```

Listing of Heat1 (cont'd)

```
C          NOTE : (1) NO INTERPOLATION IS DONE TO DETERMINE THE EXACT
C                     TIME DURING THE FINAL TIME INCREMENT AT WHICH
C                     TXREM EQUALS TREM.
C                (2) ONLY TXREM NEEDS TO BE CHECKED. IT IS PHYSICALLY
C                     IMPOSSIBLE FOR TXREM TO BE .GE. TREM WHILE
C                     TEMPERATURES AT NODES ABOVE XREM ARE.LT.TREM.
C
C
      IF(TXREM.GE.TREM) GO TO 10
C
C
C
C
C     CHECK TO DETERMINE IF THE SURFACE IS PRESENTLY INSULATED
C
      IF(SWITCH.GT.0.0) GO TO 11
C
C
C     CHECK TO DETERMINE IF THE SURFACE TEMPERATURE ( TP1(1) )
C     EQUALS OR EXCEEDS ITS MAXIMUM ALLOWABLE VALUE ( TP1MAX ).
C
      IF(TP1(1).LT.TP1MAX) GO TO 11
C
C     SET SWITCH TO STOP HEATING AND INSULATE THE SURFACE
C
      SWITCH = 1.0
C
C
C     INCREMENT INSULATION PERIOD COUNTER
C
      NINSUL = NINSUL + 1
C
C
C     TIME AT THE END OF THE CURRENT INSULATION PERIOD
C
      TEND = TIME + TINSUL
```

Listing of Heat1 (cont'd)

```
C
C     INCREMENT TIME
C
   11 TIME = TIME + DTIME
C
C     RESET ALL TEMPERATURES
C
      DO 12 I=1, M,1
   12 T(I) = TP1(I)
C
C     CHECK FOR END OF CURRENT INSULATION PERIOD
C

      IF(TIME.LE.TEND) GO TO 14
C
C     SET SWITCH TO REMOVE INSULATION AND  BEGIN REHEATING THE
C     SURFACE
C
      SWITCH = -1.0
C
C     CHECK TO DETERMINE IF PRINTING SHOULD OCCUR AT THIS TIME STEP
C
   14 IF(IPRINT.LT.IMAX) GO TO 15
C
C     RESET PRINT COUNTER
C
      IPRINT = 1
C
C     CHECK PRINT OPTION AND PRINT
C
      WRITE(5,17) TIME, T(1), TXREM
   17 FORMAT(/,3X,'TIME = ',D14.7,/,3X,'T(1) = ',E14.7,/,3X,
     1'TXREM = ', E14.7)
C
C
C
```

Listing of Heat1 (cont'd)

```
      IF(IOPT.GT.1) GO TO 16
C
C     PRINT ENTIRE TEMPERATURE PROFILE IN THE PAVEMENT
C
      X = 0.0
      DO 18 I=1, MP1,1
      TT = T(I)
C
      WRITE(5,19) X , TT
   19 FORMAT(3X,'X = ',E14.7,5X, 'T = ', E14.7)
   18 X = X + DELX
C
C
C
C
      GO TO 15
C
C     PRINT TIME AT END OF HEATING
C
   10 TIME = TIME + DTIME
C
C
      WRITE(5,20) TIME
   20 FORMAT(///,3X, 'TOTAL ELAPSED TIME = ', D14.7,//)
C
C
C     PRINT NUMBER OF INSULATION PERIODS REQUIRED
C
      WRITE(5,21) NINSUL
   21 FORMAT(///,3X,'NUMBER OF INSULATION PERIODS REQUIRED = ', I3,//)
C
C
      END
C
C
C
```

Listing of Heat1 (concluded)